Autophagy and antipsychotic treatment response:

Characterising a potential relationship in a neuropsychiatric disorders context

by

Ms. Jessica Lagerwall

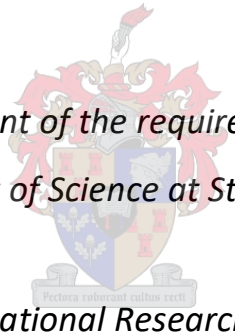

Thesis presented in partial fulfilment of the requirements for the degree of Master of Science in the Faculty of Science at Stellenbosch University

The financial assistance of the National Research Foundation (NRF) towards this research is hereby acknowledged. Opinions expressed and conclusions arrived at, are those of the author and are not necessarily to be attributed to the NRF.

Supervisor: Dr Nathaniel Wade McGregor

Co-supervisors: Prof. Louise Warnich, Prof. Ben Loos

March 2021

DECLARATION

By submitting this thesis electronically, I declare that the entirety of the work contained therein is my own, original work, that I am the sole author thereof (save to the extent explicitly otherwise stated), that reproduction and publication thereof by Stellenbosch University will not infringe any third party rights and that I have not previously in its entirety or in part submitted it for obtaining any qualification.

March 2021

ABSTRACT

Differential antipsychotic treatment outcomes continue to contribute to the global burden of age-related central nervous system (CNS) disorders. Amplifying this problem, a paucity of effective therapies exists, mainly due to unsuccessful drug discovery efforts in recent years. It is thus imperative that contemporary research contributes to the discovery of underpinning factors and causal mechanisms of these disorders for the development of effective therapeutic strategies. Moreover, it is essential that an emphasis be placed on genetic studies pertaining to patient cohorts of African descent, for which an alarming lack in literature currently exists. Macroautophagy, henceforth referred to as autophagy, is one of the main systems of degradation of cellular components. Its essential role in the homeostatic functioning of post-mitotic neurons makes it an excellent candidate mechanism when investigating the underlying factors contributing toward the development of age-related CNS disorders. In this regard, research has shown autophagy to be heavily implicated in the pathophysiology of neurodegenerative diseases, and more recently, albeit characterised to a much lesser degree, neuropsychiatric disorders. Further, the autophagy pathway has been shown to play a direct role in antipsychotic drug metabolism, thus providing impetus for more emphasis to be placed on this mechanism in drug-related research. This study thus aimed to investigate the genetic factors governing the dysregulation of autophagy to elucidate how this may inform on differential antipsychotic treatment response in a neuropsychiatric disorder context. The study used a South African cohort comprising 103 first-episode schizophrenia (FES) patients. Patients were treated with the same long-acting injectable antipsychotic, flupenthixol decanoate, and their response was measured at different time-points using the Positive and Negative Syndrome Scale (PANSS). Candidate genes associated with autophagy were identified in literature and genetic variants were subsequently prioritised using a bioinformatics pipeline. Prioritised variants were extracted from the genetic data available for the cohort and their involvement in differential treatment response was investigated. Using linear regression and mixed-effects modelling, association analyses revealed 10 significant associations, that survived Bonferroni correction for multiple testing, between prioritised genetic variants and various antipsychotic treatment outcomes all occurring under the PANSS Negative symptom domain. To inform on the extent to which an age-related CNS disease contributes to autophagy impairment, a directly converted induced neuronal (iN) cellular model was utilised by means of Huntington's disease (HD) patient-derived dermal fibroblasts. The iNs were treated pharmacologically with Torin1, an mTOR-dependent autophagy-inducing drug, and the response was assessed using immunocytochemistry and high content screening analysis. Whilst autophagy was successfully activated in the control iNs, it was inefficiently activated in the HD-iNs, suggesting a functional autophagy impairment in the diseased iNs. This impairment was further supported by the less elaborate neurite phenotype evident in the diseased iNs in comparison to the control iNs. This study was thus able to gauge the effect the age-related disease had on the autophagy mechanism of a neuronal-like cell, as well as the extent to which the autophagy-inducing drug could rescue the diseased phenotype. Ultimately, the outcomes of this study

provide novel genetic insight into the dysregulation of the autophagy pathway in neuropsychiatric disorders in a South African context. This may contribute to the future development of new and improved therapeutic strategies for the potential amelioration of neuropsychiatric disorder symptoms, with an emphasis on the negative symptoms of SCZ as well as the circumvention of adverse antipsychotic drug reactions. Furthermore, this study provides physiological insight into the dysfunctional autophagy pathway in a diseased neuronal-like cell and provides incentive for investigating the genetic findings of this study at a physiological-level using a directly converted iN cellular model in the future.

OPSOMMING

Differensiële antipsigotiese behandelingsuitkomste dra steeds by tot die wêreldwye las van ouderdomsverwante versteurings in die sentrale senuweestelsel (SSS). Hierdie probleem word vererger deur 'n gebrek aan effektiewe terapieë, hoofsaaklik as gevolg van onsuksesvolle pogings om terapeutiese middels te ontwikkel in die afgelope jare. Dit is dus noodsaaklik dat kontemporêre navorsing bydra tot die ontdekking van faktore en oorsaaklike meganismes van hierdie afwykings vir die ontwikkeling van effektiewe behandelingstrategieë. Verder is dit noodsaaklik dat klem gelê word op genetiese studies rakende pasiëntegroepe afkomstig vanuitAfrika, waarvoor daar tans 'n onrusbarende tekort aan literatuur bestaan. Makro-outofagie, wat voortaan outofagie genoem sal word, is een van die belangrikste stelsels verantwoordelik vir sellulêre komponent degenerering. Die wesenlike rol daarvan in die homeostatiese funksionering van post-mitotiese neurone maak dit 'n uitstekende kandidaatmeganisme vir die ondersoek na die onderliggende faktore wat bydra tot die ontwikkeling van ouderdomsverwante SSS-afwykings. In hierdie verband het navorsing getoon dat outofagie sterk betrokke is by die patofisiologie van neurodegeneratiewe siektes, en meer onlangs, hoewel dit in 'n baie mindere mate gekenmerk word, neuropsigiatriese afwykings. Verder is getoon dat die outofagie-weg 'n direkte rol speel in die metabolisme van antipsigotiese geneesmiddels, wat sodoende 'n verdere motivering gee vir meer klem op hierdie meganisme in geneesmiddelverwante navorsing. Hierdie studie het dus ten doel gehad om die genetiese faktore wat die wanregulering van outofagie beheer te ondersoek, om sodoende die rol van differensiële antipsigotiese behandelingsreaksie in 'n neuropsigiatriese versteuringskonteks te verstaan. Die studie het 'n Suid-Afrikaanse groep gebruik wat 103 pasiënte met skisofrenie (eerste episode) bevat. Pasiënte is behandel met dieselfde langwerkende inspuitbare antipsigotiese middel, flupenthixol-dekanoaat, en hul reaksie is op verskillende tydspunte gemeet deur die positiewe en negatiewe sindroomskaal (PANSS) te gebruik. Kandidaatgene wat met outofagie geassosieer word, is in die literatuur geïdentifiseer en genetiese variante is vervolgens geprioritiseer met behulp van 'n bioinformatika-pyplyn. Geprioritiseerde variante is onttrek uit die genetiese data wat beskikbaar is vir die groep en hul betrokkenheid by die respons van die differensiële behandeling is ondersoek. Met behulp van lineêre regressie en modellering van gemengde effekte, het assosiasie-ontledings 10 belangrike verwantskappe aan die lig gebring, na Bonferroni-regstelling vir meervoudige toetse, tussen voorkeur genetiese variante en verskillende antipsigotiese behandelingsuitkomste wat almal onder die PANSS Negatiewe simptoom domein voorkom. Om te lig te bring die mate waartoe 'n ouderdomsverwante SSS-siekte bydra tot 'n afwyking van outofagie, is 'n direk-omgeskakelde geïnduseerde neuronale (iN) sellulêre model vir Huntington-siekte (HD) pasiënt-afgeleide dermale fibroblaste gebruik. Die iN'e is farmakologies behandel met Torin1, 'n mTOR-afhanklike outofagie-induserende middel, en die respons is beoordeel met behulp van immunositochemie en hoë-inhoud-siftingsanalise . Terwyl outofagie suksesvol geaktiveer was in die kontrole iN'e, was dit ondoeltreffend geaktiveer in die HD-iN'e, wat dui op 'n funksionele outofagiese inkorting in die siek iN’e. Hierdie inkorting is

verder ondersteun deur die minder uitgebreide neurietfenotipe wat sigbaar is in die siek iN’e in vergelyking met die kontrole-iN’e. Hierdie studie kon dus die effek bepaal wat ouderdomsverwante siekte op die outofagie-meganisme van 'n neuronagtige sel gehad het, asook die mate waarin die outofagie-induserende middel die siek fenotipe kon red. Uiteindelik bied die uitkomste van hierdie studie nuwe genetiese insig in die wanregulering van die outofagie-weg in neuropsigiatriese afwykings in 'n Suid-Afrikaanse konteks. Hierdie kan bydra tot die toekomstige ontwikkeling van nuwe en verbeterde terapeutiese strategieë vir die moontlike verbetering van neuropsigiatriese versteuringsimptome, met die klem op die negatiewe simptome van SCZ sowel as die verligting/voorkoming van ongunstige antipsigotiese geneesmiddelreaksies. Verder bied hierdie studie fisiologiese insig in die disfunksionele outofagie-pad in 'n siek neuronagtige sel en bied dit 'n aansporing om die genetiese bevindings van hierdie studie op 'n fisiologiese vlak te ondersoek deur gebruik te maak van 'n direk omgeskakelde iN-sellulêre model in die toekoms.

ACKNOWLEDGEMENTS

I would like to express my sincere gratitude to the following people and institutions:

The National Research Foundation (NRF) and Stellenbosch University for financial assistance.

Dr Nathaniel McGregor, my supervisor, for your guidance, support, and mentorship throughout my postgraduate studies. You have taught me to think critically and work independently, for which I am very grateful.

Professor Louise Warnich, my co-supervisor, for your unwavering support and dedication throughout my postgraduate studies. Despite a demanding schedule, you have always found time for me. Your consistency and constructive advice have been invaluable, and your incredible success as a woman in science is inspiring.

Professor Ben Loos, my co-supervisor, your knowledgeable contributions to the physiological aspect of this project have been indispensable. Thank you for enthusiastically taking on the role as co-supervisor at such a late stage.

Professor Robin Emsley and the EONKCS team, for patient recruitment, sample collection, and clinical data.

Professor Johan Jakobsson, my supervisor at Lund University, for allowing me to be a part of the Molecular Neurogenetics Lab. This experience has taught me how valuable it is to have a diverse, yet cohesive team, as well as the importance of collaboration. The opportunity allowed for me to get a glimpse into the great possibilities of science, for which I will always be grateful.

Dr Karolina Pircs, my research project supervisor at Lund University, for your mentorship and guidance, and your dedication to my development as a scientist. Your inner drive and enthusiasm towards your research are truly inspiring. I look forward to collaborating with you in the future.

Professor Maria Swanberg, the course administrator for the Advanced Course in Neuroscience at Lund University, for granting me the opportunity to partake in this course. This course has taught me to be confident as an independent researcher and has shown me the extensive possibilities of the neuroscientific field. I have walked away with invaluable skills and networks, which will undoubtedly support me in my future career.

The Stellenbosch University International Office, especially Sarah de Villiers, for her valuable insight into the exchange student process and her assistance in the administration process.

Isabelle Jönsson, my International Administration Officer at Lund University, for her dedication to the administration process of my studying abroad, as well as her caring and supporting nature during my stay in Sweden.

Members of the Human Systems Genetics Lab, for providing me with a semblance of normality and structure during the pandemic. Lab meetings and journal clubs were always something I looked forward to in the thick of lockdown.

My family, for the emotional and financial support. Thank you for the home-cooked meals (and the video calls whilst I was away) when I needed them, and for being my sounding board whenever something was troubling me. I would not have been able to make it through this process without your careful guidance and direction.

My friends, both in South Africa and across the globe. Thank you for your constant support, for checking in on me, and for always having my back. Your friendships have meant the world to me, and I wouldn't be able to get by without them.

Alex, for providing me with unwavering emotional support throughout the last 3 years. You have taught me to be confident within myself, and to stand up for my beliefs. *Merci beaucoup pour tout.*

Harley, for your caring nature, and your ability to turn any bad day into a good one. Walks with you have been the perfect thesis-writing breaks and I can't thank you enough. I foresee plenty of walks and ball-throwing for us in the future.

TABLE OF CONTENTS

LIST OF FIGURES

LIST OF TABLES

LIST OF SYMBOLS AND ABBREVIATIONS

%	Percentage
×	multiplied by/interaction
+	Addition/positive
±	Standard error
=	Equal to
>	Greater than
≥	Greater than or equal to
<	Less than
≤	Less than or equal to
3’	3-prime end
°C	Degrees Celsius
α	Alpha
β	Beta
cm^2	Centimetre squared
µM	micromolar
µg	microgram
ɣ	Gamma
©	Copyright
™	Trademark
**	Denotes uncorrected P-value threshold of P ≤ 0.001
***	Denotes P-value below Bonferroni-corrected threshold
ADNP	Activity-dependent neuroprotective protein
ADR	Adverse drug reaction
AIM	Ancestry Informative Marker
AKT/PKB	Protein kinase B
AMBRA1	Activating molecule in Beclin-1-regulated autophagy encoding gene
ATG	Autophagy-related
ATP	Adenosine triphosphate
ATR	Antipsychotic treatment response
BECN1	Beclin-1 protein
BECN1	Beclin-1 encoding gene
bp	Base pair
CD-CV	Common disease-common variant
CGI	Clinical Global Impression
CI	Confidence interval

CNS	Central nervous system
CYP2C9	Cytochrome P450 2C9 enzyme encoding gene
CYP4F2	Cytochrome P450 Family 4 Subfamily F Member 2 encoding gene
DAPI	4', 6-diamidino-2-phenylindole
D2	Dopamine Type 2
dbSNP	Single Nucleotide Polymorphism Database
DLB	Dementia with Lewy-Bodies
DMEM	Dulbecco's Modified Eagle Medium
DMSO	Dimethyl sulfoxide
DRD2	Dopamine receptor subtype 2
DSigDB	Drug signatures database
DSM-IV	Diagnostic and Statistical Manual of Mental Diseases, Fourth Edition
ECM	Early conversion media
eQTL	Expression quantitative trait loci
FBS	Fetal bovine serum
FES	First episode schizophrenia
FGA	First generation antipsychotic
G x G	Gene-gene interaction
GABARAP	Gamma-aminobutyric acid receptor-associated protein encoding gene
G x E	Gene-environment interaction
GFP	Green fluorescent protein
GIGYF2	*GRB10 Interacting GYF Protein 2* encoding gene
GO	Gene ontology
GRch37	Human Genome Assembly version 37
GWAS	Genome-wide association study
h	Hour
HCS	High-content screening
HD	Huntington's disease
HHV8	Human herpesvirus-8
HTT	Huntingtin protein
ID	Identification number
IL	Interleukin
iN	Induced neuron
INF- γ	Interferon- γ
IRFs	Interferon response factors
KEGG	Kyoto Encyclopaedia of Genes and Genomes
KSHV	Kaposi's sarcoma-associated herpesvirus

LAMP-1	Lysosomal-associated membrane protein 1
LAMP-2	Lysosomal-associated membrane protein 2
LC3	Microtubule-associated protein 1A/1B-light chain 3
LC3-II	Lipid modified form of microtubule-associated protein 1A/1B light chain 3
LCM	Late conversion media
LD	Linkage disequilibrium
Lme4	Linear Mixed-Effects Models using 'Eigen' and S4
lmerTest	Tests in Linear Mixed Effects Models
M	Molar
MAF	Minor allele frequency
MAP2	Microtubule-associated protein 2
MAPK	Mitogen-activated protein kinase
min	Minute
mg	milligram
mHTT	Mutant huntingtin protein
miRNA	microRNA
ml	milliliter
mM	millimolar
mRNA	Messenger ribonucleic acid
mTOR	Mammalian target of rapamycin
mTORC/1	Mammalian target of rapamycin complex/1
MOI	Multiplicity of infection
n	Number of samples
NF-κB	Nuclear factor kappa B
NHGRI-EBI	National Human Genome Research Institute
NLRP3	NOD-like receptor pyrin containing 3
NLRs	NOD-like receptors
NOD	Nucleotide-binding oligomerisation domain
nM	Nanomolar
NRF	National Research Foundation
ORF	Open-reading frame
p62/SQSTM1	Sequestosome-1 protein
p150	Phosphoinositide 3-kinase regulatory subunit 4
PANSS	Positive and Negative Syndrome Scale
PARK2	*Parkin* encoding gene
DPBS	Dulbecco's Phosphate Buffered Saline
PD	Parkinson's disease

PharmGKB	Pharmacogenomics Knowledge Base
PGK	Phosphoglycerate kinase
PI3K/PtdIns3K	Phosphoinositide 3-kinase
PINK1	PTEN-induced kinase 1
PINK1	PTEN-induced kinase 1 encoding gene
PolymiRTS	Polymorphism in microRNA Target Site
PolyPhen-2	Polymorphism Phenotyping v2
r^2	Squared correlation coefficient (linkage disequilibrium measurement)
RB1CC1	RB1 inducible coiled-coil 1 encoding gene
RB1CC1/FIP200	RB1-inducible coiled-coil protein 1
REST	RE1 Silencing Transcription Factor
RNA	Ribonucleic acid
ROS	Reactive oxygen species
SA	South Africa
SAPS	Scale for Assessment of Positive Symptoms
SCID	Structural Clinical Interview for DSM-IV
SCZ	Schizophrenia
SEM	Standard error of the mean
SGA	Second generation antipsychotic
SIFT	Sorting Intolerant From Tolerant
shRNA	Short hairpin ribonucleic acid
SNP	Single nucleotide polymorphism
SQSTM1	Sequestosome-1 protein encoding gene
TFBS	Transcription factor binding site
TLRs	Toll-like receptors
TNF	Tumor necrosis factor
TRAF	Tumor necrosis factor receptor-associated factor
Ubq	Ubiquitin
ULK	Unc-51-like kinase
VPS34	Phosphatidylinositol 3-kinase VPS34 protein encoding gene
VKORC1	Vitamin K epoxide reductase encoding gene
w/	with
WMA	World Medical Association

CHAPTER 1. LITERATURE REVIEW

1.1. Antipsychotic treatment response in schizophrenia

Schizophrenia (SCZ) is a debilitating neuropsychiatric disorder for which no known cure exists (Albus, 2012). With a lifetime prevalence of 1%, it is a major contributor to the global burden of disease (Saha, Chant, Welham, *et al.*, 2005; Whiteford, Degenhardt, Rehm, *et al.*, 2013), and this is exacerbated by the paucity of effective therapies which is mainly a result of failed drug discovery efforts in recent years (Dunlop & Brandon, 2015; Wong, Yocca, Smith, *et al.*, 2010). Indeed, a systematic review which evaluated 50 studies relating to SCZ recovery found that a staggering 13.5% of the median proportion of individuals with SCZ reached clinical and social recovery criteria (Jääskeläinen, Juola, Hirvonen, *et al.*, 2013). It is therefore crucial that contemporary research contributes to discovering the underpinning factors and causal mechanisms of age-related CNS diseases like SCZ for the subsequent development of new effective therapeutic strategies.

Symptoms of SCZ are characterised according to positive and negative symptoms. Positive symptoms include delusions, hallucinations, disorganised speech, grossly disorganised or catatonic behaviour, and negative symptoms include emotional and social withdrawal, difficulty in abstract thinking as well as avolition amongst other symptoms (Wenzel, 2017). Relief from the associated symptoms of this complex disorder is primarily through the administration of antipsychotic drugs (Foster, Miller & Buckley, 2010). Research postulates that variation in antipsychotic treatment response (ATR) is evident both within and between populations. This is hypothesised to be due to an interplay between genetic and environmental factors and thus corroborates the idea that ATR is a complex trait (Foster *et al.*, 2010).

Adverse drug reactions (ADRs) are a common occurrence when considering antipsychotic treatment of SCZ patients (Müller, Chowdhury & Zai, 2013; Young, Taylor & Lawrie, 2015; Zhang, Gallego, Robinson, *et al.*, 2013). They can be defined as “an appreciably harmful or unpleasant reaction, resulting from an intervention related to the use of a medicinal product; adverse effects usually predict hazard from future administration and warrant prevention, or specific treatment, or alteration of the dosage regimen, or withdrawal of the product.” (Aronson & Ferner, 2005). This definition has been further revised to include ADRs occurring due to error, misuse or abuse, and suspected adverse reactions to unlicensed medicines (European Union, 2011). Examples of ADRs are weight gain, acute dystonia, tardive dyskinesia and drug-induced parkinsonism (Bender, Grohmann, Engel, *et al.*, 2004). Ultimately, the lack of drug compliancy due to ADRs contributes to the worsening of the progression and outcome of the disorder (Hudson, Owen, Thrush, *et al.*, 2004; Löffler, Kilian, Toumi, *et al.*, 2003; Sharif, 2008; Velligan, Weiden, Sajatovic, *et al.*, 2009, extensively reviewed by Higashi, Medic, Littlewood, *et al.*, 2013 and Wade, Tai, Awenat, *et al.*, 2017)

Antipsychotic medications are classified into first generation (FGA) and second generation (SGA) antipsychotics, both of which exhibit a variation in type, severity, and frequency of ADRs (Bender *et al.*, 2004).

FGAs, which act as dopamine receptor D_2 (DRD2) antagonists, have been in use for over half a century in the treatment of SCZ. To minimise ADRs inflicted using FGAs, SGAs were introduced. These SGAs interact with a broader range of pharmacological receptor types and are classified as serotonin-dopamine antagonists or multi-acting receptor-targeted antipsychotics (Horacek, Bubenikova-Valesova, Kopecek, *et al.*, 2006). Contradictory to the main premise of SGAs, statistical meta-analyses of clinical trials of SCZ patients demonstrate that these antipsychotics present only with heterogeneous ADRs (Leucht, Corves, Arbter, *et al.*, 2009; Smith, Leucht & Davis, 2019). Further compounding this issue, the complexity of the ATR trait begets the effectivity of both FGAs and SGAs to depend entirely on the individual patient (Bender *et al.*, 2004; Citrome, Eramo, Clement, *et al.*, 2015).

1.2. The neurodevelopmental hypothesis of schizophrenia

It is hypothesised that adult-onset neuropsychiatric disorders, such as SCZ, have their origins in the abnormal early development of the nervous system (Rapoport, Giedd & Gogtay, 2012). This is supported by numerous studies focusing on primates, as well as epidemiological, developmental and neuroimaging studies (van Os & Kapur, 2009; Owen, Sawa & Mortensen, 2016). The neurodevelopmental hypothesis of SCZ has been a prominent paradigm in SCZ research over the past three decades (Murray & Lewis, 1987; Owen & O'Donovan, 2017; Owen, O'Donovan, Thapar, *et al.*, 2011; Weinberger, 1987, 2017). Research suggests that it might be more plausible to view SCZ as a member of a wider group of overlapping syndromes, which have arisen partly from neurodevelopmental irregularities and which are not restricted to psychotic or even psychiatric disorders (Guloksuz & Van Os, 2018; Owen & O'Donovan, 2017). In this regard, SCZ should not be reduced to simply a neurodevelopmental disorder but rather a result of the interaction of neurodevelopmental risk factors with adverse social and drug risk factors, majority of which act during development and which then later culminate in the disorder in early adult life. To this end, the neurodevelopmental hypothesis has gradually transformed into the Developmental Risk Factor Model of Psychosis (reviewed in Murray, Bhavsar, Tripoli, *et al.*, 2017).

Considering the genetic risk of both SCZ and neurodevelopmental disorders, population genetics and genetic epidemiology suggest that there is an underlying spectrum of risk alleles, even within families (Daniels, Forssen, Hultman, *et al.*, 2008; Gandal, Haney, Parikshak, *et al.*, 2018; Kushima, Aleksic, Nakatochi, *et al.*, 2018; Larsson, Eaton, Madsen, *et al.*, 2005; Owen *et al.*, 2016). This implies that a general overlap in genetic risk and pathophysiology could exist between neurodevelopmental disorders (such as attention deficit hyperactivity disorder, epilepsy and autism) and SCZ, and further challenges the idea that they are completely unrelated diagnostic entities (Owen & O'Donovan, 2017; Owen *et al.*, 2011). Polygenic risk scores for SCZ have been shown to account for approximately 9% of variance in caseness in SCZ case and control studies (Vassos, Di Forti, Coleman, *et al.*, 2017), and notably have been shown to be associated with neurodevelopmental defects as well as negative symptoms in healthy children (Riglin, Collishaw, Richards, *et*

al., 2017), adolescents (Jones, Stergiakouli, Tansey, *et al.*, 2016) and adults (Van Os, Van Der Steen, Islam, *et al.*, 2017). This is further supported by findings in family studies that have identified an increased prevalence of SCZ in the parents of individuals with autism (Daniels *et al.*, 2008; Larsson *et al.*, 2005; Sullivan, Magnusson, Reichenberg, *et al.*, 2012). Along with the genetic overlap between SCZ and neurodevelopmental disorders, a phenotypic overlap is present. More specifically, this overlap concerns cognitive impairments which frequently result in a range of developmental delays and neurological soft signs such as deficits in sensory integration and motor coordination, and difficulties in performing complex motor tasks (Chisholm, Lin, Abu-Akel, *et al.*, 2015; Owen *et al.*, 2011). This symptomology overlap is evident between childhood-onset as well as adult-onset SCZ and autism spectrum disorders (Morgan, Leonard, Bourke, *et al.*, 2008; Owen & O'Donovan, 2017; Rapoport, Chavez, Greenstein, *et al.*, 2009; Stahlberg, Soderstrom, Rastam, *et al.*, 2004).

1.3. Comorbidity is evident in neurodevelopmental disorders and neurodegenerative diseases

In a similar fashion to the latter symptomological overlap between neuropsychiatric and neuro-developmental disorders, comorbidity is frequently seen between certain neurodevelopmental disorders and neurodegenerative diseases (Zhu, Casadesus, Webber, *et al.*, 2008). For instance, motor abnormality domains are shared across neurodevelopmental disorders and neurodegenerative diseases, albeit with a varying expressivity or prevalence (Peralta & Cuesta, 2017). This distinct overlap is also present when considering the manifestation of neurodegenerative diseases and ADR symptoms exhibited during the treatment of neuropsychiatric disorders. For example, tardive dyskinesia, a common ADR in SCZ patients, mimics the symptoms of Parkinson's disease (PD) and Parkinsonism disorder; more specifically, the motor dysfunction present (Cornett, Novitch, Kaye, *et al.*, 2017). Moreover, when one considers the symptoms of SCZ itself, it is striking that SCZ-like manifestations are considered to be some of the earliest markers of the autosomal dominant neurodegenerative disease Huntington's disease (HD), along with changes in striatal volume, amongst other symptoms (Duff, Beglinger & Paulsen, 2008). Huntington's disease is caused by the expansion of CAG repeats in the first exon of the huntingtin (*HTT*) gene, and results in the synthesis of a mutant form of the HTT protein, namely mHTT (Bates, Dorsey, Gusella, *et al.*, 2015). Individuals with a CAG repeat length > 40 will develop the disease, and further, the CAG repeat length is directly correlated with clinical progression and indirectly correlated with the age of onset of the disease (Langbehn, Brinkman, Falush, *et al.*, 2004). Huntington's disease is characterised by the primary degeneration of the cortico-striatal pathway (Estrada-Sánchez & Rebec, 2012; Hamilton, Haaland, Adair, *et al.*, 2003; Miller, Walker, Barton, *et al.*, 2011). These cortico-striatal neurons synapse upon cholinergic interneurons, which then regulate dopaminergic neurons *via* nicotinic receptors situated on the dopamine neurons. These then mediate the cortico-striatal control of striatal dopamine release (Kosillo, Zhang, Threlfell, *et al.*, 2016). Interestingly, ADRs occurring due to antipsychotic medication during treatment of SCZ are mainly due to the blockade of D_2

receptors on cholinergic interneurons (Kharkwal, Brami-Cherrier, Lizardi-Ortiz, *et al.*, 2016). Another interesting aspect to note is the high prevalence of neuropsychiatric symptoms throughout the different stages of the disease. For example, a study performed over 15 European countries assessing the neuropsychiatric symptoms of almost 2000 HD patients found that depression, irritability or aggression and obsessive compulsive behaviours are prevalent at all stages of the disease (Van Duijn, Craufurd, Hubers, *et al.*, 2014). Furthermore, they found that apathy occurred most often at the advanced stages of the disease.

This multi-faceted overlap is emphasised when considering the intricate mechanism and subsequent dysregulation of macroautophagy (Fujikake, Shin & Shimizu, 2018; Lee, Hwang & Lee, 2013; Schneider, Miller & Woesner, 2017; Vucicevic, Misirkic-Marjanovic, Harhaji-Trajkovic, *et al.*, 2018).

1.4. Autophagic pathway: The ‘‘raison d’être’’ of autophagy genes

There are two protein degradation systems that are of paramount importance when considering a living organism’s ability to maintain cellular homeostasis. These are ubiquitin-proteasome (UPS)-dependent protein degradation and autophagy, which itself functions *via* lysosomal degradation. Whereas the UPS is more selective in that it only degrades short-lived ubiquitinated proteins (Finley, 2009; Hershko, 1983), autophagy is responsible for the degradation of both long-lived proteins and cellular components (Groll & Huber, 2003, 2004; Klionsky, 2007). Autophagy can be categorised into three pathways, namely macroautophagy, chaperone-mediated autophagy and microautophagy. For the purpose of this study, only macroautophagy will be investigated as it is the principal and most well-characterised pathway for lysosomal degradation, and it will henceforth be referred to as autophagy.

During events such as nutrient deficiencies, hypoxia, bacterial infections and oxidative stress, autophagy occurs at an amplified rate, and in doing so contributes to the cellular adaptation to stress (Heymann, 2006). The molecularly well-understood autophagy process is regulated by approximately 30 genes from the autophagy-related (ATG) gene family. These genes were initially identified in yeast, and their orthologues were then identified in humans (Lippai & Lőw, 2014; Yang & Klionsky, 2010). The autophagy pathway plays a crucial role in maintaining proteostasis, and thus preventing proteotoxicity, by removing damaged organelles and long-lived cytoplasmic proteins, especially in neurons (Liang & Sigrist, 2018). It constitutes the autophagosome formation, maturation and lastly fusion with the lysosomes whereby the autophagic cargo is degraded *via* lysosomal proteases (Yu, Chen & Tooze, 2018) (Figure 1.1.). Autophagosomes are ubiquitously formed at the neuronal axon tip and are then retrogradely transported toward the soma, developing into fully-matured autophagosomes as they make their retrograde journey (Lee, Sato & Nixon, 2011; Maday, Wallace & Holzbaur, 2012). During autophagosome formation, membranes of autophagosomes are formed during a two-step conjugation process whereby the second step involves the association of the lipid modified form of microtubule-associated protein 1A/1B-light chain 3 (LC3-II) with the autophagosome membrane (Ichimura, Kirisako, Takao, *et al.*, 2000; Kabeya, 2000; Nath, Dancourt, Shteyn, *et al.*, 2014; Valionyte, Yang,

Roberts, *et al.*, 2020). LC3-II abundance thus represents the total number of autophagosomes, and is hence used as a biological marker for autophagosomes (Mizushima & Yoshimori, 2007). Additionally, the Lysosomal-Associated Membrane Proteins 1 and 2 (LAMP-1 and LAMP-2) carry the function of trafficking of lysosomes and autophagosome-fusion and are thus commonly used as biological markers for these organelles (Saftig, Beertsen & Eskelinen, 2008; Tanaka, Guhde, Suter, *et al.*, 2000). More specifically, LAMP-1 is indicative of the presence of early lysosomal structures and LAMP-2 is indicative of the presence of mature lysosomes (Klionsky, Abdelmohsen, Abe, *et al.*, 2016).

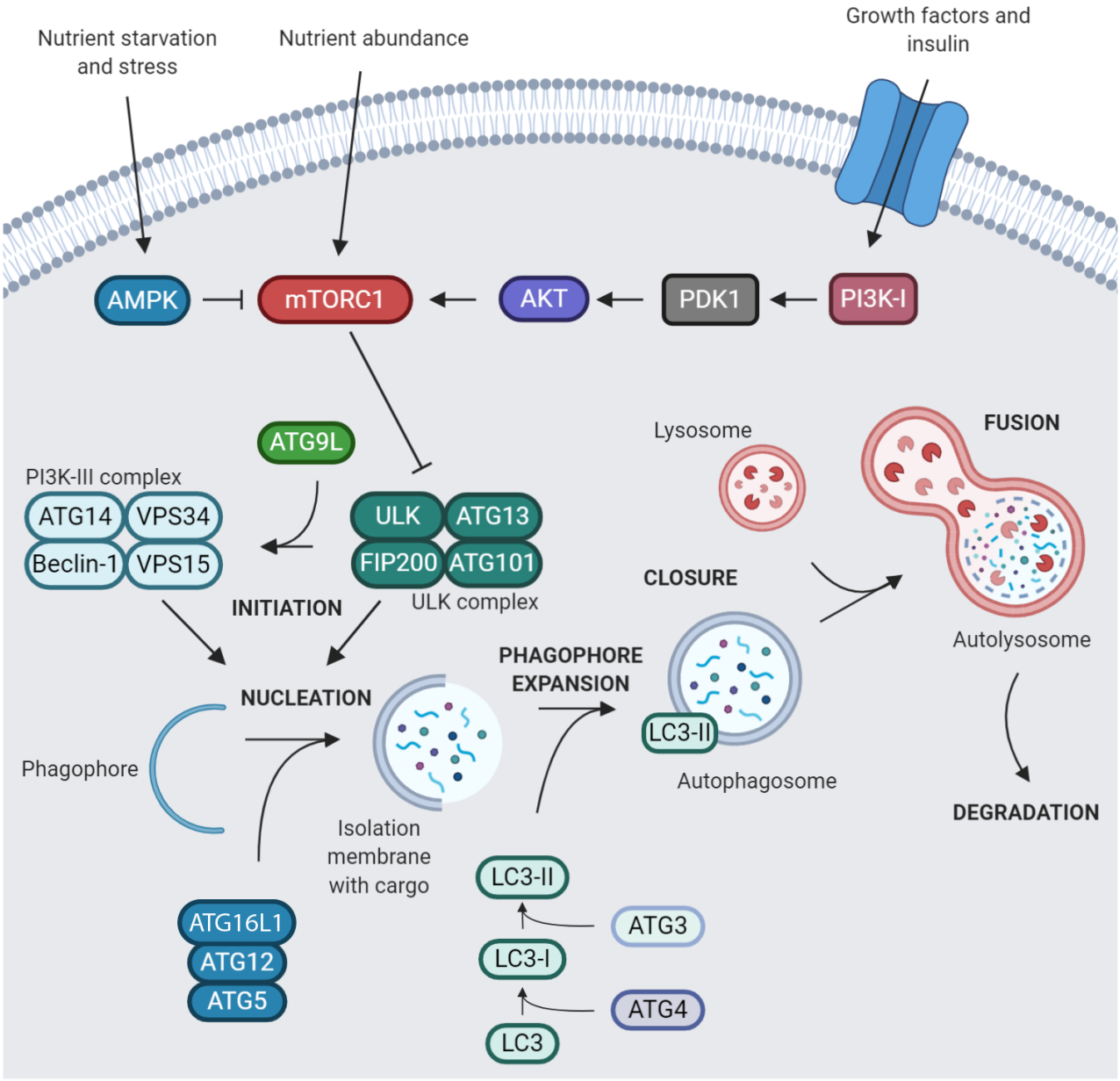

Figure 1.1. The molecular mechanisms of autophagy in mammalian cells
The mechanism of autophagy in mammalian cells. Post autophagy initiation, a phagophore nucleates and expands near the endoplasmic reticulum, in a specialised structure known as the omegasome. Closure of this entity leads to the formation of the autophagosome, and upon fusion with the lysosome the contents are degraded by hydrolytic enzymes present in the lumen of the lysosome. The ULK (Unc-51-like kinase) and PI3K (class III phosphatidylinositol 3-kinase) complexes, and the ATG9 trafficking system are required for the initiation, nucleation and expansion steps, whereas the ATG12 and LC3 conjugation systems are mainly involved in the closure of the phagophore and autophagosome-lysosome fusion. Adapted from www.invivogen.com. Created with www.BioRender.com.

Autophagy is a dynamic process in which autophagosome accumulation can either indicate an induction of autophagy or an inhibition of downstream steps following autophagosome formation. More specifically, an increased activation of autophagy from a basal level will result in an increase in autophagic structures (i.e.

autophagosomes represented by LC3-II and autolysosomes represented by LAMP-1). However, if there is any dysregulation prior to autophagosome formation, there will be a decreased number in all autophagic structures (Mizushima, Yoshimori & Levine, 2010). Alternatively, if any dysregulation occurs downstream of autophagosome formation, such as dysfunctional degradation of autophagosome contents, then there will be a resulting increase in the number of autophagosomes (LC3-II), similar to that observed in the activation of autophagy, with an accompanied decrease in autolysosomes (LAMP-1) (Mizushima *et al.*, 2010). This stresses the importance of the accurate measurement of autophagic flux, which refers to the rate at which damaged organelles and abnormal proteins are degraded *via* autophagy (Klionsky *et al.*, 2016; Loos, Toit & Hofmeyr, 2014), as both activation and dysfunction of the autophagic pathway manifest in the same molecular profile. Another informative biomarker is the p62 receptor protein (encoded by *SQSTM1*), which binds to ubiquitinated proteins and subsequently becomes incorporated into mature autophagosomes for degradation in autolysosomes (Klionsky *et al.*, 2016). Thus, by measuring the presence of both LC3-II and LAMP-1, as well as the receptor protein p62, one would be able to gain better insight into the current functional state of the autophagy pathway and discern whether there is activation or dysregulation of the pathway occurring.

1.5. Selective autophagy

1.5.1. Mitophagy

Mitophagy is a process that is defined by the selective degradation of mitochondria. *PINK1* (which encodes PTEN-induced kinase 1) is known to be a critical constituent in the mitophagy process. PINK1 is a mitochondrial outer membrane kinase, and it recruits PARK2/Parkin to the site of damage for ubiquitination and subsequent initiation of mitophagy (Youle & Narendra, 2011). Furthermore, Beclin-1 (BECN1) has been identified to relocalise at the mitochondria-associated membranes with PINK1 for the activation of mitophagy degradation through mitophagy (Gelmetti, De Rosa, Torosantucci, *et al.*, 2017). In order to prevent the accumulation of PINK1 on the membrane of healthy mitochondria and thus their degradation *via* mitophagy (Jin, Lazarou, Wang, *et al.*, 2010; Mariño, Uría, Puente, *et al.*, 2003), PINK1 is transported into the inner mitochondrial membrane for eventual degradation.

1.5.2. Xenophagy

Xenophagy is a selective autophagy pathway that targets intracellular bacteria and viruses (Gatica, Lahiri & Klionsky, 2018). Nucleotide-binding and oligomerisation domain (NOD)-like receptors (NLRs) are pattern-recognition receptors and function as innate immune receptors key to this process (Figure 1.2.). By recruiting ATG16L1 to the site of bacterial entry on the plasma membrane, NOD1 and NOD2, founding members of the NLR family, can sense the bacterial peptidoglycan and induce mitophagy for the selective removal of pathogens (Kim, Shin & Nahm, 2016). This signalling pathway can trigger the formation of inflammasomes

and can potentially activate nuclear factor κB (NF-κB), stress kinases, interferon response factors (IRFs), inflammatory caspases and autophagy (Muñoz-Wolf & Lavelle, 2016) (Figure 1.2.).

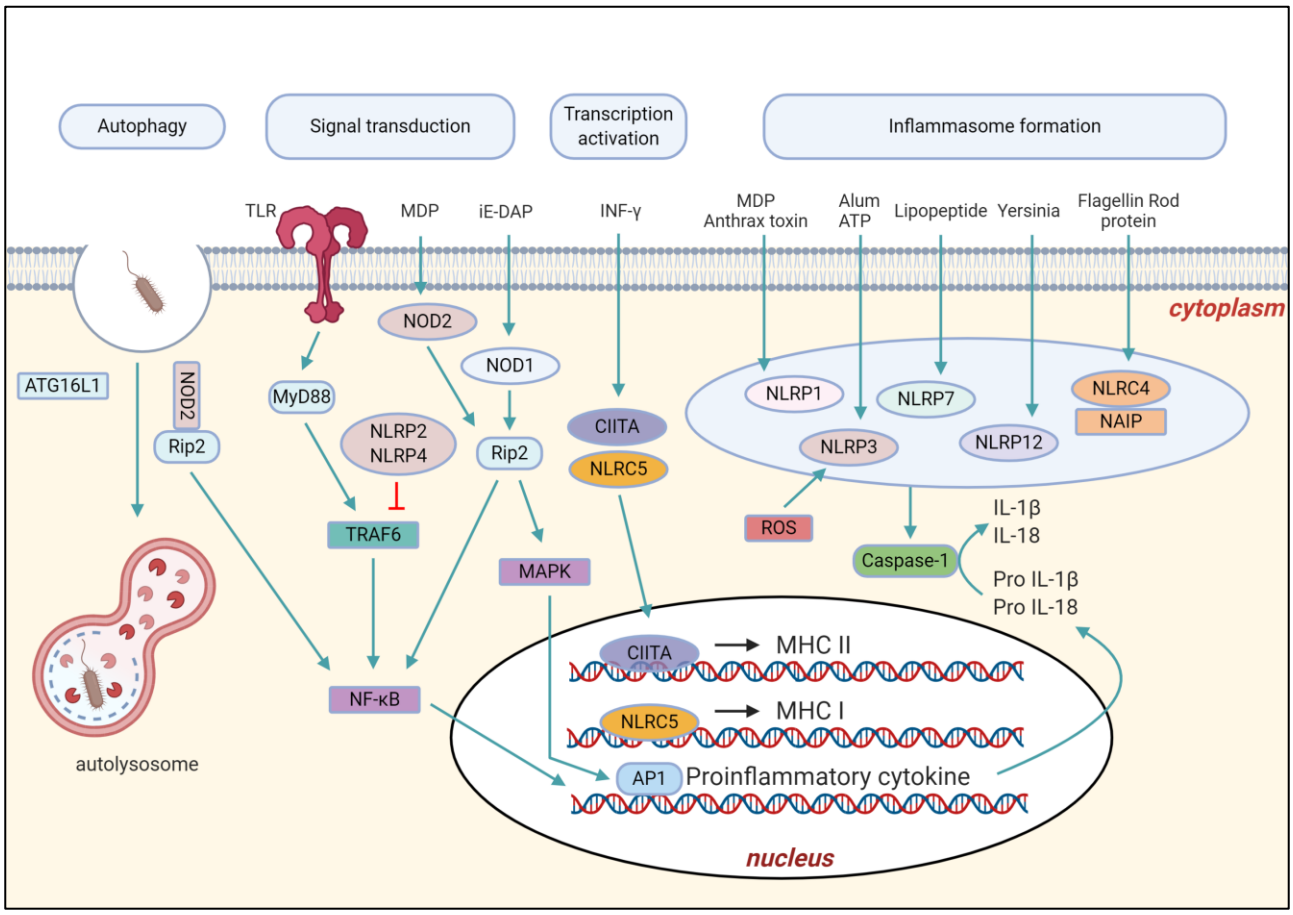

Figure 1.2. The NOD-like receptor pathway is an immune response pathway that activates autophagy amongst other processes

NOD-like receptor (NLR) functions. NLR activities can be divided into four broad groups, namely autophagy, signal transduction, transcription activation and inflammasome formation. NOD2 activates autophagy to remove pathogens by recruiting ATG16L1 to the plasma membrane at the site of bacterial entry. NOD1 and NOD2 recognise the bacterial peptidoglycan and trigger the formation of inflammasomes and can potentially activate nuclear factor κB (NF-κB), stress kinases, interferon response factors (IRFs), inflammatory caspases and autophagy. NLRs: NOD-like receptors; NF-κB: nuclear factor kappa B; MAPK: mitogen-activated protein kinase; TRAF: tumour necrosis factor (TNF) receptor-associated factor; IL: interleukin; INF-γ: interferon-γ. Adapted from Kim, Shin, *et al.*, 2016, reproduced under the Creative Commons Attribution Non-Commercial License (http://creativecommons.org/licenses/by-nc/3.0/). Created with www.BioRender-.com.

1.6. The role of autophagy in CNS disorders and diseases

The post-mitotic nature of neurons prompts the crucial functioning of protein quality control mechanisms within the CNS. Autophagy impairment is consistently implicated in neurodegenerative diseases, and more recently neuropsychiatric disorders (Bar-Yosef, Damri & Agam, 2019; Levine & Kroemer, 2008; Stamatakou, Wróbel, Hill, *et al.*, 2020). Further, this impairment is considered to be a promising link between the two (Polajnar & Žerovnik, 2014). Emerging evidence is in favour of the enhancement of autophagy for the removal

of toxic protein aggregates (Loos, Engelbrecht, Lockshin, *et al.*, 2013; Ravikumar, Stewart, Kita, *et al.*, 2003; Rubinsztein, DiFiglia, Heintz, *et al.*, 2005). These toxic protein aggregates and associated neurodegenerative diseases include but are not limited to: mHTT in HD, α-synuclein in Parkinson's disease, and amyloid-β/tau in Alzheimer's disease. Additionally, there is support for the induction of autophagy potentially ameliorating symptoms in both neurodegenerative and neuropsychiatric disorders (extensively reviewed in (Bassan, Zamostiano, Davidson, *et al.*, 2008) and (Bar-Yosef *et al.*, 2019)). For example, activity-dependent neuroprotective protein (ADNP) is necessary for brain formation and development, neuroprotection and neuroplasticity, and its interaction with LC3-II, a key component of autophagosomes, suggests its role in autophagy (Bassan *et al.*, 2008; Merenlender-Wagner, Malishkevich, Shemer, *et al.*, 2015). Abnormal expression of *ADNP* in SCZ results in an impaired autophagy mechanism and further supporting this, ADNP expression has been shown to be deregulated in the post-mortem hippocampus of SCZ patients compared to healthy matched controls (Dresner, Agam & Gozes, 2011; Merenlender-Wagner *et al.*, 2015). Notably, a study by Vulih-Shultzman *et al*. demonstrated that the administration of the peptide sequence derived from ADNP enhances autophagy in a mouse model of SCZ (Vulih-Shultzman, Pinhasov, Mandel, *et al.*, 2007). Moreover, the administration of this peptide decreased SCZ-like hyperactivity in a different mouse model of SCZ (Merenlender-Wagner, Pikman, Giladi, *et al.*, 2010). Other examples of these autophagic defects in neurodegenerative disease, such as HD, are: mutant HTT (mHTT) aggregate-mediated recruitment of beclin-1 (BECN1) or mammalian target of rapamycin (mTOR) (regulators of autophagy) (Ravikumar, Vacher, Berger, *et al.*, 2004; Shibata, Lu, Furuya, *et al.*, 2006), and both an impaired acquisition of cargo (Vicente, Talloczy, Wong, *et al.*, 2010) and increased formation of 'empty' autophagosomes (Martinez-Vicente, Talloczy, Wong, *et al.*, 2010). This provides support for the assessment of markers for both autophagic machinery (LC3-II) as well as proteinaceous cargo such as huntingtin (indicated by the presence of the p62 protein) when assessing the autophagy pathway in a neurodegenerative disease context. This is especially crucial since p62 is inversely correlated with autophagic degradation (Agholme, Agnello, Agostinis, *et al.*, 2012).

With regards to selective autophagy, particularly the mitophagy pathway, both *PINK1* and *PARK2* are mutated in the autosomal recessive forms of PD (Kitada, Asakawa, Hattori, *et al.*, 1998; Valente, Abou-Sleiman, Caputo, *et al.*, 2004), thus emphasising the crucial functioning of these genes and proteins within the pathway. In line with this, Narendra *et al*. demonstrated that PINK1 and PARK2 specifically play a role in the detection of mitochondrial depolarisation and the subsequent recruitment of autophagy machinery for the activation of mitophagy (Narendra, Jin, Tanaka, *et al.*, 2010). The malfunctioning of this process has also been gaining traction recently in SCZ studies. Bernstein *et al*. hypothesise that an enhanced expression of two alleged mitophagy receptors in oligodendrocytes in SCZ could be an indication of disrupted mitophagy, thereby influencing white matter pathology of SCZ patients (Bernstein, Keilhoff, Dobrowolny, *et al.*, 2020). Additionally, as one would expect, a disruption in the homeostasis of the xenophagy signalling pathway could cause an inflammatory state which could disrupt cellular processes and potentially lead to disease (Zhong,

Kinio & Saleh, 2013). As such, mutations in NLR proteins, as is present in Crohn's disease (an inflammatory bowel disease known to be implicated in both the peripheral and CNS), have been shown to result in an impairment of autophagy, catalysed by the inability of recruitment of ATG16L1 to the plasma membrane (Travassos, Carneiro, Ramjeet, *et al.*, 2010). Moreover, a study investigating the NLR protein subfamily NOD-like receptor pyrin containing 3 (NLRP3) identified an immune-activation by means of the NLR signalling pathway in the post-mortem prefrontal cortex of individuals with bipolar disorder and SCZ respectively (Kim, Andreazza, Elmi, *et al.*, 2016).

The precise impact of the deviation of autophagy activity from basal levels during disease progression remains to be elucidated (Lumkwana, du Toit, Kinnear, *et al.*, 2017). Recently, advances have been made regarding autophagy modulation by use of pharmacological agents (Berger, Ravikumar, Menzies, *et al.*, 2006; Hebron, Lonskaya & Moussa, 2013; Ravikumar, Duden & Rubinsztein, 2002; Ravikumar *et al.*, 2004; Rose, Menzies, Renna, *et al.*, 2010) or psychotherapy (Alirezaei, Kemball, Flynn, *et al.*, 2010; Kuma, Hatano, Matsui, *et al.*, 2004; Mizushima, Yamamoto, Matsui, *et al.*, 2004; Scott, Schuldiner & Neufeld, 2004) both *in vitro* and *in vivo.* However, there is limited research considering an effective implementation of autophagy regulation (Loos *et al.*, 2014).

1.7. Genetic regulatory components of the autophagic pathway in CNS disorders

Gene transcriptional regulation is hypothesised to be one of the key players in the pathogenesis of neurodegenerative diseases and neuropsychiatric disorders. (Bar-Yosef *et al.*, 2019). Remarkably, studies have elucidated that the innate autophagic impairment characteristic of both neurodegenerative diseases and neuropsychiatric disorders has a genetic foundation whereby differential expression in principal autophagy genes is evident (Bar-Yosef *et al.*, 2019; Narayan, Tang, Head, *et al.*, 2008; Schneider *et al.*, 2017). This genetic regulation has been reviewed extensively in Levine & Kroemer (2008). Moreover, because most CNS disorders are complex and are thus influenced by genes and their interaction with the environment, distinctions in the nature of disease could be due to mutations or epigenetic mechanisms present. Thus, further research is warranted into exact genetic mechanisms governing the impaired autophagy pathway in these disorders.

1.8. Autophagy and ATR

A noteworthy study, which screened 480 bioactive small molecules for potential autophagy-inducing proficiency, discovered that three of the eight most effective compounds were indeed the Food and Drug Administration (FDA) -approved antipsychotic drugs trifluoperazine, fluspirilene, and pimozide (Zhang, Yu, Pan, *et al.*, 2007). In fact, studies have demonstrated that antipsychotics transcriptionally and post-transcriptionally regulate autophagy (Feng, Yao & Klionsky, 2015; Vucicevic, Misirkic-Marjanovic, Paunovic, *et al.*, 2014). For instance, Vucicevic *et al.* (2014) demonstrated that the SGA olanzapine induced autophagy

in human SH-SY5Y neuronal cells. This was evident by the increase in both autophagic machinery and expression of key autophagy-related genes *ATG4B*, *ATG5* and *ATG7*. This upregulation of autophagy was shown to be due to an increased production of reactive oxygen species. In this same study, the treatment of olanzapine for 14 days in mice caused an increase in autophagosome-associated LC3B-II and mRNA encoding *ATG4B*, *ATG5*, *ATG7*, *ATG12*, *GABARAP* and *BECN1* in the brain. Antipsychotic medications are not the only FDA-approved drugs which have been gaining increasing attention considering repurposing potential for autophagic manipulation. For instance, two drugs historically used in the treatment of diabetes (De Santi, Baldelli, Diotallevi, *et al.*, 2019) and heart disease (Park, Jeong, Lee, *et al.*, 2016) respectively (namely metformin and resveratrol), have been identified as effective autophagy enhancers. This emphasises the potential of repurposing FDA-approved drugs, with a specific focus on those that historically have been utilised to treat neurodegenerative diseases. Since these drugs would be effective in the clearance of toxic protein aggregates, they might serve as a basis when investigating therapeutic strategies targeting the impaired autophagy mechanism is SCZ.

Considering the mitophagy pathway, the atypical antipsychotic drug olanzapine has been shown to cause mitochondrial damage and a subsequent enhanced level of mitophagy in serotonergic neurons (Vucicevic *et al.*, 2014). Additionally, considering literature on treatment response and the xenophagy pathway, whilst there are limited studies investigating the effects of NLR signalling on treatment response, there are myriad studies investigating toll-like receptor (TLR) signalling and ATR, specifically in SCZ patients (Balaji, Subbanna, Shivakumar, *et al.*, 2020; García-Bueno, Gassó, MacDowell, *et al.*, 2016; Kéri, Szabó & Kelemen, 2017; Mantere, Trontti, García-González, *et al.*, 2019). TLRs are very similar to NLRs in that they are both main forms of innate immune receptors and provide front-line response to pathogenic invasion or tissue damage, and signalling is involved in the pathogenesis of chronic and/or idiopathic inflammatory disorders (Fukata, Vamadevan & Abreu, 2009). The studies investigating TLR signalling and ATR demonstrate contradictory evidence regarding the effect of antipsychotics on the expression levels of TLRs. Namely, Balaji and colleagues reported an alteration in *TLR4* gene expression in drug-naïve SCZ patients, and showed that antipsychotic medication does not have any effect on this expression (Balaji *et al.*, 2020). Whilst the specific findings of TLR4 gene expression alteration in SCZ patients is in line with the findings from García-Bueno *et al.* (2016), García-Bueno and colleagues identified that this alteration was dependent on the patients' exposure to antipsychotic medication. Specifically, they demonstrated that antipsychotic-treated SCZ patients exhibited a higher expression of *TLR4* genes in comparison to controls, and this is further supported by a study by Mantere *et al.* (2019). Contradicting these results, a study by Kéri *et al*. (2017) demonstrated that antipsychotic medication stabilises the expression of an otherwise overly expressed TLR4 receptor in SCZ patients. Additionally, they suggested that the TLR pathway might play an important role in the pathophysiology of SCZ, where an increase in certain subtypes of TLRs are linked to cognitive deficits.

Hence, these findings emphasise the need for future studies to focus on investigating the relationship between ATR and the various autophagy signalling pathways.

1.9. Systems genetics approach

Contemporary pharmacogenetic and pharmacogenomic research has consistently proved that transdisciplinary, systems genetics approaches allow for the integration of ideas from distinct fields, ultimately leading to a more enhanced understanding of the research question and a better facilitation of the progress of translational research (Ciesielski, Aldrich, Marsit, *et al.*, 2016). This is especially helpful when dealing with complex disorders and complex traits, where the complexity is constituted by both environment and genetics playing a role in the manifestation of the disorder or trait. Further, results of recent meta-analyses focusing on treatment of SCZ highlight the need for the development of new treatment strategies (Galling, Roldán, Hagi, *et al.*, 2017; Gregory, Mallikarjun & Upthegrove, 2017; Samara, Dold, Gianatsi, *et al.*, 2016; Siskind, Siskind & Kisely, 2017). To this extent, there is a particular need for research to focus on pathways other than the dopaminergic blockade (Haddad & Correll, 2018). Thus, a focus on the dysfunction of the autophagy pathway is a promising candidate in this regard and represents a unique outlook on the therapeutic strategy for treatment of ADRs and the amelioration of SCZ symptoms.

There is undoubtedly an intricate overlap when considering neurodegenerative diseases, neuropsychiatric disorders, and neurodevelopmental disorders in terms of both pathophysiology and the governing genetic factors involved. Additionally, this overlap extends to the autophagy malfunction present, as well as the antipsychotic treatment of these disorders. This complex overlap is illustrated in Figure 1.3.

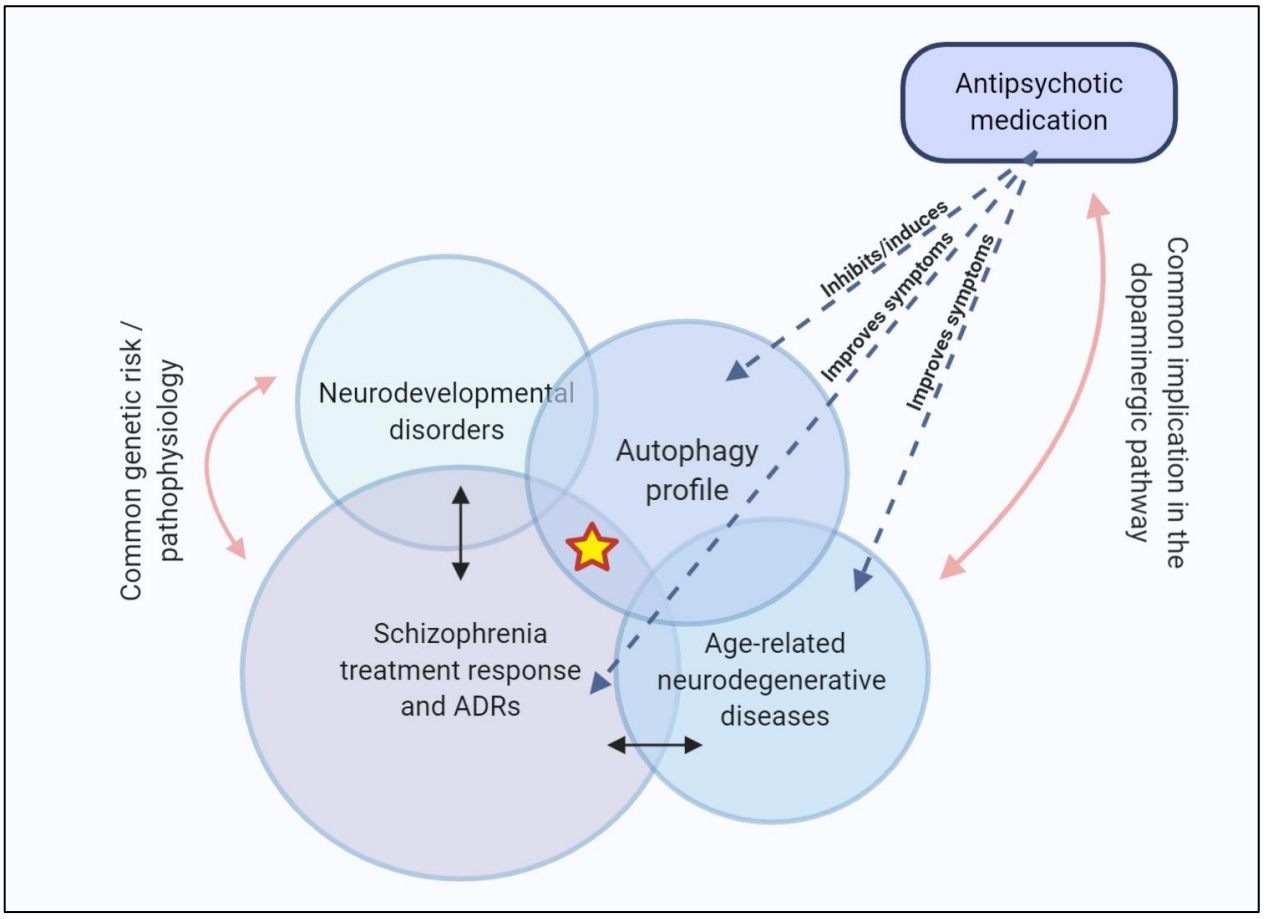

Figure 1.3. Overlap evident between neurodevelopmental disorders, antipsychotic treatment response and neurodegenerative diseases suggests autophagy plays a role in antipsychotic treatment response and adverse drug reactions of schizophrenia

Overlap between autophagy profile and neurodevelopmental and neurodegenerative diseases, as well as the overlap between these and antipsychotic treatment response in schizophrenia. Also illustrated is the interplay of antipsychotic medication on these different diseases and traits. Based on these overlapping elements, it is entirely plausible to presume that the autophagy mechanism is also highly implicated in the symptoms and adverse effects associated with schizophrenia and its treatment. Double-headed arrows indicate the overlap present between different traits/diseases. A singular arrow indicates the relationship present between the different elements. The star indicates where all elements converge (autophagy profile of individuals). ADRs: adverse drug reactions.

1.10. A new *in vitro* model to investigate autophagy

The past two decades have seen a substantial increase in the understanding of the physiological mechanisms of autophagy in a mammalian context (Bar-Yosef *et al.*, 2019; Levine & Kroemer, 2008; Lumkwana *et al.*, 2017; Nakamura & Yoshimori, 2018). An organism's maladaptation to stress due to autophagy dysregulation, as well as autophagy's crucial role in drug metabolism, are two reasons why autophagy ought to be the focal point of contemporary neuropsychiatric disorder research. Although to date neurodegenerative diseases and other inflammatory disorders are at the forefront of autophagy research (Puyal, Ginet, Grishchuk, *et al.*, 2012; Wei, Wang, Mchugh, *et al.*, 2012; Wong & Cuervo, 2010), recent years have seen an emerging role of autophagy impairment in neuropsychiatric disorders (Jia & Le, 2015; Kara, Toker, Agam, *et al.*, 2013; Yuan,

Wang, Wei, *et al.*, 2015). Further, studies have supported this role with investigations into autophagy mechanisms using various *in vitro* and *in vivo* models.

An abundance of different models exists to study autophagy, though the relevance of a model relies entirely on the investigative question at hand. A model that has only in the last decade gained traction in neuronal cell-based studies is the induced neuronal cell model (Vierbuchen, Ostermeier, Pang, *et al.*, 2010). Through the direct conversion of patient-derived fibroblasts, these induced neurons (iNs) can completely skip the intermediate pluripotent stage, in contrast to induced pluripotent stem cells. Mertens *et al*. illustrated that these iNs exhibit age-dependent regulation of genes associated with aging, thus emphasising the relevance of this model in the study of age-related diseases (Mertens, Paquola, Ku, *et al.*, 2015). Moreover, Huh and colleagues demonstrated that iNs retain age-related epigenetic signatures of the donor as well (Huh, Zhang, Victor, *et al.*, 2016). These iNs, generated through the forced expression of transcription factors, have been shown to exhibit neuronal-like morphology as well as functional aspects of neurons. Additionally, previous studies have demonstrated that action potentials can be evoked in these iNs, and have detected unprompted synaptic activity when these iNs are co-cultured with astrocytes or primary cortical neurons following transplantation (Drouin-Ouellet, Pircs, Barker, *et al.*, 2017). Hence, the iN model has proved itself to be an excellent system for the study of age-related diseases and would provide an ideal physiological background to characterise the autophagy mechanism in a diseased state.

The insight that could be gained from this *in vitro* model, together with the understanding of the genetic mechanisms governing autophagy in CNS diseases could pave the way for new therapeutic targets. This present study thus aimed to delve into the genetic and physiological mechanisms underlying autophagy pathway regulation in a neuropsychiatric disorder context to elucidate how this may inform on ATR. Further, this study aimed to develop an autophagy model using iNs in order to study the autophagy process in the future research of antipsychotic treatment response. To this end, this study utilised HD patient-derived fibroblasts to serve as a point of departure to modelling the autophagy profile in SCZ in future studies.

1.11. Overview of current study

1.11.1. Aim and objectives

This study aims to investigate the extent to which characterising autophagy dysregulation mechanisms informs on differential treatment outcomes in a South African (SA) first episode schizophrenia (FES) cohort.

This will be achieved through the following objectives:

1. Perform a literature search identifying genes shown to influence autophagy, and which have previously been implicated in either neuropsychiatric disorders, neurodegenerative diseases, or inflammatory disorders.
2. Prioritise genes using a gene-set enrichment analysis, selecting candidate genes based on significant enrichment across various relevant gene-set enrichment libraries.
3. Identify variants within these candidate genes that have a functional or regulatory impact on the autophagy mechanism using publicly available bioinformatic tools and databases.
4. Using a pathway-based approach, categorise the genes and their corresponding variants according to significantly enriched pathways using an appropriate gene-set enrichment library.
5. Perform independent association analyses on the prioritised variants within their respective pathways to see whether the prioritised variants inform on ATR in an SA FES cohort.
6. Recapitulate autophagy mechanism using a directly converted induced neuronal (iN) cell model from Huntington's disease (HD) patient-derived fibroblasts, treat the iNs pharmacologically using an autophagy enhancing drug, and assess the functional response of a neuronal-like cell to the drug to gauge the extent to which the HD mutation profile translates to autophagy dysfunction.

1.11.2. Role of incumbent

Clinical interviews, data collection, sampling and human DNA extractions were performed by trained clinicians and a laboratory technician. Genotyping was performed prior to this study by the Department of Psychiatry, Zucker Hillside Hospital, New York, USA. The role of the incumbent of this study was therefore to analyse the genetic data obtained using a bioinformatic pipeline for the purpose of identifying candidate genes and variants for this study. The incumbent performed the *in-silico* and association analyses sections of this study at Stellenbosch University, South Africa under the supervision of Dr Nathaniel McGregor, and co-supervision by Prof. Louise Warnich and Prof. Ben Loos (Section 2.5 and 2.6). Additionally, as a part of an exchange student programme, the incumbent carried out the *in vitro* model section of research (Section 2.7) at Lund University, Sweden, under the supervision of Prof. Johan Jakobsson and Dr Karolina Pircs. The lentiviral vector transfection was performed by a trained laboratory technician. The incumbent performed all cell-culture work, as well as all immunocytochemistry and statistical analyses.

1.12. Strategy

The proposed strategy for the current study is illustrated in the figure below. (Figure 1.4.)

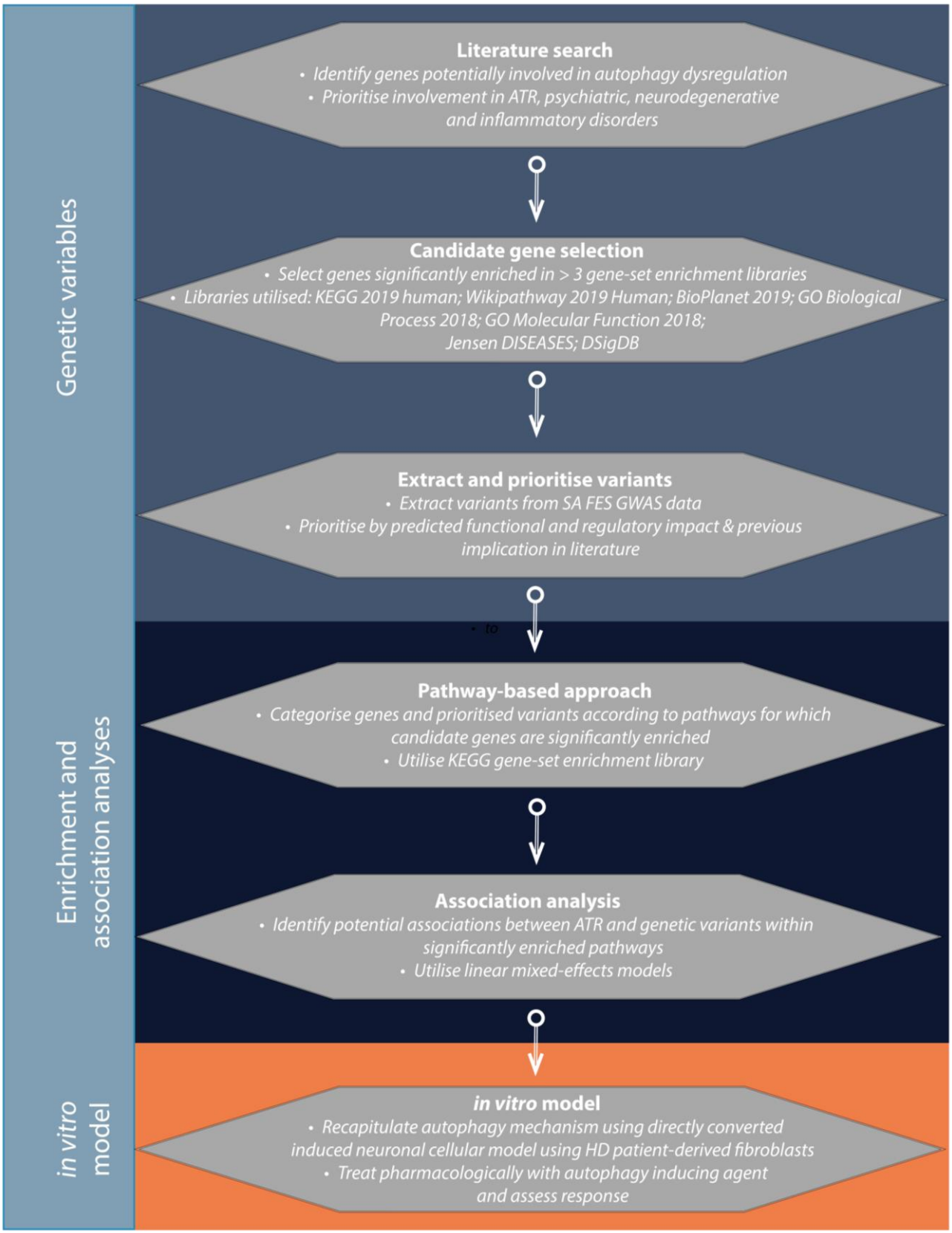

Figure 1.4. Proposed strategy of current study.
ATR: antipsychotic treatment response; SA: South African; FES: first-episode schizophrenia; GWAS: genome-wide association study; HD: Huntington's disease.

CHAPTER 2. METHODS AND MATERIALS

For accession dates to electronic sources, please refer to Supplementary table 3.

2.1. Patient cohort

Written and informed consent was imparted by all subjects (and their guardians where applicable) preceding this study and ethical clearance was obtained from the Committee for Human Research, Faculty of Health Sciences, Stellenbosch University in SA (N06/08/148). The cohort, as described previously by Chiliza, Asmal, Kilian, *et al.* (2015) and Drögemöller, Niehaus, Chiliza, *et al.* (2014), comprised 103 unrelated individuals aged between 16 and 45 years (+/- 7 years). The subjects were included in this study based on the condition that they received a Diagnostic and Statistical Manual of Mental Diseases, Fourth Edition (DSM-IV; (Bell, 1994)) diagnosis of schizophreniform, SCZ or schizoaffective disorder. Additionally, inclusion criteria encompassed the patients being drug naïve, having only been exposed to a maximum of 4 weeks of antipsychotic medication during their lifetime. Of the included subjects, 76 were male and 27 were female. Ethnicity of the subjects were as follows: 13 individuals of African descent, 82 individuals of South African Mixed Ancestry and eight individuals of European descent. Exclusion criteria were: current substance abuse, history of long-acting injectable antipsychotic treatment and significant physical illness or mental retardation.

2.2. Clinical assessments

Initially, patients were diagnosed by psychiatrists using the Structural Clinical Interview for DSM-IV (SCID, (Bell, 1994)). Treatment response was assessed according to symptom severity using the Positive and Negative Syndrome Scale (PANSS; (Kay, Opler & Lindenmayer, 1989)) as well as the Clinical Global Impressions (CGI) Scale (Busner & Targum, 2007). Patients' symptoms were assessed prior to receiving treatment, and then subsequently every two weeks for the initial six weeks, followed by every three months thereafter over a 12-month period. In order to minimise assessment bias, the psychiatrists underwent inter-rater reliability testing preceding this study, as described in Drögemöller *et al.*, 2014.

2.3. Treatment and clinical outcomes

All patients were treated with the FGA flupenthixol decanoate (Fluanxol®, Lundbeck, Copenhagen, Denmark) administered in the form of a long-acting injectable, which assists in adherence (Chiliza *et al.*, 2015). A preliminary wash-out period of 7 days comprised of a 1-3 mg/day dosage of flupenthixol decanoate administered orally. This was followed by injections of a 10 mg dosage every two weeks, with increments of 10 mg permitted every six weeks, to a maximum of 30 mg fortnightly (Chiliza *et al.*, 2015). No other antipsychotics, mood stabilisers or psychostimulants were taken in conjunction with flupenthixol decanoate – although when needed, other psychotropic medications such as benzodiazepines, antidepressants or anticholinergics were used in parallel. Patients were administered the lowest possible dose of antipsychotic

and would only be eligible for a dosage increase if they showed insufficient response over an extended period (i.e. less than 20% reduction in the PANSS total score, and minimal improvement on the CGI Scale). This was sustained until the patient went into remission (defined by (Andreasen, Carpenter, Kane, *et al.*, 2005)), or the maximum permitted dose was reached (Chiliza *et al.*, 2015). Early responders were considered as those who displayed a ≥ 25% reduction in PANSS total scores within the first six weeks (Emsley, Chiliza, Asmal, *et al.*, 2011; Emsley, Rabinowitz, Medori, *et al.*, 2007). This amounted to 77 of the patients (74.8%). At the end of the 12-month period, 58 patients (56.3%) of patients were in full remission according to the Remission in Schizophrenia Working Group criteria (Andreasen *et al.*, 2005). Non-responders were defined as those who either discontinued treatment due to poor response, had a < 25% reduction in PANSS total scores at end-point, or had a PANSS total score of > 70 at the end of the 12-month period (Chiliza *et al.*, 2015). In contrast, nine patients (8.7%) did not respond to treatment and were considered treatment refractory. An example of how a patient's PANSS score changes over time can be found in Emsley, Chiliza, Asmal, *et al.* (2017).

2.4. DNA extraction and genotyping

DNA samples as well as genome-wide genotype data were available for all individuals of the cohort prior to the commencement of this study. Using a protocol designed by Miller and colleagues (Miller, Dykes & Polesky, 1988), DNA was extracted from patient whole blood samples and subsequently genotyped using the Illumina Infinium OmniExpressExome-8 Kit (Illumina, California, USA), for roughly 1 million single nucleotide polymorphisms (SNPs) (O'Connell, McGregor, Malhotra, *et al.*, 2019). Additionally, due to the diverse ancestry of the SA cohort, Ancestry Informative Markers (AIMs) (Daya, van der Merwe, Galal, *et al.*, 2013), which are markers previously designed for this specific cohort, were included in the genotyping of this cohort for the purpose of correcting population stratification. All 103 patients were genotyped for 96 AIMs, and for each individual, ancestry proportion was estimated in ADMIXTURE (Alexander, Novembre & Lange, 2009; Drögemöller, Emsley, Chiliza, *et al.*, 2016) for the five base population groups (African San, African non-San, European, South and East Asian).

2.5. Genetic variables

Candidate gene selection, variant prioritisation, enrichment analysis and variant descriptive statistics were performed according to the pipeline depicted in Figure 2.1.

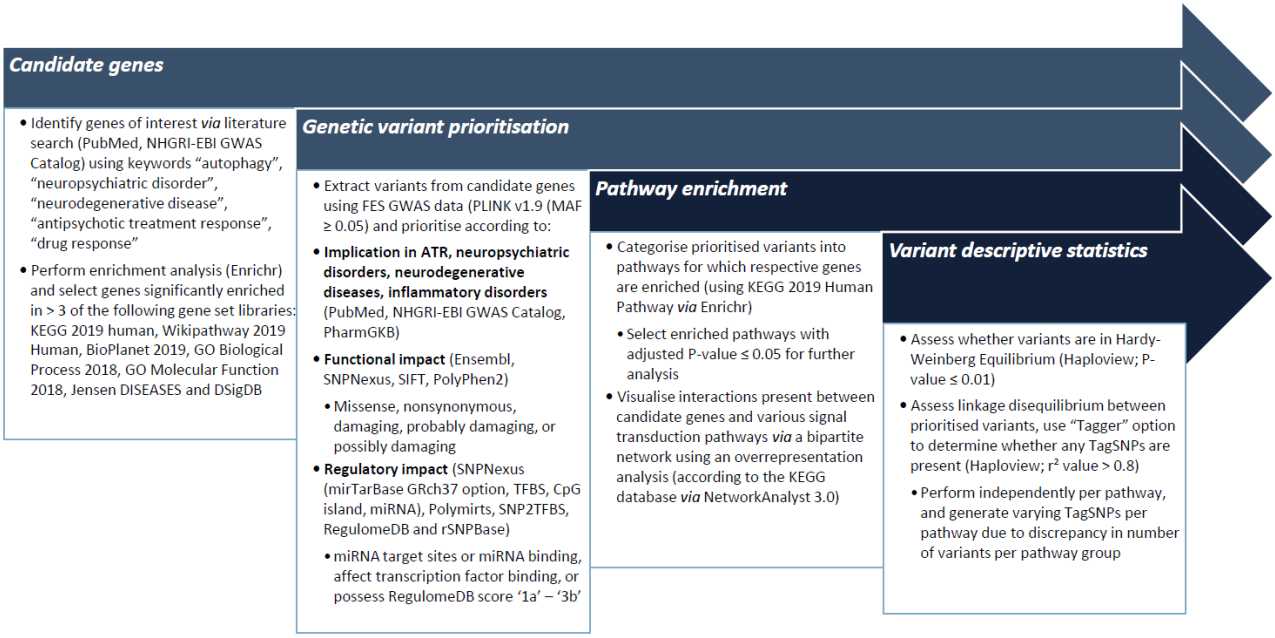

Figure 2.1. Bioinformatic pipeline followed for candidate gene selection, variant prioritisation, pathway enrichment and variant descriptive statistics

FES: First episode schizophrenia; GWAS: Genome wide association study; MAF: Minor allele frequency; ATR: Antipsychotic treatment response. Tools utilised are available at the following webpages: Pubmed (https://www.ncbi.nlm.nih.gov/pubmed/); National Human Genome Research Institute (NHGRI-EBI) genome-wide association study (GWAS) Catalog (https://www.ebi.ac.uk/gwas/); Enrichr (available at https://amp.pharm.mssm.edu/Enrichr/); PharmGKB (https://www.pharmgkb.org/); Ensembl (https://www.-ensembl.org/index.html); SNPNexus (https://www.snpnexus.org/v4/), SIFT (https://sift.bii.a-star.edu.sg/), PolyPhen2 (http://genetics.bwh.harvard.edu/pph2/), Polymirts (http://compbio.uthsc.edu/miRSNP/home-.php), SNP2TFBS (https://ccg.epfl.ch//snp2tfbs/) RegulomeDB (https://regulomedb.org/regulomesearch) and rSNPBase (http://rsnp.psych.ac.cn/); Network Analyst 3.0 (www.networkanalyst.ca).

2.5.1. Candidate genes

In order to find genes of interest, a literature search was performed using PubMed (https://www.ncbi-.nlm.nih.gov/pubmed/) as well as National Human Genome Research Institute (NHGRI-EBI) genome-wide association study (GWAS) Catalog (https://www.ebi.ac.uk/gwas/) (MacArthur, Bowler, Cerezo, *et al.*, 2017) using the keywords "autophagy", "neuropsychiatric disorder", "neurodegenerative disease", "antipsychotic treatment response" and "drug response" (Figure 2.1).

Genes identified during the literature search were investigated *via* an enrichment analysis performed through Enrichr (available at https://amp.pharm.mssm.edu/Enrichr/). The following gene-set libraries were utilised: KEGG 2019 human; Wikipathway 2019 Human; BioPlanet 2019; GO Biological Process 2018; GO Molecular Function 2018; Jensen DISEASES and DSigDB. Candidate gene selection criteria was based on a gene being significantly enriched in more than three of the abovementioned gene-set libraries (Figure 2.1).

2.5.2. Genetic variant prioritisation

Variants within the candidate genes were extracted from the SA FES GWAS data using PLINK v1.9 (Purcell, Neale, Todd-Brown, *et al.*, 2007). A common disease-common variant (CD-CV) approach was used (as is custom for complex traits such as ATR), and thus only variants with a minor allele frequency (MAF) ≥ 0.05 were included for further investigation. This allowed for the exclusion of any rare variants. Additionally, so as not to exclude any non-coding variation within the candidate genes, variants situated 1000 bp up- and downstream were also extracted (Figure 2.1).

Variants were prioritised according to previous implication in ATR (Bomba, Walter & Soranzo, 2017), neuropsychiatric disorders and neurodegenerative diseases, and their role in inflammatory disorders were also taken into account (Figure 2.1). This was based on a literature search using PubMed (https://www.ncbi.nlm.nih.gov/pubmed/) and NHGRI-EBI GWAS Catalog (MacArthur *et al.*, 2017), as well as the curated database PharmGKB (https://www.pharmgkb.org/) (Whirl-Carrillo, McDonagh, Hebert, *et al.*, 2012), which informs on genetic variation associations with drug response. Considering PharmGKB, variants were prioritised if they were identified to influence antipsychotic efficacy, toxicity, or response, according to the variant and clinical annotations stipulated in the database. However, there was a complete absence of documentation of the variants within the PharmGKB database. Hence, variants possessing similar dbSNPIDs identified to be associated with drug response as per the PharmGKB database were recorded for further investigation. This allowed for the investigation of any potential linkage disequilibrium (LD) between the variants in the process of being prioritised and the variants with similar dbSNPIDs.

Variants were prioritised based on their functional and regulatory impact according to various publicly available bioinformatic databases (Figure 2.1). More specifically, Ensembl (https://www.ensembl.org-/index.html) (Yates, Achuthan, Akanni, *et al.*, 2020), SNPNexus (https://www.snp-nexus.org/v4/) (SIFT and PolyPhen options; (Chelala, Khan & Lemoine, 2009)), SIFT (https://sift.bii.a-star.edu.sg/) (Sim, Kumar, Hu, *et al.*, 2012), PolyPhen2 (http://genetics.bwh.harvard.edu/pph2/) (Adzhubei, Jordan & Sunyaev, in press) were used in order to assess the functional consequences of variants. Considering these databases, variants were prioritised if they were identified to be missense, nonsynonymous, damaging, probably damaging, or possibly damaging. With regards to assessing the regulatory impact of variants, SNPNexus (https://www.snp-nexus.org/v4/) (mirTarBase GRch37 option, TFBS, CpG island, miRNA; (Chelala *et al.*, 2009)), Polymirts (http://compbio.uthsc.edu/miRSNP/home.php) (Bhattacharya, Ziebarth & Cui, 2014), SNP2TFBS (https://ccg.epfl.ch//snp2tfbs/) (Kumar, Ambrosini & Bucher, 2017), RegulomeDB (https://regulomedb.org-/regulome-search) (Boyle, Hong, Hariharan, *et al.*, 2012) and rSNPBase (http://rsnp.psych.ac.cn/) (Guo, Du, Chang, *et al.*, 2014) were used. Variants were prioritised if they were identified to have a potential impact on miRNA target sites (SNPNexus) or miRNA binding (Polymirts). Additionally, variants were included if they were predicted to affect transcription factor binding assessed *via* SNPNexus (TFBS option) and SNP2TFBS. Considering the RegulomeDB database, variants scoring from '1a' – '3b' were prioritised for further analysis

(scores defined in Supplementary table 1). Due to the majority of variants being predicted to be regulatory according to rSNPBase, this database was not used as a criterium for prioritisation, however information from rSNPBase was still recorded for variant annotation purposes.

2.6. Enrichment and association analyses

2.6.1. Pathway-enrichment

Prioritised variants were categorised into pathways for which their respective genes were enriched (Figure 2.1). These pathways were selected according to the gene-set library KEGG 2019 Human Pathway (Kanehisa & Goto, 2000) (Enrichr, https://academic.oup.com/nar/article/44/W1/W90/2499357). This gene-set library is a collection of pathway maps that represent knowledge on molecular interaction, reaction and relation networks for metabolism, genetic information processing, environmental information processing, cellular processes, organismal systems, human diseases and drug development pathways (Kanehisa & Goto, 2000).

In order to compute enrichment and the significance thereof, two tests are performed by Enrichr. Firstly, the Fisher's exact test (Fisher, 1992) is computed, which is a proportion test that assumes a binomial distribution and independence for probability of any gene belonging to any set. Secondly, a correction to the Fisher's exact test is computed to determine the adjusted P-value, and this was used to select for the most enriched pathways (Chen, Tan, Kou, *et al.*, 2013). Enriched pathways with an adjusted P-value ≤ 0.05 were chosen for further analysis.

The bioinformatic tool NetworkAnalyst 3.0 (Xia, Benner & Hancock, 2014; Xia, Gill & Hancock, 2015; Zhou, Soufan, Ewald, *et al.*, 2019; available at www.networkanalyst.ca), which provides network visual analytics for gene expression profiling, was employed to visualise the output from the enrichment analysis (Figure 2.1). Specifically, the interactions present between the candidate genes and various signal transduction pathways were visualised in a bipartite network using an overrepresentation analysis (ORA) according to the KEGG database (Kanehisa & Goto, 2000). ORA is a statistical technique that allows for the identification of gene sets or pathways that have a significant overlap with the selected genes of interest. Hypergeometric tests are utilised to compute P-values. Enriched gene sets are displayed in network form, where gene sets possessing overlapping genes are connected by edges. This enables for the grouping of functionally similar genes. Additionally, the nodes by which gene sets are depicted are colour-coded according to their enrichment score (P-value). Further, the size of the node is directly related to the number of genes from the gene set that are on the analysed gene list. For the purpose of gaining a broader outlook on the interactions present, *BECN1,* a key autophagy gene, was included in the list of input genes. Thus, the input genes for the gene-set enrichment analysis and network visualisation were *ATG3*, *ATG7*, *ATG12*, *ATG13*, *ATG14*, *ATG16L1*, *BECN1, GABARAP* and *PINK1*.

2.6.2. Variant descriptive statistics

In order to assess whether the prioritised variants were in Hardy-Weinberg Equilibrium (HWE), Haploview (Barrett, Fry, Maller, *et al.*, 2005) was used (significance threshold of P-value ≤ 0.01 (Wigginton, Cutler & Abecasis, 2005)). Haploview was used to calculate genotype frequencies (Figure 2.1).

The SNPStats web-tool (https://www.snpstats.net/start.htm) (Solé, Guinó, Valls, *et al.*, 2006) was used to perform LD analysis between the variants returned during the PharmGKB (Whirl-Carrillo *et al.*, 2012) searches (with similar dbSNPIDs to the variants in question) and the variants selected for prioritisation. The variants identified through PharmGKB were extracted from the SA FES GWAS data for an unbiased analysis. The analysis, however, yielded no conclusive results (no linkage was identified between the prioritised SNPs and those that were identified through PharmGKB), thus these variants were excluded from further analyses.

Haploview (Barrett *et al.*, 2005) was then used to assess LD between the prioritised variants, and the "Tagger" option was used to determine whether there were any TagSNPs that were representative of other variants. This was based on the r^2 value, where a value above 0.8 was considered indicative of a strong LD (Carlson, Eberle, Rieder, *et al.*, 2004). This analysis was performed independently for each pathway, and varying TagSNPs were generated per pathway due to the discrepancy in the number of variants per pathway group.

2.6.3. Association analyses

Linear regression modelling for this study was performed using R (R Core Team, 2020) in R Studio (Rstudio, 2020). The packages used were lme4 (Bates, Mächler, Bolker, *et al.*, 2015) and lmerTest (Kuznetsova, Brockhoff & Christensen, 2017). Independent association analyses were performed per respective pathway, as outlined in Section 2.6.1.

In order to investigate the effect of genetic variants on change in log-transformed PANSS scores over the 12-month period for each subscale (Positive, Negative, General and Total), linear mixed-effects models were used. These models were adjusted for age, gender and proportion ancestry (using the AIMs described in Section 2.4 (Daya *et al.*, 2013)), as well as log-transformed baseline PANSS scores.

Specifically, PANSS scores for the four different domains (Positive, Negative, General and Total) were modelled as functions of the interaction between time of observation (PANSS score) and the genetic variant as fixed effects. Both the genotypic and additive allelic models of inheritance were investigated, and therefore genotypes as well as the number of minor alleles (0, 1 or 2) acted as the genetic predictors in the respective models. To account for multiple measures (PANSS scores) per individual over time, a random effect was included. Variants were excluded from the analysis if the cohort included less than five minor genotypes for that variant – this was to avoid failure of the regression model converging. In total, 6 pathway-categorised groups of variants were included for analyses, as well as an independent analysis that included all 39 variants. The Bonferroni-corrected threshold (depicted by α) was used to correct for multiple testing

(varying number of variants per pathway, two modes of inheritance and four PANSS domains result in varying α-thresholds for the respective pathways). Additionally, an uncorrected significance threshold of P-value ≤ 0.001 as well as a P-value ≤ 0.05 were considered for the observation of trends.

2.7. *In vitro* model

2.7.1. Ethical considerations

Adult dermal fibroblasts acquired through collaboration with Roger A. Barker (Parkinson's Disease Research and Huntington's disease clinics at the John van Geest Centre for Brain Repair in Cambridge, United Kingdom) were used under the following ethical approval: REC 09/H0311/88. Each participant provided written informed consent and all experiments conformed to the guidelines set out in the World Medical Association (WMA) Declaration of Helsinki and the Department of Health and Human Services Belmont Report.

2.7.2. Cell culture and cell lines

Twelve fibroblast cell lines were utilised in this study, namely six HD lines and six age- and sex-matched control lines (Table 2.1.). The fibroblasts were cultured at 37 °C in 5% CO_2 in a standard fibroblast medium (DMEM (Dulbecco's Modified Eagle Medium; Gibco™) + 10% fetal bovine serum (FBS) (Biosera) + a combination of streptomycin and penicillin (100 mg/mL); Sigma-Aldrich®). The cells were subsequently dissociated using 0.05% trypsin (ScienCell), spun, and plated onto 24-well cell culture plates (Nunc™) for further growth prior to conversion.

Table 2.1. Fibroblast cell line information of Huntington's disease patients and controls

	Line name	Age of biopsy	Sex	CAG repeat
Controls	CKP	54	F	15-20
	C2	67	F	N/A
	C7	75	F	18
	CKK	27	M	17
	TS	30	M	19-24
	CGE	61	M	17-23
HD patients	HD1	53	M	19-42
	HD596	31	M	20-45
	HD635	43	M	17-42
	HDKP	28	M	15-39
	HDRH	59	M	16-39
	HDSD	43	M	19-44

Length of CAG repeat is negatively correlated with age of disease onset, and is positively correlated with symptom severity (Lee, Correia, Loupe, *et al*., 2019; Tabrizi, Scahill, Owen, *et al*., 2013). F: female; M: male; N/A: not available.

2.7.3. Viral vectors and viral transduction

In this study DNA plasmids expressing mouse open-reading frames (ORFs) for a combination of *ASCL1* and *BRN2* with short hairpin ribonucleic acid (shRNA) targeting RE1 Silencing Transcription Factor (*REST*) were generated in a third-generation lentiviral vector (previously published by Drouin-Ouellet, Lau, Brattås, *et al.*, 2017). This vector contained a non-regulated ubiquitous phosphoglycerate kinase (PGK) promoter using the same method as previously described by Zufferey, Nagy, Mandel, *et al.*, 1997, and titrated by quantitative polymerase chain reaction (qPCR) analysis (Georgievska, Jakobsson, Persson, *et al.*, 2004). Presence of all constructs had been verified *via* sequencing. Transduction was performed at a multiplicity of infection (MOI) of 20 and virus titer was 1.06×10^9 for all viruses used in this study.

2.7.4. Direct neural reprogramming

For the conversion of HD and control human dermal fibroblasts to neurons, a reprogramming induction protocol was used, which has been outlined in great detail by Drouin-Ouellet *et al.* (2017). This study,

however, made use of a modified Drouin-Ouellet protocol. Briefly, fibroblasts were plated at a density of 50 000 cells per cm² in 24-well plates (Nunc™) that prior to plating had been coated with 1% Poly-L-ornithine (Sigma-Aldrich®) incubated at 37°C overnight followed by coating with 0.5% Laminin (Invitrogen™) for 2 – 3 hours and lastly coated with 1% Fibronectin (Thermo Fisher Scientific) incubated at 37°C overnight. All 12 lines (six HD lines and six control lines) were plated in triplicate. Fibroblasts were transduced one day subsequent to plating, and three days post-transduction the fibroblast growth medium was replaced by early neural differentiation medium (NDiff227; Takara-Clontech) supplemented with growth factors at the following concentrations: LM-22A4 (2 µM, R & D Systems), GDNF (2 ng/ml, R & D Systems), NT3 (10 ng/µl, R&D Systems) and db-cAMP (0.5 mM, Sigma-Aldrich®) and the small molecules CHIR99021 (2 µM, Axon), SB-431542 (10 µM, Axon), noggin (0.5 µg/ml, R & D Systems), LDN-193189 (0.5 µM, Axon), as well as valproic acid sodium salt (VPA; 1 mM, Merck Millipore). Every two to three days, half of the neuronal differentiation medium was replenished with fresh medium. On day 18 post-transduction, the early conversion medium was changed to late conversion medium consisting of only the growth factors (LM-22A4, GDNF, NT3, and db-cAMP) until completion of the experiment.

2.7.5. Pharmacological treatment

This study made use of a potent and selective adenosine triphosphate (ATP)-competitive inhibitor of mTOR, and thus an effective autophagy-inducing reagent, Torin1 (Sigma-Aldrich®). A literature search was performed to determine the most effective concentration and duration of Torin1 treatment on neuronal cells. As a biological control, the identified potential concentrations and durations of Torin1 treatment were tested on the fibroblasts growing in standard fibroblast growth medium on 24-well plates (Nunc™).

Mature iNs were treated on Day 28 of the protocol with 250 nM of Torin1 and 250 nM of DMSO (dimethyl sulfoxide, a standard solvent and hence control used in cell culture models, Sigma-Aldrich®) for 2 hours, as this was identified to be the most suitable concentration and duration of treatment.

2.7.6. Immunocytochemistry

2.7.6.1. Torin1 treatment of fibroblasts

Cells were fixed in 4% paraformaldehyde for 10 - 15 minutes and then were washed with Dulbecco's Phosphate Buffered Saline (DPBS; Sigma-Aldrich®) twice. They were then permeabilised with 0.1% Triton X-100 in 0.1 M DPBS solution for 10 minutes. Cells were then blocked in 5% serum in 0.1 M DPBS for 30 minutes. Thereafter, cells were treated with the following primary antibodies diluted in blocking solution and left overnight: anti-rabbit LC3 (1:500) (Sigma-Aldrich® L7543) and anti-mouse p62 (1:500) (Abcam 56416). Subsequent to washing cells twice with DPBS buffer, the cells were treated with secondary antibodies diluted in blocking solution (1:200) and applied for 2 hours protected from light. Cells were then washed with DPBS and then counterstained with DAPI (4',6-diamidino-2-phenylindole) for 15 minutes. Inverted fluorescent

microscopy was used to determine the effectivity of the DAPI staining, as well as capture the presence of LC3 and p62 and following this the cells were washed twice with DPBS. Finally, cells were covered in 1 ml of DPBS.

2.7.6.2. Torin1 treatment of induced neurons

This process was repeated with the iNs. However, the primary antibodies used in this case were: anti-chicken MAP2 (microtubule-associated protein 2) (1:5000) (Abcam 5392), and anti-rabbit LC3 (1:500) (Sigma-Aldrich® L7543).

Quantification of the total number of DAPI+ and MAP2+ cells per well was performed using high-content screening (HCS) analysis using the Cellomics Array Scan (Array Scan VTI, Thermo Fisher Scientific). This is an automated process that ensures unbiased measurements between groups. The program "Target Activation" was used to obtain 100 fields of view (10× magnification) in a spiral fashion starting from the midpoint. The program "Neuronal Profiling" was used to determine the number of neurites per DAPI+ cells. The number of MAP2+ cells over the total number of DAPI+ cells in the well post-experiment was considered the neuronal purity. The number of MAP2+ cell over the total number of fibroblasts plated for reprogramming was considered the conversion efficiency. The program "Neuronal Profiling" (20x magnification) was utilised to detect cell body total area, neurite total count, neurite total length, area, and width of the cells. Further, LC3 detection was utilised to determine cell body spot total count, cell body spot total area, and neurite spot total and average count and area. This mode of detection was chosen to assess the total abundance of autophagosomes per cell, reflecting the autophagosome pool.

2.7.7. Statistical analysis

Average cell numbers per wells (as presented in Figure 3.2. D) were detected by HCS analysis based on DAPI+ nuclei. Average purity (as presented in Figure 3.2. E) was defined by measuring the number of MAP2+ cells in a well by HCS analysis.

MAP2 purity % was defined for each line using the following formula:

$$Purity = \frac{\text{number of scanned MAP2} + \text{ cells/well}}{\text{number of DAPI} + \text{cells/well}} \; x \; 100$$

Conversion efficiency (as presented in Figure 3.2. F) was defined using the following formula:

$$Efficiency = \frac{\text{number of MAP2} + \text{cells in the entire well}}{\text{number of plated cells}} \; x \; 100$$

Number of plated cells per well in a 24-well plate was 50 000 cells.

In Figure 3.2. G - K, total cell body area, neurite area, count, length, and width per cell were defined by HCS analysis. Average control values from 3 different healthy control iNs were normalised to 1, whereby values generated in treated cell lines were divided by the average of these control values.

All data are expressed as mean ± the standard error of the mean. Biological replicates (n = 3) were used for each cell line during analysis and three - three technical replicates were used for each line for each condition. An unpaired unequal Student's t-test was used in Figure 3.2. D - K to test differences between groups. Additionally, to compare treated versus non-treated data values, a paired t-test was utilised in Figure 3.3. I - L. Statistical analyses were conducted using the software GraphPad Prism version 8.3.0 (www.graphpad-.com). An α level of P-value < 0.05 was set for significance.

CHAPTER 3. RESULTS

3.1. Genetic variables

3.1.1. Candidate genes

Forty-six candidate genes were identified *via* a literature search using the terms stipulated in Section 2.5.1. These genes are presented in Supplementary table 2. Gene-set enrichment analysis was subsequently performed on these 46 genes using Enrichr. The following gene-set libraries were selected for enrichment analysis:

1. KEGG 2019 human
2. Wikipathway 2019 Human
3. BioPlanet 2019
4. GO Biological Process 2018
5. GO Molecular Function 2018
6. Jensen DISEASES
7. DSigDB

The top 10 most significantly enriched genes per library were documented. Of these, genes significantly enriched in more than 3 of these libraries were prioritised for inclusion as candidate genes in this study (10 genes in total, illustrated in Table 3.1.).

Table 3.1. Genes prioritised for inclusion in this study and their incidence in relevant gene-set enrichment libraries

Gene	Gene-set library for which gene is enriched[1]							Genomic location[2]
	BioPlanet 2019	DSigDB	GO Biological Process 2018	GO Molecular Function 2018	Jensen DISEASES	KEGG 2019 human	Wikipathway 2019 Human	
AMBRA1	✓	✗	✓	✓	✓	✓	✓	46417962..46615619
ATG3	✓	✓	✓	✗	✗	✓	✓	112251354..112280810
ATG7	✓	✓	✗	✗	✗	✗	✓	11314010..11599139
ATG12	✓	✓	✓	✗	✗	✓	✓	115163893..115177548
ATG13	✓	✗	✓	✗	✗	✓	✓	46638826..46697569
ATG14	✗	✗	✓	✓	✓	✓	✓	55833109..55878576
ATG16L1	✓	✗	✗	✓	✗	✓	✓	234160217..234204320
BECN1	✓	✓	✓	✓	✗	✓	✓	40962150..40976310
GABARAP	✓	✗	✓	✓	✗	✓	✓	7143738..7145753
PINK1	✗	✓	✓	✓	✓	✗	✗	20959948..20978004

[1]Accessed *via* Enrichr, available at https://amp.pharm.mssm.edu/Enrichr/, accessed June 2020; [2]According to GRCh37.p13 (Human Genome Assembly version 37); ✓ Indicates gene is significantly enriched in gene-set enrichment library; ✗ Indicates gene not significantly enriched in gene-set enrichment library

3.1.2. Genetic variant prioritisation

Two hundred and nineteen variants (SNPs) were extracted from the SA FES GWAS data for the 10 candidate genes. After applying a cut-off threshold of MAF ≥ 0.05, 101 variants remained.

The remaining variants were investigated with regards to their functional and regulatory impact (Supplementary table 4 and Supplementary table 5), as well as any previously reported associations with neuropsychiatric disorders, neurodegenerative diseases, inflammatory disorders and treatment response (Supplementary table 6). If deemed to have considerable regulatory or functional influence, or previously reported to be associated with any of the abovementioned factors, the variants were prioritised for inclusion for further analyses. For instance, the rs1042434 variant within *PINK1* was prioritised owing to its functional impact, as it was predicted to be a missense variant according to Ensembl (Yates *et al.*, 2020), SNPNexus (using the SIFT and Polyphen options; (Chelala *et al.*, 2009)), SIFT (Sim *et al.*, 2012) and Polyphen-2 (Adzhubei, Schmidt, Peshkin, *et al.*, 2010). Additionally, the literature search (Supplementary table 6) performed using PubMed (https://www.ncbi.nlm.nih.gov/pubmed/) as well as NHGRI-EBI GWAS Catalog (MacArthur *et al.*, 2017), revealed 15 variants that were previously reported to be associated with either a neuropsychiatric disorder, neurodegenerative disease, inflammatory disorder or treatment response. These 15 variants were subsequently prioritised for inclusion. The PharmGKB database (Whirl-Carrillo *et al.*, 2012) was similarly searched in order to identify variants with any previous report of association with drug response, however no previously reported associations were identified. Nevertheless, during this search, variants with similar dbSNPIDs were returned as hits for the respective variants. These variants were documented for further analysis which is elaborated on in section 3.2.2 below.

With regards to the regulatory impact of variants, 38 variants were identified to have a RegulomeDB (Boyle *et al.*, 2012) score ranging between “1a” and “3b” and were thus prioritised for inclusion. RegulomeDB scores classify variants according to their predicted ability to affect binding as well as their linkage to the expression of a gene target, where scores approaching “1a” represent variants with substantial binding evidence, and scores approaching “6” represent variants with minimal binding evidence (detailed in Supplementary table 1). Additionally, the presence of miRNA binding was investigated using PolymiRTs (Bhattacharya *et al.*, 2014) as well as the TarBase option on SNPNexus (Chelala *et al.*, 2009): seven variants were predicted to affect binding and were subsequently prioritised for inclusion (Supplementary table 5). Moreover, investigating transcription factor binding using SNP2TFBS (Kumar *et al.*, 2017) revealed four variants predicted to have an impact on regulation; these variants were subsequently included for further analyses (Supplementary table 5). Interestingly, of the eight variants extracted from *BECN1,* only one variant (rs9910698) survived the cut-off threshold of MAF ≥ 0.05. Upon further investigation, this variant was predicted to have minimal functional and regulatory impact and had no previously reported associations with the above-outlined terms of the literature search and was thus excluded from further analysis.

In total, 39 variants were prioritised for inclusion in this study and the corresponding genes for these variants are listed in Table 3.2.

Table 3.2. The number of variants per gene prioritised for inclusion in this study

Gene	Variant/s prioritised for inclusion
AMBRA1	2
ATG3	2
ATG7	9
ATG12	3
ATG13	5
ATG14	4
ATG16L1	8
BECN1	0
GABARAP	1
PINK1	5
Total	**39**

3.2. Enrichment and association analyses

3.2.1. Pathway-enrichment

Preceding association analysis, variants were organised according to pathways for which their corresponding genes were enriched using the gene-set library KEGG 2019 Human Pathway (Kanehisa & Goto, 2000) (accessed *via* the gene-set enrichment analysis webserver Enrichr https://academic.oup.com/nar/article-/44/W1/W90/2499357). Enriched pathways with an adjusted P-value ≤ 0.05 were selected for further analysis. These are shown in Table 3.3.

As could be predicted, the candidate genes were most significantly enriched for the autophagy pathway with an adjusted P-value of 6.21×10^{-15}. Candidate genes were likewise significantly enriched for the mitophagy pathway with an adjusted P-value of 4.18×10^{-4}. The mitophagy pathway involves the selective degradation of damaged mitochondria *via* autophagy and thus plays a crucial role in maintaining mitochondrial and metabolic homeostasis. Additionally, candidate genes were significantly enriched for the NOD-like receptor (NLR) signalling pathway and were included for further analysis (adjusted P-value 5.75×10^{-3}). The Kaposi's sarcoma-associated herpesvirus (KSHV) infection was the only other pathway for which the candidate genes were significantly enriched (adjusted P-value of 4.91×10^{-3}). These pathways, together with their P-value, adjusted P-value, odds ratio and combined scores are shown in Table 3.3.

Candidate autophagic genes previously reported to have an association with either SCZ or a neurodegenerative disease (Supplementary table 2) were independently selected for analyses to determine whether prioritised variants within these candidate genes were informative considering ATR. The genes selected for these independent analyses are listed in Table 3.3.

Table 3.3. Factors considered for the selection of enriched and curated pathways for further association analyses and their constituent genes

Pathway	P-value	Adjusted P-value	Odds Ratio	Combined Score	Genes
Autophagy*	2.02×10^{-17}	6.21×10^{-15}	138.89	5339.20	*ATG3; ATG16L1; AMBRA1; ATG14; ATG13; ATG7; GABARAP; ATG12*
Mitophagy*	2.71×10^{-6}	4.18×10^{-4}	102.56	1314.58	*PINK1; AMBRA1; GABARAP*
NOD-like receptor signaling*	5.60×10^{-5}	5.75×10^{-3}	37.45	366.69	*ATG16L1; GABARAP; ATG12*
Kaposi's sarcoma-associated herpesvirus infection*	6.38×10^{-5}	4.91×10^{-3}	35.84	346.23	*ATG3; ATG14; GABARAP*
Schizophrenia	*Previously reported association in literature*				*ATG13; ATG16L1; GABARAP; AMBRA1*
Neurodegenerative disease	*Previously reported association in literature*				*ATG12; ATG14; ATG3; ATG7; GABARAP; PINK1*

*Predicted *via* Enrichr, available at https://amp.pharm.mssm.edu/Enrichr/, accessed June 2020.

The bipartite network representative of the interactions between candidate genes and various signal transduction pathways, predicted by NetworkAnalyst (www.networkanalyst.ca) using the KEGG pathway database (Kanehisa & Goto, 2000) is displayed in Supplementary figure 2. Gene sets that were most enriched were for the autophagy pathway (both animal and other), followed by the mitophagy pathway, KSHV pathway, the NOD-like receptor pathway, FoxO signalling pathway, Apelin signalling pathway, Apoptosis, Ferroptosis and the RIG-I-like receptor signalling pathway. The P-values associated with the enrichment of these pathways is depicted in Supplementary table 22.

3.2.2. Variant descriptive statistics

Haploview (Barrett *et al.*, 2005) was utilised to assess HWE of prioritised variants using a significance threshold of P-value ≤ 0.01 (Wigginton *et al.*, 2005), and to generate genotype frequencies. No variants were out of HWE (data not shown).

LD analysis was performed using the SNPStats web-tool (Solé *et al.*, 2006) to determine whether any of the prioritised variants and PharmGKB (Whirl-Carrillo *et al.*, 2012) hits (alluded to in genetic variant prioritisation, section 3.1.2) were in LD. This analysis yielded no conclusive results and no further analysis was performed on the variants identified through PharmGKB (Whirl-Carrillo *et al.*, 2012). With regards to the prioritised variants, Haploview (Barrett *et al.*, 2005) was used to assess LD between them, as well as to determine whether there were any TagSNPs that could be utilised to represent other prioritised variants. An r^2 value above 0.8 was considered indicative of strong LD for the purpose of selecting TagSNPs (Carlson *et al.*, 2004).

Independent TagSNP analyses were performed per pathway, and varying TagSNPs were generated per pathway due to the discrepancy in the total sum of variants per pathway group. TagSNPs were identified for the "autophagy", "NOD-like receptor", "schizophrenia" pathways as well as for the "all prioritised variants" group, and the variants captured per TagSNP are shown in Table 3.4.

Table 3.4. TagSNPs predicted per pathway and their constituent SNPs

Pathway	TagSNP	SNPs captured	r^2 value
Autophagy	rs2241879	rs3828309, rs2241880, rs3792109, rs2241879	0.96
	rs10769204	rs10769204, rs10838610	1.00
NOD-like receptor	rs3792106	rs2241880, rs3828309, rs3792106, rs3792109	0.90
Schizophrenia	rs2241880	rs2241880, rs3792109, rs2241879, rs3828309	0.90
	rs10769204	rs10769204, rs10838610	1.00
All prioritised variants	rs3792109	rs3828309, rs2241880, rs3792109, rs2241879	0.94
	rs10838610	rs10838610, rs10769204	1.00

SNP: single nucleotide polymorphism; NOD: nucleotide-binding oligomerisation domain

3.2.3. Association analysis

Prioritised variants of the candidate genes enriched for each respective pathway were documented (Table 3.5.) and each pathway was analysed independently, allowing for an increase in power for association. For comparison purposes, an analysis was performed in which all variants were included (referred to as "All prioritised variants"). The Bonferroni-corrected significance thresholds per respective pathway, as well as the number of variants per pathway, are shown in Table 3.5.

Table 3.5. The number of variants per enriched pathway included for association analysis

Pathway for which prioritised genes are enriched	Number of associated variants	Bonferroni-corrected threshold*
Autophagy	34	2.08×10^{-4}
Mitophagy	8	7.81×10^{-4}
NOD-like receptor signaling	12	6.94×10^{-4}
Kaposi sarcoma-associated herpesvirus infection	7	8.93×10^{-4}
Schizophrenia	16	5.21×10^{-4}
Neurodegenerative disease	24	2.60×10^{-4}
All prioritised variants	**39**	$\mathbf{1.79 \times 10^{-4}}$

NOD: nucleotide-binding oligomerisation domain

The association analysis revealed four variants to be repeatedly associated with differential ATR outcomes in the majority of the pathways, as determined by the change in log-transformed PANSS scores over 12 months. In total, there were 10 significant associations that survived Bonferroni correction between variants and worsened treatment outcome in the Negative PANSS symptom domain, as per the positive effect estimate values (a relative increase in log-transformed PANSS scores). Table 3.6. and Table 3.7. show the association of variants with ATR under the genotypic and additive allelic models of inheritance respectively. Both Table

3.6. and Table 3.7. comprise variants that pass the Bonferroni-corrected threshold (distinguished by '***') as well as an uncorrected for multiple comparisons threshold of P-value ≤ 0.001 (distinguished by '**'). Additionally, variants that met an uncorrected threshold of P-value ≤ 0.05 are included in Supplementary table 7 to Supplementary table 20.

Table 3.6. Association analysis between genetic variants and log-transformed PANSS scores over time under the genotypic model of inheritance

Gene	dbSNPID	PANSS Domain	Contrast	ATR	Effect estimate	95% CI	P-value	α-value
Autophagy pathway								
AMBRA1	rs11819869	Negative	*TT* vs *CC*	Worsened	4.56×10^{-3}	2.04×10^{-3} to 7.07×10^{-3}	4.11×10^{-4} **	2.08×10^{-4}
ATG14	rs1538257	Negative	*TG* vs *GG*	Worsened	3.34×10^{-3}	1.39×10^{-3} to 5.30×10^{-3}	8.41×10^{-4} **	
GABARAP	rs222843	Negative	*GG* vs *AA*	Worsened	8.52×10^{-3}	3.62×10^{-3} to 1.34×10^{-2}	6.78×10^{-4} **	
Mitophagy pathway								
AMBRA1	rs11819869	Negative	*TT* vs *CC*	Worsened	4.56×10^{-3}	2.04×10^{-3} to 7.07×10^{-3}	4.11×10^{-4}***	7.81×10^{-4}
GABARAP	rs222843	Negative	*GG* vs *AA*	Worsened	8.52×10^{-3}	3.62×10^{-3} to 1.34×10^{-2}	6.78×10^{-4}***	
PINK1	rs1043424	Negative	*CC* vs *AA*	Worsened	5.96×10^{-3}	3.02×10^{-3} to 8.90×10^{-3}	7.56×10^{-5}***	
NOD-like receptor signalling pathway								
GABARAP	rs222843	Negative	*GG* vs *AA*	Worsened	8.52×10^{-3}	3.62×10^{-3} to 1.34×10^{-2}	6.78×10^{-4}***	6.94×10^{-4}
Kaposi-sarcoma-associated herpesvirus infection pathway								
ATG14	rs1538257	Negative	*TG* vs *GG*	Worsened	3.34×10^{-3}	1.39×10^{-3} to 5.30×10^{-3}	8.41×10^{-4} ***	8.93×10^{-4}
GABARAP	rs222843	Negative	*GG* vs *AA*	Worsened	8.52×10^{-3}	3.62×10^{-3} to 1.34×10^{-2}	6.78×10^{-4}***	
Schizophrenia pathway								
AMBRA1	rs11819869	Negative	*TT* vs *CC*	Worsened	4.56×10^{-3}	2.04×10^{-3} to 7.07×10^{-3}	4.11×10^{-4}***	$5{,}21 \times 10^{-4}$
GABARAP	rs222843	Negative	*GG* vs *AA*	Worsened	8.52×10^{-3}	3.62×10^{-3} to 1.34×10^{-2}	6.78×10^{-4}**	
Neurodegenerative disease pathway								
ATG14	rs1538257	Negative	*TG* vs *GG*	Worsened	3.34×10^{-3}	1.39×10^{-3} to 5.30×10^{-3}	8.41×10^{-4} **	2.60×10^{-4}
GABARAP	rs222843	Negative	*GG* vs *AA*	Worsened	8.52×10^{-3}	3.62×10^{-3} to 1.34×10^{-2}	6.78×10^{-4}**	
PINK1	rs1043424	Negative	*CC* vs *AA*	Worsened	5.96×10^{-3}	3.02×10^{-3} to 8.90×10^{-3}	7.56×10^{-5}***	
All prioritised variants								
AMBRA1	rs11819869	Negative	*TT* vs *CC*	Worsened	4.56×10^{-3}	2.04×10^{-3} to 7.07×10^{-3}	4.11×10^{-4}**	1.79×10^{-4}
GABARAP	rs222843	Negative	*GG* vs *AA*	Worsened	8.52×10^{-3}	3.62×10^{-3} to 1.34×10^{-2}	6.78×10^{-4}**	
PINK1	rs1043424	Negative	*CC* vs *AA*	Worsened	5.96×10^{-3}	3.02×10^{-3} to 8.90×10^{-3}	7.56×10^{-5}***	
ATG14	rs1538257	Negative	*TG* vs *GG*	Worsened	3.34×10^{-3}	1.39×10^{-3} to 5.30×10^{-3}	8.41×10^{-4} **	

ATR: antipsychotic treatment response; CI: confidence interval; **Illustrates P-value below the uncorrected threshold of 0.001; ***Illustrates P-value below the Bonferroni-corrected threshold α-value.

Table 3.7. Association analysis between genetic variants and log-transformed PANSS scores over time under the additive allelic model of inheritance

Gene	dbSNPID	PANSS Domain	Contrast	ATR	Effect estimate	95% CI	P-value	α-value
Autophagy pathway								
AMBRA1	rs11819869	Negative	Each *T* allele	Worsened	2.20×10^{-3}	9.46×10^{-4} to 3.46×10^{-3}	6.13×10^{-4} **	2.08×10^{-4}
Mitophagy pathway								
AMBRA1	rs11819869	Negative	Each *T* allele	Worsened	2.20×10^{-3}	9.46×10^{-4} to 3.46×10^{-3}	6.13×10^{-4}***	7.81×10^{-4}
Schizophrenia pathway								
AMBRA1	rs11819869	Negative	Each *T* allele	Worsened	2.20×10^{-3}	9.46×10^{-4} to 3.46×10^{-3}	6.13×10^{-4}**	5.21×10^{-4}
All prioritised genetic variants								
AMBRA1	rs11819869	Negative	Each *T* allele	Worsened	2.20×10^{-3}	9.46×10^{-4} to 3.46×10^{-3}	6.13×10^{-4}**	1.79×10^{-4}

ATR: antipsychotic treatment response; CI: confidence interval; **Illustrates P-value below the uncorrected threshold of 0.001; ***Illustrates P-value below the Bonferroni-corrected threshold of α-value.

The abovementioned associations between prioritised variants and ATR (shown in Table 3.6. and Table 3.7.) are elaborated on below.

3.2.3.1. Association analysis between genetic variants and log-transformed PANSS scores over time under the genotypic model of inheritance

Within the autophagy pathway, although no variants passed the Bonferroni-corrected significance threshold during association analysis, three variants were identified to trend toward significance (P-value ≤ 0.001) in their associations with treatment response. These variants were rs11819869 in *AMBRA1* (*TT* genotype; P-value = 4.11×10^{-4}), rs1538257 in *ATG14* (*TG* genotype; P-value 8.41×10^{-4}) and rs222843 in *GABARAP* (*GG* genotype; P-value = 6.78×10^{-4}). All three of these variants were associated with a trend towards significance in the PANSS Negative symptom domain for a worsened treatment outcome, indicated by a positive effect estimate value.

Association analysis within the mitophagy pathway revealed three variants to be significantly associated with ATR. These were rs11819869 in *AMBRA1* (P-value = 4.11×10^{-4}*),* rs222843 in *GABARAP* (P-value = 6.78×10^{-4}) and rs1043424 in *PINK1* (P-value = 7.56×10^{-5}). All significant associations occurred under the genotypic model of inheritance (Table 3.6.) for rs11819869 (genotype *TT*), rs222843 (genotype *GG*) and rs1043424 (genotype *CC*) within the PANSS Negative symptom domain, and specifically, all genotypes were associated with a worsened ATR with the effect estimates of 4.56×10^{-3}, 8.52×10^{-3} and 5.96×10^{-3} respectively.

In the NOD-like receptor signalling pathway, only one variant, namely rs222843 in *GABARAP*, was significantly associated with ATR. This association was only present under the genotypic model of inheritance (Table 3.6.), with a P-value of 6.78×10^{-4}. Specifically, the genotype *GG* of this variant was associated with a worsened treatment response (effect estimate 8.52×10^{-3}), characterised by an increase in log-transformed PANSS scores over the 12-month period.

Within the KSHV infection pathway, two variants were significantly associated with ATR over the 12-month period. These variants were rs1538257 in *ATG14* (P-value = 8.41×10^{-4}) and rs222843 in *GABARAP* (P-value = 6.78×10^{-4}). These significant associations were identified under the PANSS Negative symptom domain and both genotypes, *TG* for rs1538257, and *GG* for rs222843, were associated with a worsened treatment response over the 12-month period. The effect estimates for these associations for rs1538257 and rs222843 were 3.34×10^{-3} and 8.52×10^{-3} respectively under the genotypic model of inheritance (Table 3.6.).

Within the SCZ pathway, one variant, namely rs11819869 within *AMBRA1,* was significantly associated with ATR with a P-value of 4.11×10^{-4}. Specifically, the *TT* genotype was associated with a worsened treatment outcome under the PANSS Negative symptom domain, indicated by a positive effect estimate of 4.56×10^{-3}. Additionally, one variant, namely rs222843 of *GABARAP,* trended towards a significant association (P-value = 6.78×10^{-4}). The *GG* genotype of this variant was found to be associated with a worsened treatment outcome

within the PANSS Negative symptom domain as indicated by a positive effect estimate of 8.52×10^{-3} (Table 3.6.).

Within the neurodegenerative disease pathway, one variant, rs1043424 within *PINK1,* was significantly associated with ATR with a P-value of 7.56×10^{-5}. Specifically, the *CC* genotype was associated with a worsened treatment outcome under the PANSS Negative symptom domain, indicated by a positive effect estimate of 5.96×10^{-3}. Further, two variants, rs1538257 of *ATG14* and rs222843 of *GABARAP,* were trending towards significance with regards to their association with treatment response (P-value = 8.41×10^{-4} and P-value = 6.78×10^{-4} respectively). The *TG* genotype of rs1538257 and the *GG* genotype of rs222843 were both identified to be associated with a worsened treatment outcome within the PANSS Negative symptom domain as indicated by positive effect estimates of 3.34×10^{-3} and 8.52×10^{-3} respectively (Table 3.6.).

When all prioritised variants were included for analysis, only rs1043424 of *PINK1* was significantly associated with ATR over the 12-month period (P-value = 7.56×10^{-5}). Specifically, the *CC* genotype of this variant was associated with a worsened treatment outcome as indicated by the positive effect estimate of 5.96×10^{-3}. Aside from this, within the association analysis focused on all prioritised variants, three variants were identified to be trending towards significance, namely rs11819869 of *AMBRA1*, rs222843 of *GABARAP* and rs1538257 of *ATG14*. More precisely, the *TT* genotype of rs11819869, the *GG* genotype of rs222483, and the *TG* genotype of rs1538257 were all associated with a worsened treatment outcome over the 12-month period as indicated by their positive effect sizes of 4.56×10^{-3}, 8.52×10^{-3} and 3.34×10^{-3} respectively (Table 3.6.).

3.2.3.2. Association analysis between genetic variants and log-transformed PANSS scores over time under the additive allelic model of inheritance

Within the additive allelic model of inheritance (Table 3.7.), only one variant within one pathway was identified to be significantly associated with treatment response, that is rs11819869 of *AMBRA1* within the mitophagy pathway. This same variant was identified to be trending towards a significant association with treatment response in the autophagy pathway, SCZ pathway as well as in the association analysis that included all the prioritised genetic variants. The P-value for this variant within all pathways was 6.13×10^{-4}, with differing α-values for the respective analyses. In all associations within Table 3.7., the *T* allele was associated with a worsened treatment outcome for the PANSS Negative symptom domain, as indicated by a positive effect estimate value of 2.20×10^{-3}.

3.3. *In vitro* model

In order to elucidate on the physiological functioning of the autophagy mechanism under the effects of an autophagy inducing drug, as would be the case for the administration of antipsychotic medication, an *in vitro* model (namely the iN cellular model) was utilised. The iN cellular model utilised is highly applicable to age-

related disorders owing to its unique ability to retain aging-related epigenetic signatures, thus emphasising its validity in a SCZ-context. As a point of departure, an *in vitro* model of HD patient-derived dermal fibroblasts converted into iNs was utilised. The iNs were subsequently treated with an autophagy-inducing agent and the response was assessed. The impaired autophagy mechanism in neurodegenerative diseases is well-characterised, and thus the assessment of autophagy response in this *in vitro* model serves as an apt way to unravel autophagy dysfunction in a diseased state.

3.3.1. Pharmacological treatment of Huntington's disease patient and control fibroblasts

A literature search was performed so as to select the most effective concentration and duration of Torin1 treatment for the activation of autophagy in the iN cells (Chandrachud, Walker, Simas, *et al.*, 2015; du Toit, Hofmeyr, Gniadek, *et al.*, 2018; Zhou, Tan, Nicolas, *et al.*, 2013). Based on findings from the literature search, fibroblast cells were treated with 250 nM, 500 nM, 1 µM, and 10 µM Torin1 for two hours and four hours respectively (Figure 3.1.). As DMSO was used as a solvent for Torin1, cells treated with DMSO-only acted as the technical control.

Markers for ubiquitinated proteins for lysosomal degradation (p62), nucleus identification (DAPI) and autophagosomes (LC3) were visualised using inverted fluorescence microscopy. After treatment, cells with a shrunken-like appearance (Figure 3.1. C, F, H, I, K and L) were considered to be a stressed phenotype. Similarly, an aggregation of p62 dots (Figure 3.1. H, I, J, K and L) may indeed indicate autophagy decline, as p62 is selectively degraded in the autophagy process and thus negatively correlates with the autophagy process. On the other hand, a non-shrunken appearance together with an abundance of LC3 dots and subsequent p62 clearance (Figure 3.1. B) was considered a healthy phenotype – indicating an activation of autophagy had occurred. Further, the absence of both p62 and LC3 was considered to represent an increase in autophagic flux, suggesting autophagosome turnover and associated p62 clearance.

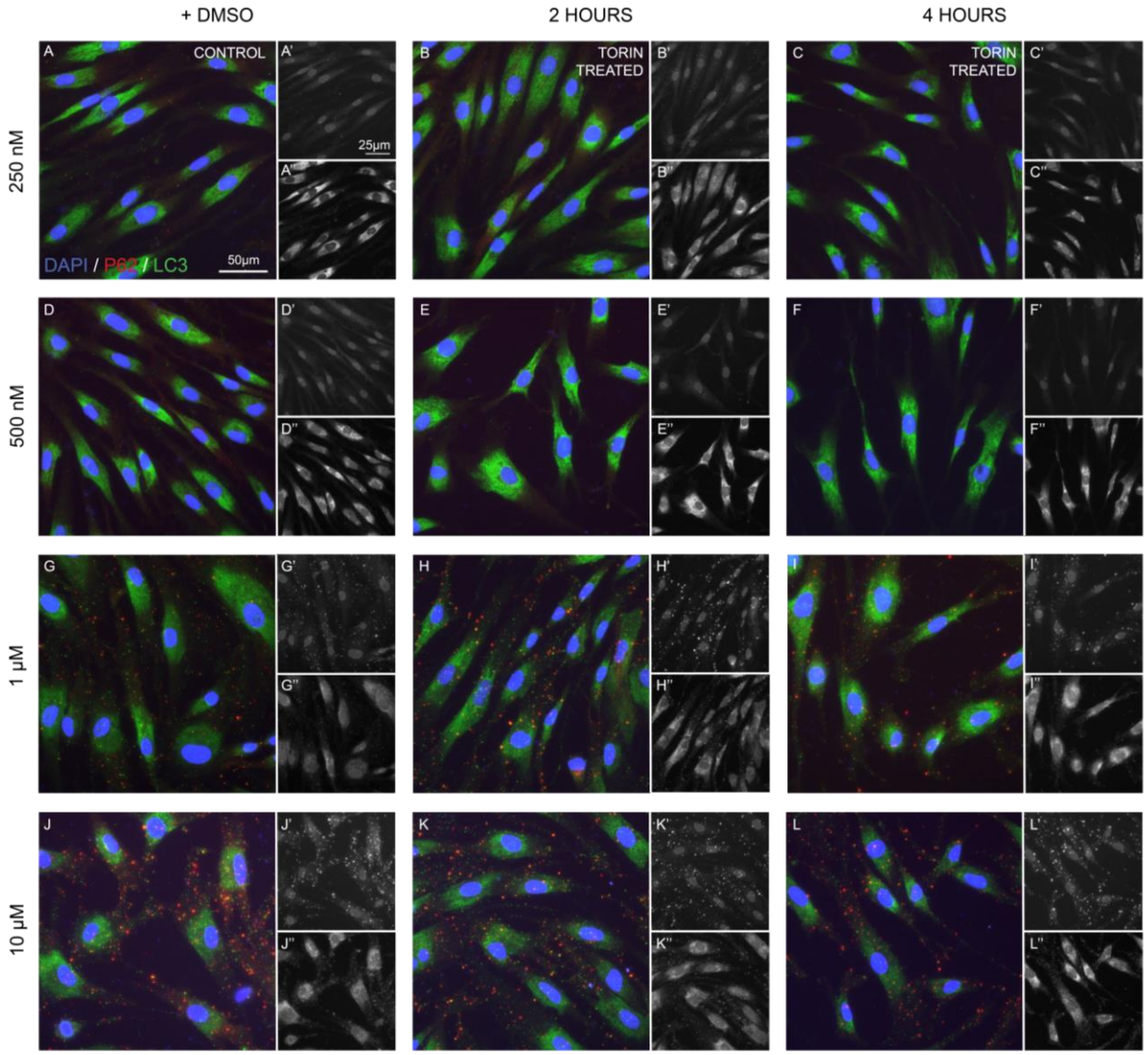

Figure 3.1. Treatment of Huntington's disease patient and control dermal fibroblasts with autophagy-inducing drug Torin1 for the selection of the concentration and duration of the drug with the greatest autophagy-inducing efficacy
A - C) Adult dermal fibroblasts treated with 250 nM DMSO 4h (A), and Torin1 2h (B) and 4h (C) respectively. A' and A'' depict the p62 puncta in red and LC3+ puncta in green, this is applicable to all treated fibroblasts in this figure. D – F) Adult dermal fibroblasts treated with 500 nM DMSO 4h (D), and Torin1 2h (E) and 4h (F) respectively. G – I) Adult dermal fibroblasts treated with 1 µM DMSO 4h (G), and Torin1 2h (H) and 4h (I) respectively. J – L) Adult dermal fibroblasts treated with 10 µM DMSO 4h (J), and Torin1 2h (K) and 4h (L) respectively. Scale bars representing 50 µm and 25 µm are included. All fibroblasts immunostained with DAPI (blue), p62 (red) and LC3 (green). DAPI stains the nuclei, p62 is a marker for ubiquitinated proteins for lysosomal degradation and LC3 is an autophagosomal marker.

A treatment of 250 nM for two hours displayed the greatest efficacy in terms of autophagy-activation and was therefore selected to be the preferred concentration and duration of Torin1 treatment to be applied on the iNs.

3.3.2. Neuronal reprogramming of Huntington's disease patient and control fibroblasts

Induced neurons were produced with a pan-neuronal phenotype through the use of a lentiviral vector yielding a large amount of mature neurons (Figure 3.2 A; Drouin-Ouellet *et al.*, 2017; Shrigley, Pircs, Barker, *et al.*, 2018). Whilst six HD and six control fibroblast cell lines were directly converted into iNs in this study, for exploratory purposes only data from three cell lines for HD and controls respectively (in triplicate) were included in the analyses.

Initially, fibroblast identity was morphologically verified and then transduced to express pro-neural factors and shRNA targeting REST. Pronounced neuronal morphology of the cells was evident by day 28. Following fixation and immunostaining, neuronal cells stained positive for the neuronal marker MAP2 (Figure 3.2. B and C).

Previous studies in the Molecular Neurogenetics Lab at Lund University (where this current study's research on the iN model was carried out), using 10 HD and 10 control iNs, have identified less elaborate neurites in HD patient iNs compared to controls (Pircs *et al*., manuscript in preparation). This is in line with what other studies have identified (Drouin-Ouellet *et al.*, 2017; Liu, Xue, Ridley, *et al.*, 2014). Immunocytochemical characterisation of the MAP2-identified iNs (Figure 3.2. B and C) confirm the discrepancy in neurite length in iNs derived from HD patients compared to controls. Quantification indicated that the purity of HD neurons was significantly higher (almost two-fold) than the control neurons (Figure 3.2. D and E) and that there was a 7 – 10% conversion efficiency of both HD and controls (Figure 3.2. F) which is in line with what limited other studies have reported (Caiazzo, Dell'Anno, Dvoretskova, *et al.*, 2011; Pfisterer, Wood, Nihlberg, *et al.*, 2011). Quantification of the neuronal profile of the iNs revealed HD-iNs have a significantly reduced total neurite count and width compared to controls, and trend towards a reduced neurite length and area compared to controls (Figure 3.2. H – K). Interestingly, HD-iNs had a significantly larger cell body total area compared to control iNs (Figure 3.2. G).

In summary, HD patient and control fibroblasts were successfully reprogrammed into iNs with an efficiency of 7 - 10 %. It was demonstrated that HD-iNs have less elaborate neurites when compared to controls.

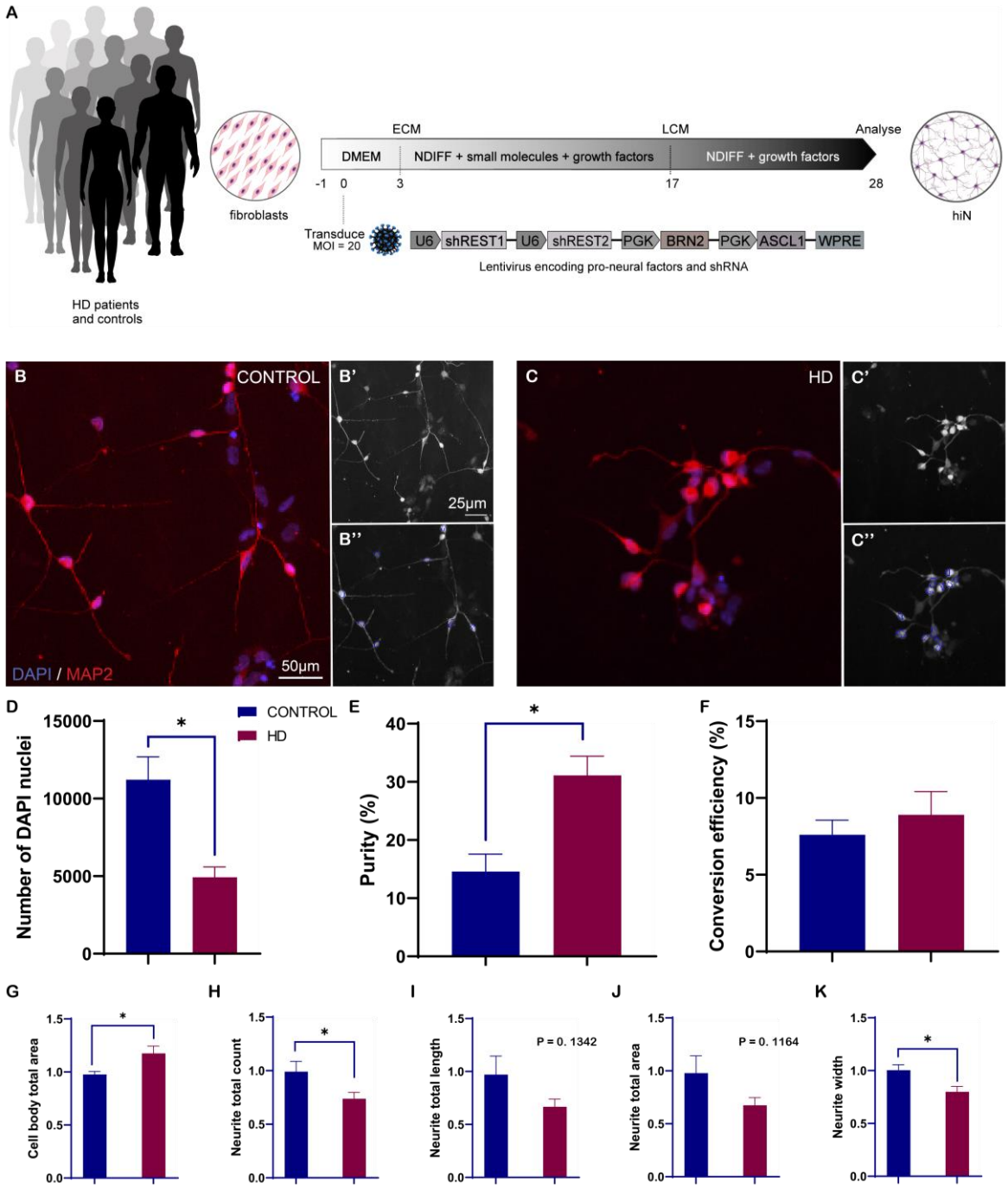

Figure 3.2. Neuronal reprogramming of Huntington's disease patient and control fibroblasts show similar rates of conversion with a reduced neuronal profile of the Huntington's disease induced neurons

A) Schematic representation of direct neuronal reprogramming of adult HD patient and control fibroblasts. B - C) Immunocytochemical characterisation of iNs from controls (B) and HD patients (C) respectively. B', B'', C' and C'' depict MAP2+ neurons defined by HCS analysis software based on area and intensity. D) Quantification of average neuronal yields per DAPI following 28 days of conversion (n = 3 for control, 9 wells analysed in total; n = 3 for HD, 7 wells analysed in total). E - F) Quantification of neuronal purity and efficiency of reprogrammed adult human dermal fibroblasts (n = 3 for control, 9 wells analysed in total; n = 3 for HD, 7 wells analysed in total). G – K) Quantification of relative cell body area, neurite total count, total length, total area, and width per cell calculated by HCS analysis defined by MAP2+ neurons (n = 3 for control, 7 wells analysed in total; n = 3 for HD, 7 wells analysed in total). Scale bars representing 50 µm and 25 µm are depicted. ECM: early conversion medium; HD: Huntington's disease; HCS: high-content screening; hiN: human induced neuron; LCM: late conversion medium; MOI: multiplicity of infection. Data

are expressed as mean ±SEM. An unpaired unequal student's t-test was used in D-K to test differences between two groups. P-value < 0.05 was set for significance, indicated with *.

Following successful conversion of the control and HD fibroblasts into iNs, iNs were treated with the autophagy-inducing drug Torin1.

3.3.3. Treatment of Huntington's disease and control iNs with autophagy-inducing drug Torin1

In this present study, iNs derived from six HD patients and six controls were treated with Torin1 for 2 hours, and subsequently fixed and immunostained with markers for DAPI, MAP2 and LC3 (due to the exploratory purposes of this study, data included in the analysis are derived from three HD-patients and three controls in triplicate only). Torin1 treatment did not affect purity, the total number of cells (as depicted by DAPI number) and conversion efficiency (Supplementary figure 1). Following analysis of the neuronal morphology of the iNs, it was revealed that Torin1 treatment did not appear to affect the neurite profile (Supplementary figure 1). Interestingly, however, it did significantly increase the cell body area, specifically in the HD-iNs (Supplementary figure 1).

Quantification through HCS revealed no significant difference in cell body spot count between the treated and non-treated controls and HD-iNs (Figure 3.3. A – D, I). However, there was a trend towards a significant difference between treated and non-treated HD-iNs in this regard, where HD-iNs presented with a higher cell body LC3 spot count (Figure 3.3. I). Treatment with Torin1 resulted in an efficient activation of autophagy in the cell body in both the control and HD-iNs, as is evident by the significant reduction in the area of the LC3+ spots (Figure 3.3. J). As LC3 is an autophagosomal marker, a reduction in size in LC3 spots could suggest an increased autophagosomal turnover, although further experiments would be needed to verify this. Interestingly, there was a trend towards an opposing effect between control and HD-iNs in the neurites. Similarly, to the LC3 cell body spot count (Figure 3.3. I) and area (Figure 3.3. J), the Torin1-treated control-iNs showed a trend towards fewer (Figure 3.3. K) LC3+ spots in the neurites compared to non-treated control-iNs. In contrast, treated HD-iNs exhibited a trend towards more (Figure 3.3. K) and larger (Figure 3.3. L) LC3+ spots in the neurites compared to non-treated HD-iNs. Interestingly, the Torin1-treated control-iNs showed a trend toward an increased autophagosome area (as depicted by LC3 spot area) in the neurites. This could possibly be indicative of more ubiquitinated proteins present within the autophagosome, although further analyses would be needed to verify this.

These results indicate that Torin1 sufficiently activated autophagy in the control iNs by lowering the abundance (and size in the case of the cell body) of LC3-tagged autophagosomes in both the cell body and neurites. In sharp contrast however, in the HD-iNs, only a decrease in autophagosome area in the cell body was evident, as well as an increase in count and size of autophagosomes in the neurites – indicating that autophagy was not effectively activated by Torin1 in the HD-iNs (Figure 3.3.).

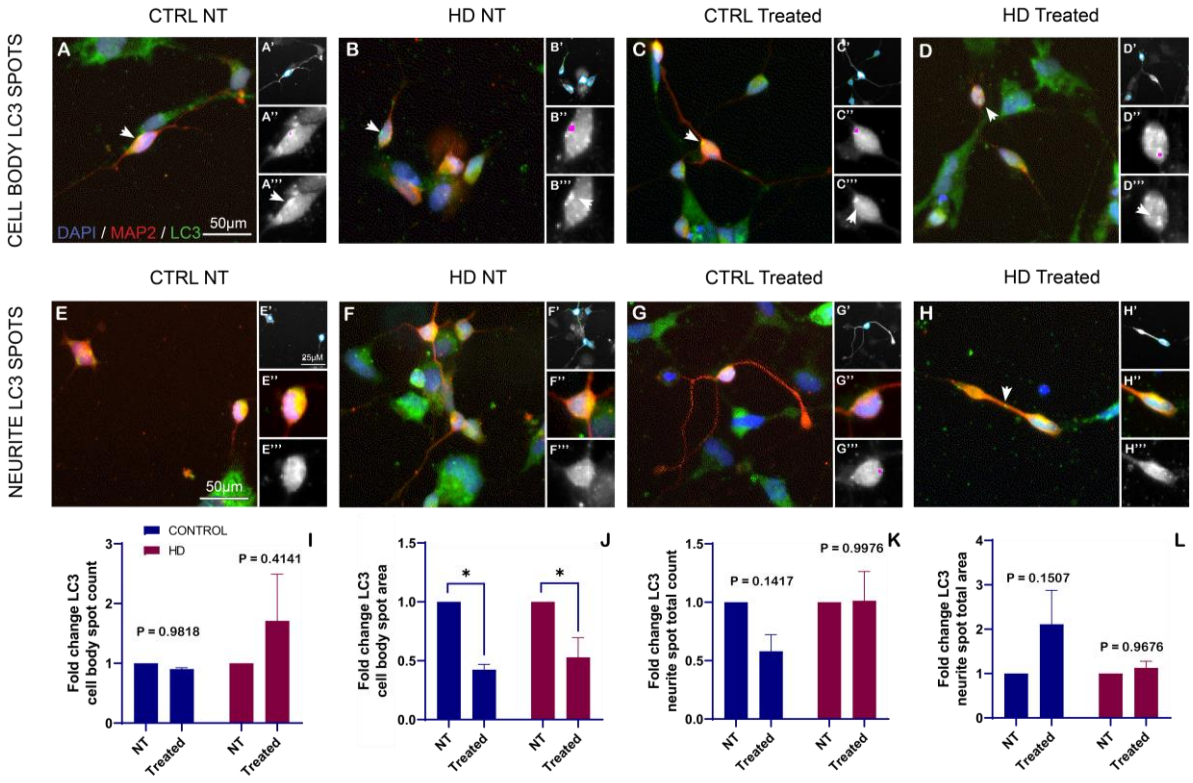

Figure 3.3. Treatment of Huntington's disease and control induced neurons with autophagy-inducing drug Torin1.
A - D) Immunocytochemical characterisation of the cell body spots of iNs before and after Torin1 treatment from controls (A, C) and HD patients (B, D) respectively. A' illustrates neuronal cell body defined by HCS software based on MAP2 staining highlighted with blue. A'' is a magnification of MAP2+ cell body (highlighted on A with arrowhead) and stained with LC3. Pink dots represent LC3+ puncta defined by intensity and area using HCS analysis software. A''' illustrates the same picture presented in A'' without the pink dots, where LC3+ puncta are highlighted by an arrowhead (Applied throughout A – D). E - H) Immunocytochemical characterisation of the neurite spots of iNs before and after Torin1 treatment from controls (E, G) and HD patients (F, H) respectively. E' illustrates neuronal cell body defined by HCS software based on MAP2 staining highlighted in blue. E'' and E''' are magnifications of E'. Pink dots represent LC3+ puncta defined by intensity and area using HCS analysis software. This is applied throughout E – H. I - L) Fold change of LC3+ spot count following Torin1 treatment in control and HD-iNs as calculated by HCS analysis (n = 3 for control, 14 wells analysed in total and n = 3 for HD, 14 wells analysed in total). All scale bars represent 50 µm. iNs: induced neurons; HD: Huntington's disease; HCS: high-content screening; NT: non-treated. Data are expressed as mean ±SEM. Paired t-test was performed in I – L to compare differences between treated and non-treated control- and HD-iNs. P-value < 0.05 set for significance, indicated with *.

Thus, autophagy was successfully activated in the control iNs, and was inefficiently activated in the HD-iNs. Moreover, there was a distinct morphological phenotype evident in the HD-iNs, particularly relating to a less complex neurite morphology. The results of this *in vitro* model thus indicate the presence of a disease-related autophagy impairment in HD, and thus alludes to the potential disease-related autophagy impairment that is likely present in a SCZ context, as is supported by the genetic results of this study.

CHAPTER 4. DISCUSSION

Using a systems genetics approach, this study investigated the role of the autophagy mechanism in treatment response outcomes of SA FES patients. This was achieved through gene-set- and pathway-enrichment analyses, followed by association analyses. Additionally, by conducting a functional analysis using a novel *in vitro* model, this study investigated the autophagy mechanism under a diseased state from a physiological standpoint.

4.1. Genetic variables

4.1.1. Candidate genes and prioritised variants

The autophagy pathway continues to prove itself an excellent candidate for unravelling genetic diseases and disorders (both complex and Mendelian), and more recently, the therapeutics thereof (Bar-Yosef *et al.*, 2019; Djajadikerta, Keshri, Pavel, *et al.*, 2020). Hence, in this study, genes associated with the core mechanisms of autophagy were considered the primary investigative target.

Candidate genes identified in the literature were selected for inclusion in this study based on their previous implication in autophagy and ATR, neuropsychiatric disorders, neurodegenerative diseases, or inflammatory disorders. A total of 46 genes were identified through a literature search, which emphasises and provides support for the genetic overlap between autophagy and diseases and disorders of the CNS as well as inflammatory disorders (Supplementary table 2). A gene-set enrichment analysis was employed to further prune the list of literature-identified genes, and the candidate genes included for further analysis comprised six of the *ATG* genes (*ATG3, ATG7, ATG12, ATG13, ATG14* and *ATG16L1*), as well as four autophagy-associated genes (*AMBRA1, GABARAP, PINK1* and *BECN1*) (Table 3.1**.**). The regulatory and functional consequences of the variants within these candidate genes (Supplementary table 4 and Supplementary table 5) served as the bases for variant prioritisation and as no variants within *BECN1* met the inclusion criteria, they were excluded from further analysis in this study.

4.1.2. A promising link between ATR, autophagy-related candidate genes and prioritised variants

Whilst the number of studies that examine the relationship between autophagy genes and variants and ATR is limited, several studies have demonstrated that various antipsychotic drugs can modulate autophagy through the mTOR pathway (Brandão-Teles, de Almeida, Cassoli, *et al.*, 2019; Kim, Park, Yu, *et al.*, 2018; Shin, Lee, Choi, *et al.*, 2013). The mTOR pathway encompasses the candidate genes of this study *ATG14, BECN1* and *ATG13* amongst others, corroborating the candidacy of this pathway for pharmacological modulation. Providing further evidence for the suitability of this pathway, another study has implicated the mTOR

pathway in extrapyramidal symptom susceptibility (Mas, Gassó, Ritter, *et al.*, 2015). Interestingly, the antipsychotic drug utilised in this study (flupenthixol decanoate) has been demonstrated to act *via* the PI3K pathway, a signalling cascade involved in the induction of autophagy by directly impacting the mTOR pathway (Figure 4.1.). A cancer-based study, aiming to uncover the exact mechanisms of flupenthixol decanoate as an anti-cancer drug, elucidated that flupenthixol docks to the ATP binding pocket of PI3K α and indeed inhibits the activity of this complex and consequently the PI3K/AKT pathway (Dong, Chen, Li, *et al.*, 2019). Another cancer-based study investigating the mechanisms of thioxanthone, of which thioxanthene (flupenthixol) is a reduction product, confirmed the autophagy induction properties of this compound (Lima, Sousa, Paiva, *et al.*, 2016). Furthermore, trifluoperazine, an antipsychotic structurally and pharmacologically similar to flupenthixol and which has been shown to have analogous effects on the CNS (Ernst, Malone, Rowan, *et al.*, 1999; https://www.drugs.com/mmx/flupenthixol-decanoate.html) was identified to be one of the eight most effective autophagy enhancing compounds (Zhang *et al.*, 2007) compared to 480 other bioactive compounds tested, further supporting the autophagy-inducing effect of flupenthixol decanoate.

These findings emphasise the need to elucidate the functional consequences of dysregulation of this pathway to further clarify its role as a therapeutic target.

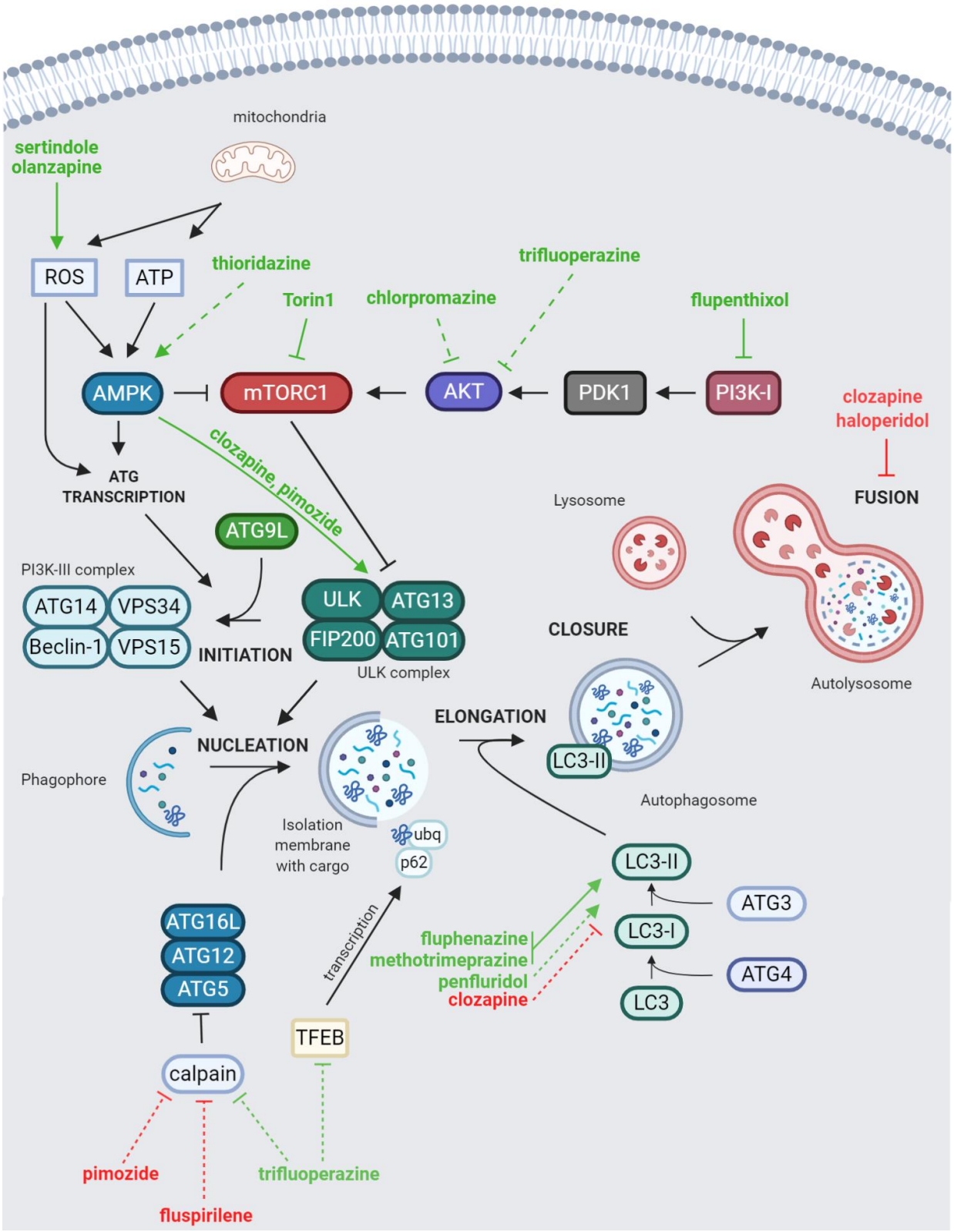

Figure 4.1. Mechanisms of autophagy regulation by antipsychotic drugs
Arrowheads represent activation and bar-heads represent inhibition of regulation by antipsychotics. Full lines represent modulation in neuronal cells, dashed lines represent modulation in non-neuronal cells. Drug names illustrated in red indicate autophagy inhibition, and those in green indicate autophagy activation. Some drugs are shown to modulate LC3 conversion only as no specific underlying mechanism has previously been described in literature. ROS: reactive oxygen species; Ubq: ubiquitin. Adapted from (Vucicevic *et al*., 2018), under the Creative Commons Attribution Non-Commercial License (http://-creativecommons.org/licenses/by-nc/3.0/). Created using BioRender (www.biorender.com).

4.1.3. Dysregulation of the autophagy-related candidate genes could lead to SCZ-related pathophysiology

The candidate genes in this study, as supported by approximately two decades of studies (Levine & Kroemer, 2008; Mizushima & Komatsu, 2011; Nishimura & Tooze, 2020; Yim & Mizushima, 2020), are known to control the formation of the double-membraned structures that transport intracytoplasmic contents to the lysosome for degradation (Figure 1.1.). The critical role of these genes in maintaining cellular homeostasis and protein and organelle quality control necessitates their optimum functioning, and this is emphasised when one considers the fundamental role of the induction of autophagy in synaptic transmission and long-term memory formation (Levenga, Wong, Milstead, *et al.*, 2017; Radwanska, Medvedev, Pereira, *et al.*, 2011). The expected interaction between the candidate genes and various signal transduction pathways is depicted in Supplementary figure 2, highlighting the intricacy and dependency of their relationship. Hence, it is rational to hypothesise that any dysregulation or alteration of the autophagy pathway could result in catastrophic downstream events that result in an impaired ability of an organism to adapt to stress, potentially leading to disease. As expected, the autophagy induction signalling cascade that includes the serine/threonine kinase AKT, mTOR, *ATG13, ATG14*, as well as *BECN1*, has previously been implicated in the pathophysiology of SCZ (Kitagishi, Kobayashi, Kikuta, *et al.*, 2012). This is supported by a recent study by Chadha and Meador-Woodruff (2020), which provides direct evidence of a reduced expression of AKT and mTOR proteins in the dorsolateral prefrontal cortex of SCZ patients compared to controls. This is additionally supported by Merenlender-Wagner *et al.* (2015), who identified a statistically significant reduction in the expression levels of BECN1 in the hippocampus of SCZ patients, as well as Rietschel, Mattheisen, Degenhardt, *et al.* (2012), which show *ATG13* to be in strong LD with a chromosomal region associated with SCZ. Similarly to the latter study (Rietschel *et al.*, 2012), *ATG16L1,* the gene transcribing a core protein involved in the expansion of the phagophore, has been shown to interact with *GIGYF2*, a gene located in an identified risk locus for SCZ (Ripke, O'Dushlaine, Chambert, *et al.*, 2013). Furthermore, associations exist between the $GABA_A$-receptor gene cluster and SCZ (Petryshen, Middleton, Tahl, *et al.*, 2005), specifically an enhanced binding of the receptors on prefrontal cortex neurons of SCZ patients has been identified (Benes, Vincent, Marie, *et al.*, 1996). Thus, the dysregulation of the candidate genes in this study (through mechanisms that may partly involve the prioritised variants) might contribute to both differential treatment outcomes as well as SCZ pathophysiology (Figure 1.3.).

4.1.4. Candidate genes and prioritised variants provide evidence of autophagy-profile overlap between age-related CNS diseases and disorders

One of the main premises of this study is the apparent overlap between an impaired autophagy mechanism and neuropsychiatric disorders, neurodevelopmental disorders and neurodegenerative diseases (overlap depicted in Figure 1.3.). The candidate genes in this study were selected based on this premise, and this is

supported by an array of studies that provide evidence for the dysregulation of these genes and proteins that leads to calamitous downstream effects that ultimately cause these devastating disorders and diseases. For instance, using both *in vitro* and *in vivo* experiments, a study revealed that AMBRA1 positively regulates the PI3K complex by directly binding to BECN1, and AMBRA1 deficiency leads to severe neurodevelopmental defects in mice (Maria Fimia, Stoykova, Romagnoli, *et al.*, 2007). Additionally, a study discovered that the upstream ULK1 complex critically regulates ATG14 and the PI3K complex to control autophagy activity, and this regulation is compromised in a mouse model of HD due to mHTT-induced proteotoxic stress (Wold, Lim, Lachance, *et al.*, 2016). Studies implicate these alterations in Dementia with Lewy Bodies (DLB), PD and HD. Case in point: GABARAPs, which play a crucial role in autophagosome formation, were discovered to be at a decreased level in DLB, and immunohistochemical staining revealed that these GABARAP proteins, as well as LC3, were localised within Lewy Bodies in both PD and DLB (Tanji, Mori, Kakita, *et al.*, 2011). To this degree, ATG3, a protein likewise involved in the second UBL conjugation system of the elongation phase of autophagy, has been hypothesised to be involved in the age of onset of HD (Metzger, Saukko, Van Che, *et al.*, 2010; Yang & Klionsky, 2010).

Hence, there is convincing evidence supporting the implication of the candidate autophagic genes and prioritised variants of this study in the mechanism of ATR as well as the mechanism of disease *via* a dysregulation of the autophagy pathway (Figure 1.3.), and further exploration in this regard is warranted.

4.2. Enrichment and association analyses

4.2.1. Candidate gene and genetic variant enrichment in autophagy-related pathways

There is a profound intricacy in the autophagy mechanism, where its activation and inhibition are entirely dependent upon the crosstalk between proteins within different signal transduction pathways (Supplementary figure 2.). Analysing this mechanism and its integral components (i.e. the candidate genes and prioritised variants within the context of this study) and their association with ATR might thus best be represented by categorising the components into functionally relevant pathways. This study utilised pathway-enrichment analysis to achieve this mechanistic insight, and categorised prioritised variants into the most significantly enriched signal transduction pathways. Pathways for which the candidate genes and corresponding prioritised variants were significantly enriched according to the KEGG-database (Kanehisa & Goto, 2000) include the autophagy pathway, mitophagy pathway, NOD-like receptor pathway and KSHV pathway (Table 3.3., Supplementary figure 2.). Additionally, due to the known overlap between the autophagy profile in both neuropsychiatric disorders and neurodegenerative diseases, prioritised variants previously implicated in SCZ or neurodegenerative disease, as per literature findings (Supplementary table 6.), were respectively categorised as such for further analysis.

The significant enrichment of these pathways in this study is not unwarranted. Considering the implication of the mitophagy pathway in both neuropsychiatric (Bernstein *et al.*, 2020) and neurodegenerative disease (Kitada *et al.*, 1998; Valente *et al.*, 2004), as well as its role in antipsychotic drug-metabolism (Vucicevic *et al.*, 2014), this pathway is a prime candidate for ATR studies. The KSHV pathway, on the other hand, has a direct impact on xenophagy, and comprises genes that encode for inhibitory proteins that target different phases of the autophagic process (Klionsky *et al.*, 2016; Lee, Li, Lee, *et al.*, 2009; Liang, Chang, Brulois, *et al.*, 2013). A growing body of evidence suggests that the eight viruses that belong to the family of human Herpesviridae are indeed a risk factor for developing SCZ (Arias, Sorlozano, Villegas, *et al.*, 2012; Brown, 2011; Cannon, Laney & Pellett, 2003; Dickerson, Kirkpatrick, Boronow, *et al.*, 2006; Prasad, Watson, Dickerson, *et al.*, 2012; Yolken, Torrey, Lieberman, *et al.*, 2011). Human herpesvirus-8 (HHV8) was the most recently discovered of these viruses and has been identified to be implicated in the development of Kaposi sarcoma (Cannon *et al.*, 2003), hence the name “Kaposi’s sarcoma-associated herpesvirus infection”.

Therefore, with known previous associations between the significantly enriched pathways in this study and drug-metabolism, positive symptoms of SCZ, and SCZ risk, there is strong evidence to suggest that an association between ATR and the prioritised variants of this study exists, and this could be highlighted by analysing the distinct signal transduction pathways.

4.2.2. Association analysis reveals autophagic genetic variants predict ATR

Association analyses were performed in this study to investigate the potential presence of associations between prioritised genetic variants and ATR, as determined by the change in log-transformed PANSS scores over time. These analyses revealed 10 unique significant associations between four genetic variants within four different candidate genes and antipsychotic treatment outcomes that were below the Bonferroni-corrected α-value threshold (Table 3.6. and Table 3.7.). Interestingly, these genetic variants were found to be predictive of a worsened treatment outcome, specifically with regards to the PANSS Negative symptom domain. These variants were rs11819869 in *AMBRA1*, rs1538257 in *ATG14*, rs222843 in *GABARAP* and rs1043424 in *PINK1.* Whilst all of these associations were a novel finding in terms of ATR (to our knowledge), previous studies have identified an association between rs11819869 in *AMBRA1* and SCZ risk (Rietschel *et al.*, 2012). Of greater interest are the associations identified in previous studies between rs222843 in *GABARAP* and rs1043424 in *PINK1,* which respectively have been found to be associated with vulnerability to nicotine dependence and predicting treatment outcome in colorectal cancer, further highlighting the complexity of the ATR trait and its overlap with other disorders and treatment response phenotypes.

Whilst significant associations between genetic variants and ATR provide promising insight into the mechanisms governing treatment response, trends towards significant associations present with a comparable relevance when considering complex traits and diseases such as ATR and SCZ. The importance of acknowledging the trends towards significance in neuropsychiatric disorders has been highlighted by

Schork and colleagues (Schork, Won, Appadurai, *et al.*, 2019). Thus, whilst this study reports on the significant associations discovered between genetic variants and ATR, trends towards significance are likewise paid heed.

4.2.2.1. Significant associations between variants and ATR all predict a worsened treatment outcome for the PANSS Negative symptom domain

4.2.2.1.1. *AMBRA1* variant rs11819869 and ATR

In this study, the rs11819869 variant in *AMBRA1*, specifically the *TT* genotype, was identified to be significantly associated with a worsened treatment outcome within the mitophagy pathway and the SCZ pathway, under the genotypic model of inheritance (Table 3.6.). Further supporting this is the significant association between the *T* allele of the rs11819869 variant and a worsened treatment response for the Negative symptom domain, identified within the mitophagy pathway under the additive allelic model of inheritance (Table 3.7.). Upon further investigation into the functional and regulatory impact of this variant (Supplementary table 4 and Supplementary table 5), it was revealed that this variant is predicted to affect *AMBRA1* gene expression by modulating activities of distal regulatory elements (Guo *et al.*, 2014). Further, rs11819869 has been predicted to be an expression quantitative trait locus (eQTL) of the *AMBRA1* gene (Supplementary table 5). Upon further investigation, it is evident that this eQTL prediction is supported by single tissue expression data analysed within GTEx (GTEx Consortium, 2013), whereby the *TT* genotype is associated with an enhanced expression of the neighbouring gene *PACSIN3* in the cerebellum (normalised effect size: 0.3; P-value: 2.5×10^{-5}; available at https://www.gtexportal.org/home/snp/rs11819869, accessed 6 March 2021). Interestingly, rs11819869 is additionally predicted to play a role in RNA-binding protein mediated regulation as per rSNPBase (Guo *et al.*, 2014) (Supplementary table 5.). These RNA-binding proteins control gene expression through the stabilisation and destabilisation of mRNAs in response to stress or extracellular signals, and their alteration have previously been associated with various diseases (Lukong, Chang, Khandjian, *et al.*, 2008), including SCZ (Chénard & Richard, 2008).

As *AMBRA1* is a positive regulator of the autophagy key player *BECN1*, and because antipsychotic agents have been shown to act on the AMPK-ULK1-BECN1 signalling pathway in a rat model (Kim *et al.*, 2018), it is entirely plausible that any disruption in *AMBRA1* gene expression by variant rs11819869 would result in ineffective drug metabolism and a coupled variation in antipsychotic treatment outcome. The same holds true for any neighbouring genes this variant disrupts that play a role in this crucial pathway. While there is currently a paucity in the literature concerning a relationship between autophagy genes and variants and ATR, the findings of this study are indirectly supported by previous literature. The literature does however implicate rs11819869 and other variants within *AMBRA1* to be associated with both SCZ and autism spectrum disorder (Mitjans, Begemann, Ju, *et al.*, 2017; Rietschel *et al.*, 2012). In fact, rs11819869 has previously been shown to alter impulsivity-related traits on a behavioural and imaging genetics level (Heinrich, Nees, Lourdusamy,

et al., 2013; Rietschel *et al.*, 2012). This is predictable, as *AMBRA1* is a gene with a crucial role in neurodevelopment and its complete knock-out in animal models has been shown to lead to severe brain morphological defects (Maria Fimia *et al.*, 2007; Mizushima & Levine, 2010; Vázquez, Arroba, Cecconi, *et al.*, 2012).

4.2.2.1.2. *ATG14* variant rs1538257 and ATR

In this study, the *TG* genotype of rs1538257 in *ATG14* was discovered to be significantly associated with a worsened treatment outcome in the enriched KSHV infection pathway, as well as trending towards significant associations in the autophagy pathway and neurodegenerative disease pathway (Table 3.6.). Upon further investigation into the functional and regulatory roles of this variant, it was revealed that this variant is predicted to be a regulatory variant, potentially altering gene expression by modulating the actions of both proximal and distal regulatory elements of *ATG14*. Additionally, as indicated by RegulomeDB (Boyle *et al.*, 2012), this variant is predicted to be an eQTL and affect transcription factor binding (Supplementary table 5). Therefore, this variant has potential regulatory power over the expression of *ATG14* and could play a notable role in drug action. Upon further investigation using the gene expression data available on GTEx (GTEx Consortium, 2013), it is evident that this variant is indeed an eQTL and in addition to being associated with the disruption of *ATG14* expression in the cerebellum and basal ganglia, it is also associated with a disruption of gene expression of *RP11-665C16.6*, *WDHD1* and *FBXO34* in the frontal cortex, basal ganglia and cerebellum, respectively (available at https://www.gtexportal.org/home/snp/rs1538257, accessed 6 March 2021). As is the case with *AMBRA1* and *BECN1*, *ATG14* is involved in the core nucleation phase of autophagy, and thus any mutations in this gene lead to impaired autophagosome formation. Further, the antipsychotic medication utilised in this study, flupenthixol decanoate, has been shown to act directly on this pathway (Dong *et al.*, 2019) to induce autophagy (Figure 4.1.). As autophagy is an essential factor in drug action, rs1538257 of *ATG14* impairing autophagy and potentially blocking the interaction of this drug with the proteins of the pathway could explain why rs1538257 was identified to be associated with a worsened treatment outcome in this study. Another interesting aspect is the fact that this significant association occurred within the KSHV pathway. This virus is known to encode for inhibitory proteins that target various stages of autophagy (Klionsky *et al.*, 2016; Lee *et al.*, 2009; Liang *et al.*, 2013), and a high prevalence of this viral infection (HHV8) has been identified in a cohort of 108 SCZ patients (Hannachi, El Kissi, Samoud, *et al.*, 2014). Moreover, they showed that there was a statistically significant association with this viral infection and positive symptoms, assessed using the Scale for the Assessment of Positive Symptoms (SAPS), which is a rating scale utilised to measure positive symptoms in SCZ (β-coefficient = -0.263, P-value = 0.014, CI 0.598 to 0.989) (Andreasen, 1984; Hannachi *et al.*, 2014). Whilst a direct comparison cannot be made between the findings of this study and the abovementioned study (Hannachi *et al.*, 2014) due to the absence of viral-infection status of the cohort, the effect of these identified variants on viral infection and coupled drug response would be an interesting aspect to investigate in the future.

4.2.2.1.3. *GABARAP* variant rs222843 and ATR

The *GABARAP* variant rs222843 was identified to be significantly associated with a worsened treatment response for the PANSS Negative symptom domain in this study under the genotypic model of inheritance, specifically the *GG* genotype (Table 3.6.). These significant associations occurred within the pathways responsible for selective autophagy, namely the mitophagy pathway, the NLR pathway and the KSHV pathway. Assessment of trends towards significance revealed that the *G* allele of rs222843 was indeed trending towards an association with a worsened treatment response within these pathways (Supplementary table 10, Supplementary table 12 and Supplementary table 14). By investigating the variant's functional and regulatory impact (Supplementary table 4 and Supplementary table 5), it is evident that the significant associations with ATR are supported. For instance, rs222843 is predicted to be an eQTL site in both brain and nerve tissues (GTEx Consortium, 2013), affect transcription factor binding, and increase DNAse activity (Supplementary table 5). Furthermore, it is predicted to be a regulatory variant, modulating the activity of both proximal and distal elements (Supplementary table 5). *GABARAP* is known to interact with the γ_2-subunit of the $GABA_A$-receptor, and interactions between these two, as well as with tubulin, have been shown to enhance clustering of the receptor, alter its channel kinetics and increase its trafficking to the plasma membrane in neurons (Chen, Wang, Vicini, *et al.*, 2000; Leil, 2004; Wang, Bedford, Brandon, *et al.*, 1999). Whilst the antipsychotic medication utilised in this study is a D_1- and D_2-receptor antagonist, there is a well-established antagonistic relationship between dopaminergic and GABAergic neurons (Bouarab, Thompson & Polter, 2019; Valenti & Grace, 2010). Thus, rs222843 could be decreasing the number of available $GABA_A$-receptors, and consequently increasing the excitation of dopaminergic neurons through the mediation of fast synaptic inhibition mechanisms (Vithlani, Terunuma & Moss, 2011). Hence, the action of the antipsychotic medication might not be enough to circumvent this increase in excitability of dopaminergic neurons, thus contributing to a worsened treatment outcome. To our knowledge, the findings of this study present a novel association between rs222843 and ATR. Previous studies have however discovered variants within *GABARAP* to be associated with nicotine and alcohol dependence (Cui, Seneviratne, Gu, *et al.*, 2012; Lou, Ma, Sun, *et al.*, 2007), and deletions in the related gene *GABARAPL1* have additionally been identified in individuals with autism spectrum disorder (Griswold, Ma, Cukier, *et al.*, 2012), which provides further evidence for the intricate overlap between neurodevelopmental and neuropsychiatric disorders.

As an omnipresent receptor expressed in the brain, $GABA_A$-receptors play a critical role in regulating synaptic processes (Kaar, Natesan, McCutcheon, *et al.*, 2020). Moreover, the α_5-subtype of the $GABA_A$-receptor has recently gained traction as a therapeutic target in SCZ (Kaar *et al.*, 2020), supporting the implication of rs222843 in differential treatment outcomes. Due to the high degree of heterogeneity in GABA receptor subtypes, as well as the wide distribution of these receptors within the brain, GABA receptors have great therapeutic potential as primary targets for certain antipsychotics. For instance, a study investigating the ability of olanzapine (Eli Lilly and Company, 1996, 2006) to trigger neuronal autophagy in mice, discovered

that the administration of this atypical antipsychotic drug increased the levels of mRNA encoding *GABARAP*, as well as the majority of other genes implicated in the elongation phase of autophagy, thus indicating the induction of autophagy (Figure 4.1.) (Vucicevic *et al.*, 2014). Of note, this study subsequently utilised the inhibition of autophagy to reveal the neurotoxic effects of olanzapine, and provided evidence for autophagy acting as a protective mechanism against olanzapine-mediated neurotoxicity (Vucicevic *et al.*, 2014).

According to a study that investigated the role of rs222843 in nicotine addiction, this variant is situated in the promoter region of GABARAP, and the *G* allele contributes to an increase in expression of *GABARAP* by nearly two-fold (Cui *et al.*, 2012; Lou *et al.*, 2007). This is specifically interesting, as in this study, it is the *GG* genotype that contributes towards a worsened treatment outcome. Further, in this study, this association with a worsened treatment outcome was specifically for the PANSS Negative symptom domain. This is plausible, as the negative symptoms of SCZ have been hypothesised to manifest due to reduced D_1-receptor activation in the prefrontal cortex, decreased activity of the caudate nucleus, as well as potential alterations in D_3-receptors (extensively reviewed by Brisch, Saniotis, Wolf, *et al.*, 2014). In line with this, there is evidence for D_1-receptors in GABAergic interneurons (Goldman-Rakic, Muly & Williams, 2000). Thus, the overexpression of *GABARAP*, as well as the antipsychotic medication-influenced hyperactivity decrease of the mesolimbic dopaminergic pathway (Brisch *et al.*, 2014), could both potentially lead to the inhibition of dopaminergic neurons thus contributing to negative symptoms. This is in line with the previous literature which predicts that the negative symptoms of SCZ are either directly or indirectly associated with GABAergic function (Taylor, Demeter, Phan, *et al.*, 2014). Unfortunately, poor treatment response is a very real challenge in the treatment of neuropsychiatric disorders such as SCZ. As most antipsychotic drugs target DRD_2 in the dopaminergic system, the one third of SCZ patients who have functional dopaminergic systems thus will not respond to these dopamine-specific drugs (Ackenheil & Weber, 2004). Interestingly, recent studies suggest that FES patients who are non-responders to antipsychotic treatment have glutamatergic and GABAergic abnormalities, specifically a higher level of glutamate (Bojesen, Ebdrup, Jessen, *et al.*, 2020; Egerton, Broberg, Van Haren, *et al.*, 2018; de la Fuente-Sandoval, Reyes-Madrigal, Mao, *et al.*, 2018), compared to responders who have a higher level of striatal dopamine activity (Wulff, Nielsen, Rostrup, *et al.*, 2019).

The evident role of $GABA_A$-receptors supports the association between the rs222843 variant and ATR identified in this study. Furthermore, as GABA neurons are expressed ubiquitously in the brain, the alteration in expression of *GABARAP* by rs222843 could render downstream effects not limited to the mesolimbic system, ultimately contributing to a worsened treatment outcome, specifically for negative symptoms of SCZ.

4.2.2.1.4. *PINK1* variant rs1042434 and ATR

The final variant identified to be significantly associated with treatment response as predicted by log-transformed PANSS scores was rs1042434 in *PINK1*. Specifically, the significant association took place within

the mitophagy and neurodegenerative disease pathways, between the *CC* genotype of rs1042434 and worsened ATR for the PANSS Negative symptom domain under the genotypic model of inheritance (Table 3.6.). Further, there is a trend toward a significant association between the *C* allele of rs102434 and worsened treatment response, according to the additive allelic model of inheritance for the mitophagy and neurodegenerative disease pathway (Supplementary table 10 and Supplementary table 18). By solely looking at the predicted regulatory and functional impact of this variant, the significant association with treatment response could be expected (Supplementary table 4 and Supplementary table 5). This variant is a missense variant according to Ensembl (Yates *et al.*, 2020). While this nonsynonymous mutation is predicted to be benign, this variant is predicted to affect transcription factor binding and to regulate the expression of *PINK1* through distal elements. Additionally, rs1042434 is predicted to mediate RNA binding proteins, thus fine-tuning the expression of *PINK1*. Upon further investigation in GTEx (GTEx Consortium, 2013), it was revealed that indeed the *CC* genotype of this variant is associated with a decreased expression of *PINK1* (cortex, putamen and cerebellum) as well as the neighbouring gene *FAM43B* (cerebellum and cerebellar hemisphere) (according to https://www.gtexportal.org/home/snp/rs1043424, accessed 6 March 2021). As *PINK1* is a vital gene within the mitophagy pathway, any dysregulation could result in an impairment of mitophagy and the inability to adapt to changing environments. Previous literature shows that certain antipsychotic drugs can have a damaging effect on mitochondria and a subsequent activation of the mitophagy pathway (Vucicevic *et al.*, 2014), thus necessitating the optimal functioning of this pathway, including the genes therein. Therefore, a mutation within a gene as critical as *PINK1* could mean that the damaging effects of the antipsychotic are compounded, with a failed activation of the mitophagy pathway ultimately resulting in a worsened treatment outcome.

4.2.2.2. Evidence in support of intertwined relationship between ATR, autophagy integrity and age-related disorders and diseases

An additional noteworthy finding of this study provides further evidence in support of the intricate overlap between the autophagy profiles in neuropsychiatric disorders and neurodegenerative diseases, and the cascading effect that impairment in the autophagy profile has on ATR (Figure 1.3.). Specifically, this study identified an intertwined relationship between the induction stage of the autophagy pathway and the longevity pathway (an enrichment of *ATG13* in longevity pathway depicted in Supplementary table 21). ATG13 is a stabilising entity within the complex required for autophagy induction (ULK1/2-ATG13-RB1CC1) (Jung, Jun, Ro, *et al.*, 2009), and acts as a direct substrate of the mTOR pathway, emphasising the critical role of ATG13 in the activation of autophagy and maintaining neuronal integrity. A plethora of studies exist providing evidence for the entanglement between lifespan regulation pathways and cognitive decline or neurodegeneration (reviewed extensively in (Gkikas, Petratou & Tavernarakis, 2014). For instance, aging is known to be the number one risk factor for neurodegenerative diseases. Additionally, both neuropsychiatric disorders such as SCZ, as well as neurodegenerative diseases, are considered to be age-related disorders due

to their known association with age-related memory impairment amongst other symptoms. Thus, the findings of this study are in line with previous literature considering the overlap depicted in Figure 1.3. Furthermore, variants within *ATG13* (rs10769204, rs10838610 and rs13448) were identified to be trending towards a significant association with ATR (Supplementary table 7, Supplementary table 8, Supplementary table 15, Supplementary table 16, Supplementary table 19, Supplementary table 20). These associations showed that under the genotypic model of inheritance, the variants were predictive of an improved treatment outcome (rs10769204; *TT* vs *CC* genotype, where each *T* allele contributes to an improved response according to the additive allelic model of inheritance and rs10838610; *AA* vs *GG* genotype where each *A* allele contributes towards an improved response) and a worsened treatment outcome (rs13448; *CT* vs *TT* genotype) respectively, all for the PANSS Negative symptom domain.

4.2.2.3. The abundance of significant associations with the PANSS Negative symptom domain

The treatment of negative symptoms has long since posed an issue, with no specific treatment showing benefits over another. Currently, there is a lack of evidence-based treatments of negative symptoms, as well as limited understanding regarding the aetiology and pathophysiology related to the negative symptoms of SCZ (Remington, Foussias, Fervaha, *et al.*, 2016).

The findings of this study, specifically the exclusivity of significant associations between variants and poorer treatment response for negative symptoms (Table 3.6. and Table 3.7.), are particularly interesting if one considers that most antipsychotic medications are designed to treat positive symptoms of SCZ (Lee, Takeuchi, Fervaha, *et al.*, 2015). Furthermore, Barnes, Huxley-Jones, Maycox, *et al.* (2011) performed a transcriptional analysis of mRNA expression levels in post-mortem samples from 19 controls and 23 SCZ patients and discovered that an alteration in autophagic gene expression was present in the brain region responsible for the development of positive symptoms (Brodmann area 22). Interestingly however, this autophagic dysregulation was not present in the brain region associated with negative symptoms of SCZ (Brodmann area 10). Hence, this is inconsistent with the findings of this study, where multiple significant associations were identified between autophagic genetic variants and negative symptoms of SCZ, albeit in the context of treatment response. Thus, this study provides evidence for new therapeutic targets and pathways for the respite against the negative symptoms of SCZ.

An intriguing finding of the same study (Barnes *et al.*, 2011), is the identification of a significant enrichment of the process of cell adhesion mediated by amyloid proteins, with marginal gene expression changes in amyloid proteins in the Brodmann 10 brain region. Whilst these gene expression changes were not significant, it does suggest a potential link between SCZ negative symptoms and amyloid pathology (supported by (Seshadri, Kamiya, Yokota, *et al.*, 2010)), which in itself could be affecting autophagy functioning (Bar-Yosef *et al.*, 2019). This provides further support for the overlapping autophagy impairment in SCZ and neurodegenerative disease proposed in this study and emphasises the warrant for further

investigation into the exact involvement of the autophagy mechanism in the worsened treatment trajectory for negative symptoms.

4.3. *In vitro* model

4.3.1. New *in vitro* model provides insight into disease-related impairments of autophagy

To our knowledge, of the minimal studies that have utilised iNs in the context of SCZ (Passeri, Jones-Brando, Bordón, *et al.*, 2016; Passeri, Wilson, Primerano, *et al.*, 2015; Siegert, Seo, Kwon, *et al.*, 2015), there are no studies that investigate the autophagy mechanism in SCZ patients. This highlights the immense gap in knowledge surrounding the autophagy mechanism in a SCZ-context and emphasises the need for SCZ-based studies to uncover the genetic and physiological underpinnings of the autophagy mechanism to gain insight into the age-dependent pathogenesis of SCZ as well as differential treatment outcomes. The findings of this study could perhaps provide direction in this regard, both genetically (Section 3.2.3.) and physiologically (Section 3.3.). In this study, primarily due to available resources, the applicability of the iN cellular model to age-related diseases, as well as the fact that the autophagy mechanism is far better studied in the context of neurodegenerative diseases, an iN model was utilised by means of HD patient-derived fibroblasts (Figure 3.2. A). These iNs were then subsequently treated with an autophagy-inducing pharmacological agent, namely Torin1. Whilst Torin1 could efficiently activate autophagy in the control-iNs, the same efficient induction effect was not evident in the HD-iNs (Figure 3.3.). Further, following HCS analyses and immunocytochemical analyses, it was discovered that the HD-iNs indeed exhibited a distinct morphological phenotype, specifically less elaborate neurites with regards to neurite width and count, as well as a larger soma (Figure 3.2. G - J).

Considering the response of the HD- and control-iNs to the autophagy-inducing agent Torin1, there are several aspects to note. Firstly, the mHTT protein, characteristic of HD, had a direct effect on the basic functioning of the autophagy pathway (Figure 3.3.). This is evident by the increase in total LC3 puncta (and therefore autophagosomes) abundance coupled with a decrease in size of LC3 puncta (autophagosomes) in the HD-iN soma (Figure 3.3. I and J). As the lipidated form of LC3 (LC3-II) is ultimately removed from the mature autophagosome outer membrane (reviewed in Yang & Klionsky, 2010), the findings of this study could be indicative of a late stage autophagy defect, where a failure in the maturation of autophagosomes exists and thus fusion with the lysosome does not ensue. This late-stage autophagy defect is entirely plausible, seeing as advanced forms of HD are associated with progressive defects of the lysosome and proteasome (Cortes & La Spada, 2014). Additionally, a less complex neurite morphology of the HD-patient iNs versus the control-iNs (Figure 3.2.) was observed, and this has been detected in several other models of HD, including post-mortem tissue (Ferrante, Kowall & Richardson, 1991; Liu *et al.*, 2014; Rong, McGuire, Fang, *et al.*, 2006; Victor, Richner, Olsen, *et al.*, 2018). In order to induce autophagy, the effects of the pharmacological agent had to overcome the damaging effects of mHTT. In the case of this study, this was unsuccessful, and the iNs were largely unresponsive, suggesting an autophagy dysfunction. Different drivers could exist for this

dysfunction. Firstly, it is possible that Torin1 was indeed successful in activating the initial stages of autophagy, (hence the increase in the number of autophagosomes/LC3 puncta present in the neurites of the treated *versus* non-treated HD-iNs; Figure 3.3. K and L), and the autophagosomes were successfully transported towards the soma (Maday *et al.*, 2012), yet the failure occurred downstream in the autophagy pathway (hence the lingering presence of the autophagosomes/LC3 puncta in the soma; Figure 3.3. I). Secondly, it is plausible that the increase in autophagosomes in both the neurite and soma (Figure 3.3.) represent the increase in formation of empty autophagosomes in the HD-iNs (Vicente *et al.*, 2010), which is plausible given that cargo recognition failure is a common occurrence in HD patient-derived cells (Martinez-Vicente *et al.*, 2010). Further, perhaps what has been observed in this study is a combination of both – an effective induction of autophagy in the HD-iNs, followed by the increased formation of empty autophagosomes, and the inadequate elimination of these autophagosomes due to other mHTT-mediated effects.

The HD patients included in this study were characterised by differing CAG-repeat domains, ranging from 39 to 42 CAG-repeats when considering the upper limit predicted (Table 2.1.). Risk of developing HD ranges according to the number of CAG-repeats an individual possesses within the *HTT* gene. While it is not certain that individuals with 36 to 39 CAG-repeats will develop HD symptoms (most of them will not), individuals with more than 40 CAG-repeats will undoubtedly develop the disease (Ross & Tabrizi, 2011). Thus, interesting to note is the fact that within this study, individuals with HD possessing 39 CAG-repeats had an autophagy impairment equivalent to those with a higher number of CAG-repeats. Whilst the data per individual is not shown, it was evident that the HD-iNs derived from individuals with 39 CAG-repeats (HDKP and HDRH; Table 2.1.) displayed similar autophagy profiles compared to HD-iNs derived from individuals with a higher number of CAG-repeats, thus variation in CAG-repeat number did not seem to influence autophagy impairment. That said, however, as only 6 cell-lines were used in triplicate for this study, it is imperative that this is investigated in a larger cohort to verify whether there indeed is no association between the number of CAG-repeats in an individual with HD and the extent to which the autophagy mechanism of their cells is impaired.

Although an HD model was utilised in this study as opposed to a SCZ model, this experiment still emphasises the intricacies involved in the activation of the autophagy pathway in a diseased-state, and highlights the probable hurdles to be expected when studying the autophagy mechanism in a SCZ context. Specifically, this model allows valuable insight into an autophagy mechanism that is negatively regulated by both genetic (mHTT) and environmental (pharmacological agent) factors, and in this regard is similar to the autophagy mechanism in SCZ (Figure 1.3.). Further, a valuable lesson can be drawn from this model when considering the study of the autophagy pathway in SCZ: HD is a heritable neurodegenerative disease with a specific mutated protein, mHTT, that directly alters pathways and causes downstream effects, and this was evident when observing the autophagy mechanism in this study (Figure 3.2. and Figure 3.3.). A similarly complex scenario exists in SCZ. SCZ is a complex disorder with an array of interacting factors that function in a vast

collection of pathways to eventually culminate as the disorder. Thus, when using this iN model to investigate the autophagy mechanism in SCZ, it is imperative to focus on the malfunctioning of the autophagy pathway and to investigate how and which antipsychotic medications affect the autophagy process, and whether they can successfully rescue the dysregulation of autophagy evident in SCZ. Additionally, from a neuropsychiatric disorder standpoint, using an antipsychotic drug that activates or inhibits autophagy regardless of the physiological effects of SCZ should be taken into consideration. Finally, considering the pharmacological agent utilised in this study, Torin1 is an mTOR-dependent autophagy inducer (Figure 4.1.). Interestingly, studies have shown that antipsychotic medications used to treat SCZ such as pimozide (Kim, Jeong, Nah, *et al.*, 2017), clozapine (Kim *et al.*, 2018) and chlorpromazine (Shin *et al.*, 2013) act in a similar manner to Torin1, enhancing autophagy *via* mTOR inhibition (Figure 4.1.). Nevertheless, the extent of autophagy impairment in SCZ is yet to be determined and the effect of these Torin-like antipsychotic medications should be tested directly on SCZ-iNs. Finally, perhaps the solution to the inefficient activation of autophagy in HD-iNs in this study is to use a pharmacological agent that activates autophagy independent of mTOR (Rubinsztein, Codogno & Levine, 2012; Sarkar, 2013).

4.4. Genetic studies in diverse populations

In this study, the majority of the FES patients were of SA Mixed-Ancestry - a highly admixed, and thus genetically diverse population. This study thus contributes to the genetic data concerning African populations, for which there is currently a grave underrepresentation in genetics-based studies (Sirugo, Williams & Tishkoff, 2019). In fact, as of 2018, most GWAS studies that aimed to identify genetic variants associated with complex traits were based on European (52%) or Asian (21%) populations, with the percentage of African studies amounting to a deplorable 9.56% (Sirugo *et al.*, 2019). This underrepresentation of ethnically diverse populations contributes to the ineffective treatment strategies and overall immense knowledge gap surrounding complex diseases and traits (Sirugo *et al.*, 2019). This is because genetic associations identified within non-African populations cannot necessarily be replicated in African or other ethnically diverse populations. This is due to several factors, namely: i) differences in LD across ethnicities which influence the accuracy of tagging SNPs capturing causal variants in a single population; ii) differences in genetic architecture due to population-specific variation and changes in allele frequencies as a result of genetic drift, local selection or both; iii) local adaptation; iv) epistasis due to differences in genetic backgrounds (G x G); and v) gene-environment (G x E) interactions that differ across population groups (Sirugo *et al.*, 2019). This emphasises the need for genetic studies to be performed on diverse populations, and this is particularly important in studies that focus on drug response. For instance, in European populations, causal variants within *CYP2C9, VKORC1*, and *CYP4F2* genes were identified to be associated with drug response, but when investigated in populations of African descent these SNPs were unable to explain any variance in drug metabolism (Johnson, Caudle, Gong, *et al.*, 2017).

Thus, due to low levels of LD within the population of this present study, any associations identified within this study could potentially inform on therapeutic development, precision medicine initiatives, and contribute to global equity in relation to genomics (Hindorff, Bonham, Brody, *et al.*, 2018).

CHAPTER 5. LIMITATIONS, FUTURE PROSPECTS AND CONCLUSION

5.1. Limitations of this study

The small sample size could potentially be viewed as a limitation of this study. However, as an exploratory analysis with a primary focus of investigating the presence and subsequent extent of certain associations, the current cohort does not hinder this purpose and successfully provides insight into the research question. Further, albeit small, the cohort is extremely well clinically-characterised. This is captured in the way that all SCZ patients were first-episode and treatment-naïve at the commencement of this study. Additionally, patients were treated with the same long-acting injectable antipsychotic (thus ensuring adherence throughout the 12 months). Thus, confounders relating to stage of illness, treatment duration, drug heterogeneity and non-adherence were not an issue. Additionally, it has been hypothesised that pharmacogenetic studies that use a cohort comprising of FES patients potentially provide enhanced power when investigating treatment response (Zhang & Malhotra, 2013). Finally, a study by Samuels, Burn & Chinnery (2009) has argued that smaller, well-characterised cohorts maintain the same power as larger cohorts of patients that are characterised to a lesser extent.

In this study, the common disease-common variant (CD-CV) approach was used, which assumes that complex traits such as ATR are rather the culmination of many variants with small effect sizes, rather than just a few causal variants contributing towards the trait's genetic and phenotypic makeup (also known as the infinitesimal or polygenic model; (Barton, Etheridge & Véber, 2017)). In this study, the MAF was accordingly set at ≥ 0.05 (Section 2.5.2.). Therefore, some variants were excluded from further investigation regardless of whether they were explicitly considered to be rare or common within the cohort; this approach thus automatically excludes variants that simply lay on the cusp of presenting as common variants within the cohort. This issue is further compounded by the fact that the cohort used in this study was genotyped using HumanOmniExpressExome BeadChip (Illumina), which genotypes over 240 000 functional exonic markers as well as over 700 000 genome-wide markers that provide coverage of common variants with a MAF > 0.05 (Illumina, 2011). Therefore, genes which are known to have a critical role in autophagy and that could potentially provide valuable information regarding treatment response in this cohort, for instance *BECN1*, had zero variants that survived the MAF threshold in this study.

Similarly, when considering the CD-CV *versus* rare variant approach, most approaches focus solely on the contribution of one or the other (either of rare or common variants). Whilst this is widely accepted, there is strong empirical evidence for the contribution of both extremes within complex diseases. Research over the years has stressed the importance of the contributions of rare variants in the genetics of complex disease. For instance, nearly a decade ago, Gibson hypothesised that common variants establish background risk for complex diseases, and environmental effects and rare variants provide the necessary momentum that

ultimately results in an individual developing a disease (Gibson, 2012). Current views are very much in line with this, especially due to the now widespread use of whole-genome sequencing and imputation technologies, which allow for the identification of rare variants (Momozawa & Mizukami, 2020). Additionally, these authors emphasise the distinguished roles that rare variants play in complex disease due to their distinctive features. Specifically, because rare variants display lower LD with flanking variants, they provide hypothesis-free evidence for gene causality. Further, due to their large effect on gene functionality and expression, as well as their population specificity, they serve as a precise target for drug functional analysis to gain insight into disease mechanisms. (Momozawa & Mizukami, 2020). Additionally, autophagy is a mechanism that is constitutive and very well-conserved among organisms, and thus perhaps a rare variant, large effect size approach could be insightful with regards to identifying causal autophagic variants contributing towards phenotypic variation in the ATR trait. Therefore, the fact that a wider allele frequency range was not utilised in the current study could be considered a limitation.

Although the action of log-transforming PANSS scores contribute to the improvement of linearity and homoscedasticity of linear regression models, there are some limitations that encumber this method. For instance, whilst log-transforming the outcome variable to satisfy model assumptions is a common procedure in linear regression analyses, most model diagnostics are based on visual assessments and can thus be highly subjective. In the case of this study, perhaps the use of nonparametric statistical models would be more informative considering the variance of PANSS scores (Lever, Krzywinski & Altman, 2016), thus avoiding overfitting of data and improving the fidelity of results. Furthermore, in this study, to determine the association between log-transformed PANSS scores and different genotypes or number of minor alleles over time, raw effect estimates were utilised. Whilst the raw effect estimate is indicative of the direction of ATR, one would have to back-transform the effect estimate and express it as a percentage of change in PANSS score over time to gain more context of the impact of the variant on ATR. However, due to the small sizes of the raw effect estimates, emphasis was rather placed on the direction of response for the purpose of this exploratory analysis.

With regards to the *in vitro* model, the sole use of the mTOR-inhibitory drug, Torin1, could be considered a limitation. Since the mTORC regulates crucial mechanisms such as protein translation and cell growth, perhaps expanding the range of pharmacological agents used to include a pharmacological agent that induces autophagy independently of the mTORC would be a safer option from a clinical standpoint (Rubinsztein *et al.*, 2012; Sarkar, 2013) (Figure 4.1.). Indeed, this combinatory treatment targeting both mTOR-dependent and -independent pathways is supported in literature. Research shows that a combinatory treatment targeting both pathways demonstrates great efficacy in terms of activating autophagy and allows for a significant rescue in neurodegeneration in fly models of HD (Sarkar, Krishna, Imarisio, *et al.*, 2008). Thus, this provides a point of reference for future endeavours concerning the pharmacological activation of autophagy in SCZ iN models.

An additional potential limitation of the *in vitro* model is the fact that the iNs were of a pan-neuronal subtype. Medium spiny neurons within the striatum are particularly vulnerable to selective degeneration in HD, and thus perhaps this study would be rendered more informative if this subtype were used. The use of further differentiated patient-derived iNs into a subtype specific to the disease being investigated would allow insight into any additional disease-specific phenotypes that may be absent in the pan-neuronal iN model. Nevertheless, this study utilises the iN model as a point of departure for future studies focusing on autophagy impairment in SCZ, and thus the utilisation of HD-iNs of a pan-neuronal subtype assists in achieving the aim of this study, and paves the way for future studies to use SCZ patient-derived iNs.

5.2. Future considerations

The significant associations (Table 3.6 and Table 3.7) as well as trends towards significant associations (Supplementary table 7 to Supplementary table 20) between genetic variants and various treatment outcomes identified in this present study should be replicated in other homogenous cohorts to confirm the findings of this study. Additionally, the significant associations identified in this study (Table 3.6 and Table 3.7) provide ideal candidates for future functional analysis studies focusing on differential treatment response in SCZ. For example, SCZ patient-derived fibroblasts with the desired mutation (SNP) can be directly converted into iNs, and one could characterise the precise effect these mutations have on the dysregulation of the autophagy mechanism, and thus the overall contribution to differential response to antipsychotic drugs. In the event that SCZ patients do not harbour the desired mutation, fibroblasts can be targeted with gene-editing systems such as CRISPR (clustered regularly interspaced short palindromic repeats)/Cas9, thus inducing these specific mutations. This could provide insight of paramount importance into the metabolism of antipsychotic drugs in SCZ patients, as well as point towards more effective therapeutic strategies in SCZ as well as CNS disorders in general.

Additionally, as this study demonstrated genetic variations in the autophagic genes to be associated with differential treatment outcomes specifically in the PANSS Negative symptom domain, future studies should investigate how the autophagy machinery is regulated by these genetic variants and how this contributes to the worsening of these negative symptoms. Moreover, a special emphasis should be placed on the specific pathways identified in this study to be implicated in the negative symptoms of SCZ. This could potentially provide insight into new therapeutics for these symptoms, which is especially imperative since currently there is a lack of effective therapies that exist that target the negative symptoms of SCZ.

Future research could focus on the production of tests aimed at identifying proxy-biomarkers indicative of autophagy impairment. For instance, a test designed to detect proxy-biomarkers in tissues such as blood serves as a good starting point as blood is easily accessible and is amenable to predictive testing. Once the proxy-biomarkers have been identified, one would have more indication of the autophagy status of the individual and thus more insight into the potential effectivity of pharmacological agents. Additionally, going

one step further, the test could identify markers that give a specific indication of the stage of autophagy pathway malfunctioning, if any. This would provide further insight into potential therapeutic targets of the cell or tissue being investigated. Additionally, as the complexity of SCZ lends itself to a discrepancy in the nature of the disorder between patients, the autophagy defect might be characteristic to only some patients. In this case, a biomarker detecting the fidelity of the autophagy mechanism in an individual will allow for a more personalised treatment approach and is imperative for a more improved treatment strategy.

Future investigation into the autophagic flux of the *in vitro* model is warranted, utilising the data obtained for the lysosomal marker LAMP-1 (data not included as it is beyond the scope of this study). Further, as this *in vitro* model only utilised Torin1, the response to an autophagy enhancing drug was assessed and not autophagic flux *per se*. Future studies should thus focus on the quantification of autophagic flux, which can be performed by inhibiting one of the late-stage steps in the autophagic pathway (by means of bafilomycin or leupeptin for instance) and subsequently measuring the basal rate of accumulation in the substrate for the inhibited step (conceptually described and demonstrated in Loos, Toit & Hofmeyr, 2014). This will allow for the discernment between basal and induced autophagic flux and will provide insight regarding some of the hypotheses formulated in this study, particularly concerning the presence and absence of LC3-positive structures. Furthermore, future studies could employ electron microscopy techniques to evaluate ultrastructural detail such as the nature of cargo within autophagosomes to further elucidate the extent to which autophagy is impaired in a diseased state.

Further, as the iN model allows for the differentiation of iNs into specific neuronal subtypes, it would be informative for future studies to differentiate SCZ patient-derived fibroblasts into a subtype of iNs most highly implicated in the pathology of the disorder, namely dopaminergic, glutamatergic, serotonergic and GABAergic neurons. The subtype chosen should depend on the particular focus of the study.

5.3. Conclusion

This study provides insight into the genetic interplay between autophagy genetic variants and ATR, and as an exploratory study provides support for future research to investigate this in more detail. Specifically, this study elucidates genetically enriched pathways for candidate autophagy genes that contribute towards differential treatment response. By performing independent association analyses for the enriched pathways, this study was able to draw significant associations between autophagic genetic variants and differential treatment outcomes in a SA FES SCZ cohort. Specifically, associations between variants and a worsened treatment outcome for the Negative PANSS symptom domain were identified. Additionally, this study recapitulated the autophagy mechanism in an induced neuronal cellular model, thus providing insight into age-related diseases and the associated dysregulation of the autophagy mechanism. This study additionally highlights the paucity in the current literature in terms of studies investigating autophagy impairment in neuropsychiatric disorders, especially as a potential therapeutic target. Support is provided for future studies

to focus on the use of induced neuronal cellular models to characterise the autophagy mechanisms in SCZ. Additionally, studies should investigate the effect of various antipsychotic drugs on the autophagic mechanism in SCZ, specifically taking into account the potential of these drugs to ameliorate the negative symptoms of SCZ.

REFERENCES

Ackenheil, M. & Weber, K. 2004. Differing response to antipsychotic therapy in schizophrenia: Pharmacogenomic aspects. *Dialogues in Clinical Neuroscience*. 6(1):71–77.

Adzhubei, I., Jordan, D.M. & Sunyaev, S.R. (in press). Predicting Functional Effect of Human Missense Mutations Using PolyPhen-2. *Current Protocols in Human Genetics*. 76(1):7.20.1-7.20.41.

Adzhubei, I.A., Schmidt, S., Peshkin, L., Ramensky, V.E., Gerasimova, A., Bork, P., Kondrashov, A.S. & Sunyaev, S.R. 2010. A method and server for predicting damaging missense mutations. *Nature Methods*. 7(4):248–249.

Agholme, L., Agnello, M., Agostinis, P., Aguirre-ghiso, J.A., Ahn, H.J., Ait-mohamed, O., Brown, E.J., Brumell, J.H., et al. 2012. Guidelines for the use and interpretation of assays for monitoring autophagy. *Autophagy*. 8(April):445–544.

Albus, M. 2012. Clinical courses of schizophrenia. *Pharmacopsychiatry*. 45 Suppl 1(S 01):S31-5.

Alexander, D.H., Novembre, J. & Lange, K. 2009. Fast model-based estimation of ancestry in unrelated individuals. *Genome research*. 19(9):1655–64.

Alirezaei, M., Kemball, C.C., Flynn, C.T., Wood, M.R., Whitton, J.L. & Kiosses, W.B. 2010. Short-term fasting induces profound neuronal autophagy. *Autophagy*. 6(6):702–710.

Andreasen, N.C. 1984. Scale for the Assessment of Positive Symptoms. *Medicine*. 1984:1–21.

Andreasen, N.C., Carpenter, W.T., Kane, J.M., Lasser, R.A., Marder, S.R. & Weinberger, D.R. 2005. Remission in schizophrenia: proposed criteria and rationale for consensus. *The American journal of psychiatry*. 162(3):441–9.

Arias, I., Sorlozano, A., Villegas, E., Luna, J. de D., McKenney, K., Cervilla, J., Gutierrez, B. & Gutierrez, J. 2012. Infectious agents associated with schizophrenia: A meta-analysis. *Schizophrenia Research*. 136(1–3):128–136.

Aronson, J.K. & Ferner, R.E. 2005. Clarification of terminology in drug safety. *Drug safety*. 28(10):851–70.

Balaji, R., Subbanna, M., Shivakumar, V., Abdul, F., Venkatasubramanian, G. & Debnath, M. 2020. Pattern of expression of Toll like receptor (TLR)-3 and -4 genes in drug-naïve and antipsychotic treated patients diagnosed with schizophrenia. *Psychiatry research*. 285:112727.

Bar-Yosef, T., Damri, O. & Agam, G. 2019. Dual role of autophagy in diseases of the central nervous system. *Frontiers in Cellular Neuroscience*. 13(May):1–14.

Barnes, M.R.E., Huxley-Jones, J., Maycox, P.R., Lennon, M., Thornber, A., Kelly, F., Bates, S., Taylor, A., et al. 2011. Transcription and pathway analysis of the superior temporal cortex and anterior prefrontal cortex in schizophrenia. *Journal of Neuroscience Research*. 89(8):1218–1227.

Barrett, J.C., Fry, B., Maller, J. & Daly, M.J. 2005. Haploview: Analysis and visualization of LD and haplotype maps. *Bioinformatics*. 21(2):263–265.

Barton, N.H., Etheridge, A.M. & Véber, A. 2017. The infinitesimal model: Definition, derivation, and implications. *Theoretical population biology*. 118:50–73.

Bassan, M., Zamostiano, R., Davidson, A., Pinhasov, A., Giladi, E., Perl, O., Bassan, H., Blat, C., et al. 2008. Complete Sequence of a Novel Protein Containing a Femtomolar-Activity-Dependent Neuroprotective Peptide. *Journal of Neurochemistry*. 72(3):1283–1293.

Bates, D., Mächler, M., Bolker, B.M. & Walker, S.C. 2015. Fitting linear mixed-effects models using lme4. *Journal of Statistical Software*. 67(1).

Bates, G.P., Dorsey, R., Gusella, J.F., Hayden, M.R., Kay, C., Leavitt, B.R., Nance, M., Ross, C.A., et al. 2015.

Bell, C.C. 1994. DSM-IV: Diagnostic and Statistical Manual of Mental Disorders. *JAMA: The Journal of the*

American Medical Association. 272(10):828.

Bender, S., Grohmann, R., Engel, R.R. & Degner, D. 2004. Severe Adverse Drug Reactions in Psychiatric Inpatients Treated with Neuroleptics. *Pharmacopsychiatry*. 37:46–53.

Benes, F.M., Vincent, S.L., Marie, A. & Khan, Y. 1996. Up-regulation of GABA(A) receptor binding on neurons of the prefrontal cortex in schizophrenic subjects. *Neuroscience*. 75(4):1021–1031.

Berger, Z., Ravikumar, B., Menzies, F.M., Oroz, L.G., Underwood, B.R., Pangalos, M.N., Schmitt, I., Wullner, U., et al. 2006. Rapamycin alleviates toxicity of different aggregate-prone proteins. *Human Molecular Genetics*. 15(3):433–442.

Bernstein, H.-G., Keilhoff, G., Dobrowolny, H. & Steiner, J. 2020. Enhanced mitochondrial autophagy (mitophagy) in oligodendrocytes might play a role in white matter pathology in schizophrenia. *Medical hypotheses*. 134:109443.

Bhattacharya, A., Ziebarth, J.D. & Cui, Y. 2014. PolymiRTS Database 3.0: linking polymorphisms in microRNAs and their target sites with human diseases and biological pathways. *Nucleic acids research*. 42(Database issue):D86-91.

Bieri, G., Lucin, K.M., O'Brien, C.E., Zhang, H., Villeda, S.A. & Wyss-Coray, T. 2018. Proteolytic cleavage of Beclin 1 exacerbates neurodegeneration. *Molecular Neurodegeneration*. 13(1):68.

Bojesen, K.B., Ebdrup, B.H., Jessen, K., Sigvard, A., Tangmose, K., Edden, R.A.E., Larsson, H.B.W., Rostrup, E., et al. 2020. Treatment response after 6 and 26 weeks is related to baseline glutamate and GABA levels in antipsychotic-naïve patients with psychosis. *Psychological Medicine*. 50(13):2182–2193.

Bomba, L., Walter, K. & Soranzo, N. 2017. The impact of rare and low-frequency genetic variants in common disease. *Genome biology*. 18(1):77.

Bouarab, C., Thompson, B. & Polter, A.M. 2019. VTA GABA Neurons at the Interface of Stress and Reward. *Frontiers in neural circuits*. 13:78.

Boyle, A.P., Hong, E.L., Hariharan, M., Cheng, Y., Schaub, M.A., Kasowski, M., Karczewski, K.J., Park, J., et al. 2012. Annotation of functional variation in personal genomes using RegulomeDB. *Genome Research*. 22(9):1790–1797.

Brandão-Teles, C., de Almeida, V., Cassoli, J.S. & Martins-de-Souza, D. 2019. Biochemical Pathways Triggered by Antipsychotics in Human Oligodendrocytes: Potential of Discovering New Treatment Targets. *Frontiers in Pharmacology*. 10:186.

Brisch, R., Saniotis, A., Wolf, R., Bielau, H., Bernstein, H.-G., Steiner, J., Bogerts, B., Braun, K., et al. 2014. The role of dopamine in schizophrenia from a neurobiological and evolutionary perspective: old fashioned, but still in vogue. *Frontiers in psychiatry*. 5:47.

Brown, A.S. 2011. The environment and susceptibility to schizophrenia. *Progress in Neurobiology*. 93(1):23–58.

Busner, J. & Targum, S.D. 2007. The clinical global impressions scale: applying a research tool in clinical practice. *Psychiatry (Edgmont)*. 4(7):28–37.

Caiazzo, M., Dell'Anno, M.T., Dvoretskova, E., Lazarevic, D., Taverna, S., Leo, D., Sotnikova, T.D., Menegon, A., et al. 2011. Direct generation of functional dopaminergic neurons from mouse and human fibroblasts. *Nature*. 476(7359):224–227.

Cannon, M.J., Laney, A.S. & Pellett, P.E. 2003. Human herpesvirus 8: Current issues. *Clinical Infectious Diseases*. 37(1):82–87.

Carlson, C.S., Eberle, M.A., Rieder, M.J., Yi, Q., Kruglyak, L. & Nickerson, D.A. 2004. Selecting a Maximally Informative Set of Single-Nucleotide Polymorphisms for Association Analyses Using Linkage Disequilibrium. *American Journal of Human Genetics*. 74(1):106–120.

Chadha, R. & Meador-Woodruff, J.H. 2020. Downregulated AKT-mTOR signaling pathway proteins in

dorsolateral prefrontal cortex in Schizophrenia. *Neuropsychopharmacology*. 45(6):1059–1067.

Chandrachud, U., Walker, M.W., Simas, A.M., Heetveld, S., Petcherski, A., Klein, M., Oh, H., Wolf, P., et al. 2015. Unbiased cell-based screening in a neuronal cell model of batten disease highlights an interaction between Ca2+ homeostasis, autophagy, and CLN3 protein function. *Journal of Biological Chemistry*. 290(23):14361–14380.

Chelala, C., Khan, A. & Lemoine, N.R. 2009. SNPnexus: A web database for functional annotation of newly discovered and public domain single nucleotide polymorphisms. *Bioinformatics*. 25(5):655–661.

Chen, D., Pang, S., Feng, X., Huang, W., Hawley, R.G. & Yan, B. 2013. Genetic analysis of the ATG7 gene promoter in sporadic Parkinson's disease. *Neuroscience Letters*. 534(1):193–198.

Chen, E.Y., Tan, C.M., Kou, Y., Duan, Q., Wang, Z., Meirelles, G.V., Clark, N.R. & Ma'ayan, A. 2013. Enrichr: interactive and collaborative HTML5 gene list enrichment analysis tool. *BMC bioinformatics*. 14:128.

Chen, L., Wang, H., Vicini, S. & Olsen, R.W. 2000. The γ-aminobutyric acid type A (GABA(A)) receptor-associated protein (GABARAP) promotes GABA(A) receptor clustering and modulates the channel kinetics. *Proceedings of the National Academy of Sciences of the United States of America*. 97(21):11557–11562.

Chénard, C.A. & Richard, S. 2008. New implications for the QUAKING RNA binding protein in human disease. *Journal of neuroscience research*. 86(2):233–42.

Chiliza, B., Asmal, L., Kilian, S., Phahladira, L. & Emsley, R. 2015. Rate and predictors of non-response to first-line antipsychotic treatment in first-episode schizophrenia. *Human Psychopharmacology*. 30(3):173–182.

Chisholm, K., Lin, A., Abu-Akel, A. & Wood, S.J. 2015. The association between autism and schizophrenia spectrum disorders: A review of eight alternate models of co-occurrence. *Neuroscience & Biobehavioral Reviews*. 55:173–183.

Ciesielski, T.H., Aldrich, M.C., Marsit, C.J., Hiatt, R.A. & Williams, S.M. 2016. Transdisciplinary approaches enhance the production of translational knowledge. *Translational Research*. 182:123–134.

Citrome, L., Eramo, A., Clement, F., Duffy, R.A., Legacy, S., Offord, S., Krasa, H., Johnston, S., et al. 2015. Lack of tolerable treatment options for patients with schizophrenia. *Neuropsychiatric Disease and Treatment*. (December):3095.

Cornett, E.M., Novitch, M., Kaye, A.D., Kata, V. & Kaye, A.M. 2017. Medication-induced tardive dyskinesia: A review and update. *Ochsner Journal*. 17(2):162–174.

Cortes, C.J. & La Spada, A.R. 2014. The many faces of autophagy dysfunction in Huntington's disease: From mechanism to therapy. *Drug Discovery Today*. 19(7):963–971.

Cui, W.-Y., Seneviratne, C., Gu, J. & Li, M.D. 2012. Genetics of GABAergic signaling in nicotine and alcohol dependence. *Human genetics*. 131(6):843–55.

Daniels, J.L., Forssen, U., Hultman, C.M., Cnattingius, S., Savitz, D.A., Feychting, M. & Sparen, P. 2008. Parental Psychiatric Disorders Associated With Autism Spectrum Disorders in the Offspring. *PEDIATRICS*. 121(5):e1357–e1362.

Daya, M., van der Merwe, L., Galal, U., Möller, M., Salie, M., Chimusa, E.R., Galanter, J.M., van Helden, P.D., et al. 2013. A panel of ancestry informative markers for the complex five-way admixed South African coloured population. *PloS one*. 8(12):e82224.

Dickerson, F., Kirkpatrick, B., Boronow, J., Stallings, C., Origoni, A. & Yolken, R. 2006. Deficit Schizophrenia: Association With Serum Antibodies to Cytomegalovirus. *Schizophrenia Bulletin*. 32(2):396–400.

Djajadikerta, A., Keshri, S., Pavel, M., Prestil, R., Ryan, L. & Rubinsztein, D.C. 2020. Autophagy Induction as a Therapeutic Strategy for Neurodegenerative Diseases. *Journal of molecular biology*. 432(8):2799–2821.

Dong, C., Chen, Y., Li, H., Yang, Y., Zhang, H., Ke, K., Shi, X.-N., Liu, X., et al. 2019. The antipsychotic agent

flupentixol is a new PI3K inhibitor and potential anticancer drug for lung cancer. *International journal of biological sciences*. 15(7):1523–1532.

Dresner, E., Agam, G. & Gozes, I. 2011. Activity-dependent neuroprotective protein (ADNP) expression level is correlated with the expression of the sister protein ADNP2: Deregulation in schizophrenia. *European Neuropsychopharmacology*. 21(5):355–361.

Drögemöller, B.I., Niehaus, D.J., Chiliza, B., Merwe, L. van der, Asmal, L., Malhotra, A.K., Wright, G.E., Emsley, R., et al. 2014. Patterns of variation influencing antipsychotic treatment outcomes in South African first-episode schizophrenia patients. *Pharmacogenomics*. 15(2):189–199.

Drögemöller, B.I., Emsley, R., Chiliza, B., van der Merwe, L., Wright, G.E.B., Daya, M., Hoal, E., Malhotra, A.K., et al. 2016. The identification of novel genetic variants associated with antipsychotic treatment response outcomes in first-episode schizophrenia patients. *Pharmacogenetics and Genomics*. 26(5):235–242.

Drouin-Ouellet, J., Pircs, K., Barker, R.A., Jakobsson, J. & Parmar, M. 2017. Direct neuronal reprogramming for disease modeling studies using patient-derived neurons: What have we learned? *Frontiers in Neuroscience*. 11:530.

Drouin-Ouellet, J., Lau, S., Brattås, P.L., Rylander Ottosson, D., Pircs, K., Grassi, D.A., Collins, L.M., Vuono, R., et al. 2017. REST suppression mediates neural conversion of adult human fibroblasts via microRNA-dependent and -independent pathways. *EMBO Molecular Medicine*. 9(8):1117–1131.

Duff, K., Beglinger, L.J. & Paulsen, J.S. 2008. “Pre-symptomatic” Huntington’s Disease. in *Handbook of Clinical Neurology*. 589–598.

Van Duijn, E., Craufurd, D., Hubers, A.A.M., Giltay, E.J., Bonelli, R., Rickards, H., Anderson, K.E., Van Walsem, M.R., et al. 2014. Neuropsychiatric symptoms in a European Huntington’s disease cohort (REGISTRY). *Journal of Neurology, Neurosurgery and Psychiatry*.

Dunlop, J. & Brandon, N.J. 2015. Schizophrenia drug discovery and development in an evolving era: are new drug targets fulfilling expectations? *Journal of psychopharmacology (Oxford, England)*. 29(2):230–238.

Egerton, A., Broberg, B. V., Van Haren, N., Merritt, K., Barker, G.J., Lythgoe, D.J., Perez-Iglesias, R., Baandrup, L., et al. 2018. Response to initial antipsychotic treatment in first episode psychosis is related to anterior cingulate glutamate levels: a multicentre 1 H-MRS study (OPTiMiSE). *Molecular Psychiatry*. 23(11):2145–2155.

Eli Lilly and Company. 1996. Zyprexa (olanzapine) antipsychotic approval package.

Eli Lilly and Company. 2006. Zyprexa (package insert).

Emsley, R., Rabinowitz, J., Medori, R. & Early Psychosis Global Working Group. 2007. Remission in early psychosis: Rates, predictors, and clinical and functional outcome correlates. *Schizophrenia research*. 89(1–3):129–39.

Emsley, R., Chiliza, B., Asmal, L. & Lehloenya, K. 2011. The concepts of remission and recovery in schizophrenia. *Current opinion in psychiatry*. 24(2):114–21.

Emsley, R., Chiliza, B., Asmal, L., Kilian, S., Riaan Olivier, M., Phahladira, L., Ojagbemi, A., Scheffler, F., et al. 2017. Neurological soft signs in first-episode schizophrenia: State- and trait-related relationships to psychopathology, cognition and antipsychotic medication effects. *Schizophrenia research*. 188:144–150.

Ernst, M., Malone, R.P., Rowan, A.B., George, R., Gonzalez, N.M. & Silva, R.R. 1999. Antipsychotics (Neuroleptics). *Practitioner’s Guide to Psychoactive Drugs for Children and Adolescents*. 297–327.

Estrada-Sánchez, A.M. & Rebec, G. V. 2012. Corticostriatal dysfunction and glutamate transporter 1 (GLT1) in Huntington’s disease: Interactions between neurons and astrocytes. *Basal Ganglia*. 2(2):57–66.

European Union. 2011. Directive 2010/84/EU of the European Parliament and of the Council of 15 December 2010 amending, as regards pharmacovigilance, Directive 2001/83/EC on the Community code relating

to medicinal products for human use. 2010(December 2010):1–44. [Online], Available: https://publications.europa.eu/en/publication-detail/-/publication/38408e8a-b7bc-467b-8b54-22309d9710e0/language-en.

Feng, Y., Yao, Z. & Klionsky, D.J. 2015. How to control self-digestion: transcriptional, post-transcriptional, and post-translational regulation of autophagy. *Trends in Cell Biology*. 25(6):354–363.

Ferrante, R.J., Kowall, N.W. & Richardson, E.P. 1991. Proliferative and degenerative changes in striatal spiny neurons in Huntington's disease: a combined study using the section-Golgi method and calbindin D28k immunocytochemistry. *The Journal of neuroscience : the official journal of the Society for Neuroscience*. 11(12):3877–87.

Finley, D. 2009. Recognition and processing of ubiquitin-protein conjugates by the proteasome. *Annual review of biochemistry*. 78:477–513.

Fisher, R.A. 1992. Statistical Methods for Research Workers. in. 66–70.

Flupentixol decanoate - DrugBank. n.d. [Online], Available: https://www.drugbank.ca/salts/DBSALT000928 [2020, September 09].

Foster, A., Miller, D.D. & Buckley, P. 2010. Pharmacogenetics and Schizophrenia. *Clinics in Laboratory Medicine*. 30(4):975–993.

Fujikake, N., Shin, M. & Shimizu, S. 2018. Association between autophagy and neurodegenerative diseases. *Frontiers in Neuroscience*. 12(MAY):255.

Fukata, M., Vamadevan, A.S. & Abreu, M.T. 2009. Toll-like receptors (TLRs) and Nod-like receptors (NLRs) in inflammatory disorders. *Seminars in immunology*. 21(4):242–53.

Galling, B., Roldán, A., Hagi, K., Rietschel, L., Walyzada, F., Zheng, W., Cao, X.-L., Xiang, Y.-T., et al. 2017. Antipsychotic augmentation vs. monotherapy in schizophrenia: systematic review, meta-analysis and meta-regression analysis. *World Psychiatry*. 16(1):77–89.

Gandal, M.J., Haney, J.R., Parikshak, N.N., Leppa, V., Ramaswami, G., Hartl, C., Schork, A.J., Appadurai, V., et al. 2018. Shared molecular neuropathology across major psychiatric disorders parallels polygenic overlap. *Science (New York, N.Y.)*. 359(6376):693–697.

García-Bueno, B., Gassó, P., MacDowell, K.S., Callado, L.F., Mas, S., Bernardo, M., Lafuente, A., Meana, J.J., et al. 2016. Evidence of activation of the Toll-like receptor-4 proinflammatory pathway in patients with schizophrenia. *Journal of psychiatry & neuroscience : JPN*. 41(3):E46-55.

Gatica, D., Lahiri, V. & Klionsky, D.J. 2018. Cargo recognition and degradation by selective autophagy. *Nature cell biology*. 20(3):233–242.

Gelmetti, V., De Rosa, P., Torosantucci, L., Marini, E.S., Romagnoli, A., Di Rienzo, M., Arena, G., Vignone, D., et al. 2017. PINK1 and BECN1 relocalize at mitochondria-associated membranes during mitophagy and promote ER-mitochondria tethering and autophagosome formation. *Autophagy*. 13(4):654–669.

Georgievska, B., Jakobsson, J., Persson, E., Ericson, C., Kirik, D. & Lundberg, C. 2004. Regulated Delivery of Glial Cell Line-Derived Neurotrophic Factor into Rat Striatum, Using a Tetracycline-Dependent Lentiviral Vector. *Human Gene Therapy*. 15(10):934–944.

Gibson, G. 2012. Rare and common variants: twenty arguments. *Nature reviews. Genetics*. 13(2):135–145.

Gkikas, I., Petratou, D. & Tavernarakis, N. 2014. Longevity pathways and memory aging. *Frontiers in Genetics*. 5:155.

Glatt, S., Chandler, S., Bousman, C., Chana, G., Lucero, G., Tatro, E., May, T., Lohr, J., et al. 2012. Alternatively Spliced Genes as Biomarkers for Schizophrenia, Bipolar Disorder and Psychosis: A Blood-Based Spliceome-Profiling Exploratory Study. *Current Pharmacogenomics and Personalized Medicine*. 7(3):164–188.

Goldman-Rakic, P.S., Muly, E.C. & Williams, G. V. 2000. D(1) receptors in prefrontal cells and circuits. *Brain*

research. Brain research reviews. 31(2–3):295–301.

Gregory, A., Mallikarjun, P. & Upthegrove, R. 2017. Treatment of depression in schizophrenia: systematic review and meta-analysis. *The British journal of psychiatry : the journal of mental science*. 211(4):198–204.

Griswold, A.J., Ma, D., Cukier, H.N., Nations, L.D., Schmidt, M.A., Chung, R.-H., Jaworski, J.M., Salyakina, D., et al. 2012. Evaluation of copy number variations reveals novel candidate genes in autism spectrum disorder-associated pathways. *Human molecular genetics*. 21(15):3513–3523.

Groll, M. & Huber, R. 2003. Substrate access and processing by the 20S proteasome core particle. *The international journal of biochemistry & cell biology*. 35(5):606–616.

Groll, M. & Huber, R. 2004. Inhibitors of the eukaryotic 20S proteasome core particle: a structural approach. *Biochimica et biophysica acta*. 1695(1–3):33–44.

GTEx Consortium. 2013. The Genotype-Tissue Expression (GTEx) project. *Nature genetics*. 45(6):580–5.

Guloksuz, S. & Van Os, J. 2018.

Guo, L., Du, Y., Chang, S., Zhang, K. & Wang, J. 2014. rSNPBase: a database for curated regulatory SNPs. *Nucleic acids research*. 42(Database issue):D1033-1039.

Haddad, P.M. & Correll, C.U. 2018. The acute efficacy of antipsychotics in schizophrenia: a review of recent meta-analyses. *Therapeutic advances in psychopharmacology*. 8(11):303–318.

El Haddad, S., Serrano, A., Moal, F., Normand, T., Robin, C., Charpentier, S., Valery, A., Brulé-Morabito, F., et al. 2020. Disturbed expression of autophagy genes in blood of Parkinson's disease patients. *Gene*. 738:144454.

Hamilton, J.M., Haaland, K.Y., Adair, J.C. & Brandt, J. 2003. Ideomotor limb apraxia in Huntington's disease: implications for corticostriate involvement. *Neuropsychologia*. 41(5):614–621.

Hannachi, N., El Kissi, Y., Samoud, S., Nakhli, J., Letaief, L., Gaabout, S., Ali, B.B.H. & Boukadida, J. 2014. High prevalence of Human Herpesvirus 8 in schizophrenic patients. *Psychiatry research*. 216(2):192–197.

Hebron, M.L., Lonskaya, I. & Moussa, C.E.-H. 2013. Nilotinib reverses loss of dopamine neurons and improves motor behavior via autophagic degradation of -synuclein in Parkinson's disease models. *Human Molecular Genetics*. 22(16):3315–3328.

Hedrich, K., Hagenah, J., Djarmati, A., Hiller, A., Lohnau, T., Lasek, K., Grünewald, A., Hilker, R., et al. 2006. Clinical spectrum of homozygous and heterozygous PINK1 mutations in a large German family with Parkinson disease: role of a single hit? *Archives of neurology*. 63(6):833–838.

Heinrich, A., Nees, F., Lourdusamy, A., Tzschoppe, J., Meier, S., Vollstädt-Klein, S., Fauth-Bühler, M., Steiner, S., et al. 2013. From gene to brain to behavior: Schizophrenia-associated variation in AMBRA1 alters impulsivity-related traits. *European Journal of Neuroscience*. 38(6):2941–2945.

Heras-Sandoval, D., Pérez-Rojas, J.M., Hernández-Damián, J. & Pedraza-Chaverri, J. 2014. The role of PI3K/AKT/mTOR pathway in the modulation of autophagy and the clearance of protein aggregates in neurodegeneration. *Cellular Signalling*. 26(12):2694–2701.

Hershko, A. 1983. Ubiquitin: roles in protein modification and breakdown. *Cell*. 34(1):11–12.

Heymann, D. 2006. Autophagy: A protective mechanism in response to stress and inflammation. *Current opinion in investigational drugs (London, England : 2000)*. 7(5):443–450. [Online], Available: http://www.ncbi.nlm.nih.gov/pubmed/16729721.

Higashi, K., Medic, G., Littlewood, K.J., Diez, T., Granström, O. & De Hert, M. 2013. Medication adherence in schizophrenia: factors influencing adherence and consequences of nonadherence, a systematic literature review. *Therapeutic Advances in Psychopharmacology*. 3(4):200–218.

Hindorff, L.A., Bonham, V.L., Brody, L.C., Ginoza, M.E.C., Hutter, C.M., Manolio, T.A. & Green, E.D. 2018. Prioritizing diversity in human genomics research. *Nature reviews. Genetics*. 19(3):175–185.

Horacek, J., Bubenikova-Valesova, V., Kopecek, M., Palenicek, T., Dockery, C., Mohr, P. & H??schl, C. 2006. Mechanism of Action of Atypical Antipsychotic Drugs and the Neurobiology of Schizophrenia. *CNS Drugs*. 20(5):389–409.

Hudson, T.J., Owen, R.R., Thrush, C.R., Han, X., Pyne, J.M., Thapa, P. & Sullivan, G. 2004. A Pilot Study of Barriers to Medication Adherence in Schizophrenia. *The Journal of Clinical Psychiatry*. 65(2):211–216.

Huh, C.J., Zhang, B., Victor, M.B., Dahiya, S., Batista, L.F.Z., Horvath, S. & Yoo, A.S. 2016. Maintenance of age in human neurons generated by microRNA-based neuronal conversion of fibroblasts. *eLife*. 5.

Ibáñez, P., Lesage, S., Lohmann, E., Thobois, S., Michele, G. De, Borg, M., Agid, Y., Dürr, A., et al. 2006. Mutational analysis of the PINK1 gene in early-onset parkinsonism in Europe and North Africa. *Brain*. 129(3):686–694.

Ichimura, Y., Kirisako, T., Takao, T., Satomi, Y., Shimonishi, Y., Ishihara, N., Mizushima, N., Tanida, I., et al. 2000. A ubiquitin-like system mediates protein lipidation. *Nature*. 408(6811):488–492.

Illumina. 2011. *HumanExome BeadChips*. [Online], Available: http://www.illumina.com/ [2020, September 25].

Jääskeläinen, E., Juola, P., Hirvonen, N., McGrath, J.J., Saha, S., Isohanni, M., Veijola, J. & Miettunen, J. 2013. A systematic review and meta-analysis of recovery in schizophrenia. *Schizophrenia Bulletin*.

Jia, J. & Le, W. 2015. Molecular network of neuronal autophagy in the pathophysiology and treatment of depression. *Neuroscience bulletin*. 31(4):427–434.

Jin, S.M., Lazarou, M., Wang, C., Kane, L.A., Narendra, D.P. & Youle, R.J. 2010. Mitochondrial membrane potential regulates PINK1 import and proteolytic destabilization by PARL. *The Journal of cell biology*. 191(5):933–942.

Johnson, J.A., Caudle, K.E., Gong, L., Whirl-Carrillo, M., Stein, C.M., Scott, S.A., Lee, M.T., Gage, B.F., et al. 2017. Clinical Pharmacogenetics Implementation Consortium (CPIC) Guideline for Pharmacogenetics-Guided Warfarin Dosing: 2017 Update. *Clinical pharmacology and therapeutics*. 102(3):397–404.

Jones, H.J., Stergiakouli, E., Tansey, K.E., Hubbard, L., Heron, J., Cannon, M., Holmans, P., Lewis, G., et al. 2016. Phenotypic manifestation of genetic risk for schizophrenia during adolescence in the general population. *JAMA Psychiatry*.

Jung, C.H., Jun, C.B., Ro, S.-H., Kim, Y.-M., Otto, N.M., Cao, J., Kundu, M. & Kim, D.-H. 2009. ULK-Atg13-FIP200 complexes mediate mTOR signaling to the autophagy machinery. *Molecular biology of the cell*. 20(7):1992–2003.

Kaar, S.J., Natesan, S., McCutcheon, R. & Howes, O.D. 2020. Antipsychotics: Mechanisms underlying clinical response and side-effects and novel treatment approaches based on pathophysiology. *Neuropharmacology*. 172:107704.

Kabeya, Y. 2000. LC3, a mammalian homologue of yeast Apg8p, is localized in autophagosome membranes after processing. *The EMBO Journal*. 19(21):5720–5728.

Kanehisa, M. & Goto, S. 2000. KEGG: kyoto encyclopedia of genes and genomes. *Nucleic acids research*. 28(1):27–30.

Kara, N.Z., Toker, L., Agam, G., Anderson, G.W., Belmaker, R.H. & Einat, H. 2013. Trehalose induced antidepressant-like effects and autophagy enhancement in mice. *Psychopharmacology*. 229(2):367–375.

Kay, S.R., Opler, L.A. & Lindenmayer, J.P. 1989. The Positive and Negative Syndrome Scale (PANSS): Rationale and standardisation. *British Journal of Psychiatry*. 155(NOV. SUPPL. 7):59–65.

Kéri, S., Szabó, C. & Kelemen, O. 2017. Antipsychotics influence Toll-like receptor (TLR) expression and its relationship with cognitive functions in schizophrenia. *Brain, behavior, and immunity*. 62:256–264.

Kharkwal, G., Brami-Cherrier, K., Lizardi-Ortiz, J.E., Nelson, A.B., Ramos, M., Del Barrio, D., Sulzer, D., Kreitzer,

A.C., et al. 2016. Parkinsonism Driven by Antipsychotics Originates from Dopaminergic Control of Striatal Cholinergic Interneurons. *Neuron*. 91(1):67–78.

Kim, H.K., Andreazza, A.C., Elmi, N., Chen, W. & Young, L.T. 2016. Nod-like receptor pyrin containing 3 (NLRP3) in the post-mortem frontal cortex from patients with bipolar disorder: A potential mediator between mitochondria and immune-activation. *Journal of psychiatric research*. 72:43–50.

Kim, S.H., Park, S., Yu, H.S., Ko, K.H., Park, H.G. & Kim, Y.S. 2018. The antipsychotic agent clozapine induces autophagy via the AMPK-ULK1-Beclin1 signaling pathway in the rat frontal cortex. *Progress in neuro-psychopharmacology & biological psychiatry*. 81:96–104.

Kim, Y.D., Jeong, E. Il, Nah, J., Yoo, S.-M., Lee, W.J., Kim, Y., Moon, S., Hong, S.-H., et al. 2017. Pimozide reduces toxic forms of tau in TauC3 mice via 5' adenosine monophosphate-activated protein kinase-mediated autophagy. *Journal of neurochemistry*. 142(5):734–746.

Kim, Y.K., Shin, J.S. & Nahm, M.H. 2016. NOD-Like Receptors in Infection, Immunity, and Diseases. *Yonsei medical journal*. 57(1):5–14.

Kitada, T., Asakawa, S., Hattori, N., Matsumine, H., Yamamura, Y., Minoshima, S., Yokochi, M., Mizuno, Y., et al. 1998. Mutations in the parkin gene cause autosomal recessive juvenile parkinsonism. *Nature*. 392(6676):605–8.

Kitagishi, Y., Kobayashi, M., Kikuta, K. & Matsuda, S. 2012. Roles of PI3K/AKT/GSK3/mTOR Pathway in Cell Signaling of Mental Illnesses. *Depression Research and Treatment*. 2012:1–8.

Klionsky, D.J. 2007. Autophagy: from phenomenology to molecular understanding in less than a decade. *Nature reviews. Molecular cell biology*. 8(11):931–937.

Klionsky, D.J., Abdelmohsen, K., Abe, A., Abedin, M.J., Abeliovich, H., Acevedo Arozena, A., Adachi, H., Adams, C.M., et al. 2016. Guidelines for the use and interpretation of assays for monitoring autophagy (3rd edition). *Autophagy*. 12(1):1–222.

Kosillo, P., Zhang, Y.-F., Threlfell, S. & Cragg, S.J. 2016. Cortical Control of Striatal Dopamine Transmission via Striatal Cholinergic Interneurons. *Cerebral Cortex*. 26(11):4160–4169.

Kuma, A., Hatano, M., Matsui, M., Yamamoto, A., Nakaya, H., Yoshimori, T., Ohsumi, Y., Tokuhisa, T., et al. 2004. The role of autophagy during the early neonatal starvation period. *Nature*. 432(7020):1032–1036.

Kumar, S., Ambrosini, G. & Bucher, P. 2017. SNP2TFBS – a database of regulatory SNPs affecting predicted transcription factor binding site affinity. *Nucleic Acids Research*. 45(D1):D139–D144.

Kushima, I., Aleksic, B., Nakatochi, M., Shimamura, T., Okada, T., Uno, Y., Morikawa, M., Ishizuka, K., et al. 2018. Comparative Analyses of Copy-Number Variation in Autism Spectrum Disorder and Schizophrenia Reveal Etiological Overlap and Biological Insights. *Cell Reports*. 24(11):2838–2856.

Kuznetsova, A., Brockhoff, P.B. & Christensen, R.H.B. 2017. lmerTest Package: Tests in Linear Mixed Effects Models. *Journal of Statistical Software*. 82(13).

de la Fuente-Sandoval, C., Reyes-Madrigal, F., Mao, X., León-Ortiz, P., Rodríguez-Mayoral, O., Jung-Cook, H., Solís-Vivanco, R., Graff-Guerrero, A., et al. 2018. Prefrontal and Striatal Gamma-Aminobutyric Acid Levels and the Effect of Antipsychotic Treatment in First-Episode Psychosis Patients. *Biological Psychiatry*. 83(6):475–483.

Langbehn, D.R., Brinkman, R.R., Falush, D., Paulsen, J.S. & Hayden, M.R. 2004. A new model for prediction of the age of onset and penetrance for Huntington's disease based on CAG length. *Clinical Genetics*.

Larsson, H.J., Eaton, W.W., Madsen, K.M., Vestergaard, M., Olesen, A.V., Agerbo, E., Schendel, D., Thorsen, P., et al. 2005. Risk Factors for Autism: Perinatal Factors, Parental Psychiatric History, and Socioeconomic Status. *American Journal of Epidemiology*. 161(10):916–925.

Lee, J.-M., Correia, K., Loupe, J., Kim, K.-H., Barker, D., Hong, E.P., Chao, M.J., Long, J.D., et al. 2019. CAG Repeat Not Polyglutamine Length Determines Timing of Huntington's Disease Onset. *Cell*. 178(4):887–900.

Lee, J.-S., Li, Q., Lee, J.-Y., Lee, S.-H., Jeong, J.H., Lee, H.-R., Chang, H., Zhou, F.-C., et al. 2009. FLIP-mediated autophagy regulation in cell death control. *Nature Cell Biology*. 11(11):1355–1362.

Lee, J., Takeuchi, H., Fervaha, G., Sin, G.L., Foussias, G., Agid, O., Farooq, S. & Remington, G. 2015. Subtyping Schizophrenia by Treatment Response: Antipsychotic Development and the Central Role of Positive Symptoms. *The Canadian Journal of Psychiatry*. 60(11):515–522.

Lee, K.-M., Hwang, S.-K. & Lee, J.-A. 2013. Neuronal Autophagy and Neurodevelopmental Disorders. *Experimental Neurobiology*. 22(3):133.

Lee, S., Sato, Y. & Nixon, R.A. 2011. Lysosomal proteolysis inhibition selectively disrupts axonal transport of degradative organelles and causes an Alzheimer's-like axonal dystrophy. *Journal of Neuroscience*. 31(21):7817–7830.

Leil, T.A. 2004. GABAA Receptor-Associated Protein Traffics GABAA Receptors to the Plasma Membrane in Neurons. *Journal of Neuroscience*. 24(50):11429–11438.

Leucht, S., Corves, C., Arbter, D., Engel, R.R., Li, C. & Davis, J.M. 2009. Second-generation versus first-generation antipsychotic drugs for schizophrenia: a meta-analysis. *The Lancet*. 373(9657):31–41.

Levenga, J., Wong, H., Milstead, R.A., Keller, B.N., LaPlante, L.E. & Hoeffer, C.A. 2017. AKT isoforms have distinct hippocampal expression and roles in synaptic plasticity. *eLife*. 6.

Lever, J., Krzywinski, M. & Altman, N. 2016. Model selection and overfitting. *Nature Methods*. 13(9):703–704.

Levine, B. & Kroemer, G. 2008. Autophagy in the Pathogenesis of Disease. *Cell*. 132(1):27–42.

Li, Y., Tomiyama, H., Sato, K., Hatano, Y., Yoshino, H., Atsumi, M., Kitaguchi, M., Sasaki, S., et al. 2005. Clinicogenetic study of PINK1 mutations in autosomal recessive early-onset parkinsonism. *Neurology*. 64(11):1955–7.

Li, Y., Huang, J., Pang, S., Wang, H., Zhang, A., Hawley, R.G. & Yan, B. 2017. Novel and functional ATG12 gene variants in sporadic Parkinson's disease. *Neuroscience letters*. 643:22–26.

Liang, Y. & Sigrist, S. 2018. Autophagy and proteostasis in the control of synapse aging and disease. *Current opinion in neurobiology*. 48:113–121.

Liang, Q., Chang, B., Brulois, K.F., Castro, K., Min, C.-K., Rodgers, M.A., Shi, M., Ge, J., et al. 2013. Kaposi's sarcoma-associated herpesvirus K7 modulates Rubicon-mediated inhibition of autophagosome maturation. *Journal of virology*. 87(22):12499–12503.

Lima, R., Sousa, D., Paiva, A., Palmeira, A., Barbosa, J., Pedro, M., Pinto, M., Sousa, E., et al. 2016. Modulation of Autophagy by a Thioxanthone Decreases the Viability of Melanoma Cells. *Molecules*. 21(10):1343.

Lippai, M. & Lőw, P. 2014. The Role of the Selective Adaptor p62 and Ubiquitin-Like Proteins in Autophagy. *BioMed Research International*. 2014:1–11.

List of Phenothiazine antipsychotics - Drugs.com. n.d. [Online], Available: https://www.drugs.com/drug-class/phenothiazine-antipsychotics.html [2020, September 09].

Liu, Y., Xue, Y., Ridley, S., Zhang, D., Rezvani, K., Fu, X.-D. & Wang, H. 2014. Direct Reprogramming of Huntington's Disease Patient Fibroblasts into Neuron-Like Cells Leads to Abnormal Neurite Outgrowth, Increased Cell Death, and Aggregate Formation. *PLoS ONE*. 9(10):e109621.

Löffler, W., Kilian, R., Toumi, M. & Angermeyer, M.C. 2003. Schizophrenic Patients' Subjective Reasons for Compliance and Noncompliance with Neuroleptic Treatment. *Pharmacopsychiatry*. 36(3):105–112.

Loos, B., Engelbrecht, A.-M., Lockshin, R.A., Klionsky, D.J. & Zakeri, Z. 2013. The variability of autophagy and cell death susceptibility. *Autophagy*. 9(9):1270–1285.

Loos, B., Toit, A. du & Hofmeyr, J.-H.S. 2014. Defining and measuring autophagosome flux—concept and reality. *Autophagy*. 10(11):2087–2096.

Lou, X.-Y., Ma, J.Z., Sun, D., Payne, T.J. & Li, M.D. 2007. Fine mapping of a linkage region on chromosome

17p13 reveals that GABARAP and DLG4 are associated with vulnerability to nicotine dependence in European-Americans. *Human Molecular Genetics*. 16(2):142–153.

Lukong, K.E., Chang, K., Khandjian, E.W. & Richard, S. 2008. RNA-binding proteins in human genetic disease. *Trends in Genetics*. 24(8):416–425.

Lumkwana, D., du Toit, A., Kinnear, C. & Loos, B. 2017. Autophagic flux control in neurodegeneration: Progress and precision targeting—Where do we stand? *Progress in Neurobiology*. 153:64–85.

MacArthur, J., Bowler, E., Cerezo, M., Gil, L., Hall, P., Hastings, E., Junkins, H., McMahon, A., et al. 2017. The new NHGRI-EBI Catalog of published genome-wide association studies (GWAS Catalog). *Nucleic Acids Research*. 45(D1):D896–D901.

Maday, S., Wallace, K.E. & Holzbaur, E.L.F. 2012. Autophagosomes initiate distally and mature during transport toward the cell soma in primary neurons. *Journal of Cell Biology*. 196(4):407–417.

Mantere, O., Trontti, K., García-González, J., Balcells, I., Saarnio, S., Mäntylä, T., Lindgren, M., Kieseppä, T., et al. 2019. Immunomodulatory effects of antipsychotic treatment on gene expression in first-episode psychosis. *Journal of Psychiatric Research*. 109:18–26.

Maria Fimia, G., Stoykova, A., Romagnoli, A., Giunta, L., Di Bartolomeo, S., Nardacci, R., Corazzari, M., Fuoco, C., et al. 2007. Ambra1 regulates autophagy and development of the nervous system. *Nature*. 447(7148):1121–1125.

Mariño, G., Uría, J.A., Puente, X.S., Quesada, V., Bordallo, J. & López-Otín, C. 2003. Human autophagins, a family of cysteine proteinases potentially implicated in cell degradation by autophagy. *The Journal of biological chemistry*. 278(6):3671–8.

Martinez-Vicente, M., Talloczy, Z., Wong, E., Tang, G., Koga, H., Kaushik, S., de Vries, R., Arias, E., et al. 2010. Cargo recognition failure is responsible for inefficient autophagy in Huntington's disease. *Nature Neuroscience*. 13(5):567–576.

Mas, S., Gassó, P., Ritter, M.A., Malagelada, C., Bernardo, M. & Lafuente, A. 2015. Pharmacogenetic predictor of extrapyramidal symptoms induced by antipsychotics: multilocus interaction in the mTOR pathway. *European neuropsychopharmacology : the journal of the European College of Neuropsychopharmacology*. 25(1):51–9.

Merenlender-Wagner, A., Pikman, R., Giladi, E., Andrieux, A. & Gozes, I. 2010. NAP (davunetide) enhances cognitive behavior in the STOP heterozygous mouse—A microtubule-deficient model of schizophrenia. *Peptides*. 31(7):1368–1373.

Merenlender-Wagner, A., Malishkevich, A., Shemer, Z., Udawela, M., Gibbons, A., Scarr, E., Dean, B., Levine, J., et al. 2015. Autophagy has a key role in the pathophysiology of schizophrenia. *Molecular Psychiatry*. 20(1):126–132.

Mertens, J., Paquola, A.C.M., Ku, M., Hatch, E., Böhnke, L., Ladjevardi, S., McGrath, S., Campbell, B., et al. 2015. Directly Reprogrammed Human Neurons Retain Aging-Associated Transcriptomic Signatures and Reveal Age-Related Nucleocytoplasmic Defects. *Cell stem cell*. 17(6):705–718.

Metzger, S., Saukko, M., Van Che, H., Tong, L., Puder, Y., Riess, O. & Nguyen, H.P. 2010. Age at onset in Huntington's disease is modified by the autophagy pathway: implication of the V471A polymorphism in Atg7. *Human Genetics*. 128(4):453–459.

Miller, B.R., Walker, A.G., Barton, S.J. & Rebec, G. V. 2011. Dysregulated Neuronal Activity Patterns Implicate Corticostriatal Circuit Dysfunction in Multiple Rodent Models of Huntington's Disease. *Frontiers in systems neuroscience*. 5(MAY 2011):26.

Miller, S.A., Dykes, D.D. & Polesky, H.F. 1988. A simple salting out procedure for extracting DNA from human nucleated cells. *Nucleic acids research*. 16(3):1215.

Mitjans, M., Begemann, M., Ju, A., Dere, E., Wüstefeld, L., Hofer, S., Hassouna, I., Balkenhol, J., et al. 2017. Sexual dimorphism of AMBRA1-related autistic features in human and mouse. *Translational Psychiatry*.

7(10):e1247–e1247.

Mizushima, N. & Komatsu, M. 2011. Autophagy: renovation of cells and tissues. *Cell*. 147(4):728–41.

Mizushima, N. & Levine, B. 2010. Autophagy in mammalian development and differentiation. *Nature cell biology*. 12(9):823–30.

Mizushima, N. & Yoshimori, T. 2007. How to interpret LC3 immunoblotting. *Autophagy*. 3(6):542–5.

Mizushima, N., Yamamoto, A., Matsui, M., Yoshimori, T. & Ohsumi, Y. 2004. In Vivo Analysis of Autophagy in Response to Nutrient Starvation Using Transgenic Mice Expressing a Fluorescent Autophagosome Marker. *Molecular Biology of the Cell*. 15(3):1101–1111.

Mizushima, N., Yoshimori, T. & Levine, B. 2010. Methods in mammalian autophagy research. *Cell*. 140(3):313–26.

Momozawa, Y. & Mizukami, K. 2020. Unique roles of rare variants in the genetics of complex diseases in humans. *Journal of human genetics*. (Epub ahead of print.).

Morgan, V.A., Leonard, H., Bourke, J. & Jablensky, A. 2008. Intellectual disability co-occurring with schizophrenia and other psychiatric illness: population-based study. *British Journal of Psychiatry*. 193(5):364–372.

Müller, D.J., Chowdhury, N.I. & Zai, C.C. 2013. The pharmacogenetics of antipsychotic-induced adverse events. *Current opinion in psychiatry*. 26(2):144–50.

Muñoz-Wolf, N. & Lavelle, E.C. 2016. Innate Immune Receptors. *Methods in molecular biology (Clifton, N.J.)*. 1417:1–43.

Murray, R.M. & Lewis, S.W. 1987. Is schizophrenia a neurodevelopmental disorder? *British medical journal (Clinical research ed.)*. 295(6600):681–2.

Murray, R.M., Bhavsar, V., Tripoli, G. & Howes, O. 2017. 30 Years on: How the Neurodevelopmental Hypothesis of Schizophrenia Morphed into the Developmental Risk Factor Model of Psychosis. *Schizophrenia Bulletin*.

Nakamura, S. & Yoshimori, T. 2018. Autophagy and Longevity. *Molecules and cells*. 41(1):65–72.

Narayan, S., Tang, B., Head, S.R., Gilmartin, T.J., Sutcliffe, J.G., Dean, B. & Thomas, E.A. 2008. Molecular profiles of schizophrenia in the CNS at different stages of illness. *Brain Research*. 1239:235–248.

Narendra, D.P., Jin, S.M., Tanaka, A., Suen, D.-F., Gautier, C.A., Shen, J., Cookson, M.R. & Youle, R.J. 2010. PINK1 is selectively stabilized on impaired mitochondria to activate Parkin. *PLoS biology*. 8(1):e1000298.

Nath, S., Dancourt, J., Shteyn, V., Puente, G., Fong, W.M., Nag, S., Bewersdorf, J., Yamamoto, A., et al. 2014. Lipidation of the LC3/GABARAP family of autophagy proteins relies on a membrane-curvature-sensing domain in Atg3. *Nature Cell Biology*. 16(5):415–424.

Nishimura, T. & Tooze, S.A. 2020. Emerging roles of ATG proteins and membrane lipids in autophagosome formation. *Cell Discovery*. 6(1):32.

O'Connell, K.S., McGregor, N.W., Malhotra, A., Lencz, T., Emsley, R. & Warnich, L. 2019. Variation within voltage-gated calcium channel genes and antipsychotic treatment response in a South African first episode schizophrenia cohort. *The pharmacogenomics journal*. 19(1):109–114.

van Os, J. & Kapur, S. 2009. Schizophrenia. *The Lancet*. 374(9690):635–645.

Van Os, J., Van Der Steen, Y., Islam, M.A., Gülöksüz, S., Rutten, B.P. & Simons, C.J. 2017. Evidence that polygenic risk for psychotic disorder is expressed in the domain of neurodevelopment, emotion regulation and attribution of salience. *Psychological Medicine*.

Owen, M.J. & O'Donovan, M.C. 2017. Schizophrenia and the neurodevelopmental continuum:evidence from genomics. *World Psychiatry*. 16(3):227–235.

Owen, M.J., O'Donovan, M.C., Thapar, A. & Craddock, N. 2011. Neurodevelopmental hypothesis of

schizophrenia. *British Journal of Psychiatry*. 198(3):173–175.

Owen, M.J., Sawa, A. & Mortensen, P.B. 2016. Schizophrenia. *Lancet (London, England)*. 388(10039):86–97.

Park, D., Jeong, H., Lee, M.N., Koh, A., Kwon, O., Yang, Y.R., Noh, J., Suh, P.-G., et al. 2016. Resveratrol induces autophagy by directly inhibiting mTOR through ATP competition. *Scientific Reports*. 6(1):21772.

Passeri, E., Wilson, A.M., Primerano, A., Kondo, M.A., Sengupta, S., Srivastava, R., Koga, M., Obie, C., et al. 2015. Enhanced conversion of induced neuronal cells (iN cells) from human fibroblasts: Utility in uncovering cellular deficits in mental illness-associated chromosomal abnormalities. *Neuroscience research*. 101:57–61.

Passeri, E., Jones-Brando, L., Bordón, C., Sengupta, S., Wilson, A.M., Primerano, A., Rapoport, J.L., Ishizuka, K., et al. 2016. Infection and characterization of Toxoplasma gondii in human induced neurons from patients with brain disorders and healthy controls. *Microbes and infection*. 18(2):153–8.

Peralta, V. & Cuesta, M.J. 2017. Motor Abnormalities: From Neurodevelopmental to Neurodegenerative Through “Functional” (Neuro)Psychiatric Disorders. *Schizophrenia Bulletin*. 43(5):956–971.

Petryshen, T.L., Middleton, F.A., Tahl, A.R., Rockwell, G.N., Purcell, S., Aldinger, K.A., Kirby, A., Morley, C.P., et al. 2005. Genetic investigation of chromosome 5q GABAA receptor subunit genes in schizophrenia. *Molecular psychiatry*. 10(12):1074–88, 1057.

Pfisterer, U., Wood, J., Nihlberg, K., Hallgren, O., Bjermer, L., Westergren-Thorsson, G., Lindvall, O. & Parmar, M. 2011. Efficient induction of functional neurons from adult human fibroblasts. *Cell Cycle*. 10(19):3311–3316.

Polajnar, M. & Žerovnik, E. 2014. Impaired autophagy: a link between neurodegenerative and neuropsychiatric diseases. *Journal of Cellular and Molecular Medicine*. 18(9):1705–1711.

Prasad, K.M., Watson, A.M.M., Dickerson, F.B., Yolken, R.H. & Nimgaonkar, V.L. 2012. Exposure to Herpes Simplex Virus Type 1 and Cognitive Impairments in Individuals With Schizophrenia. *Schizophrenia Bulletin*. 38(6):1137–1148.

Purcell, S., Neale, B., Todd-Brown, K., Thomas, L., Ferreira, M.A.R., Bender, D., Maller, J., Sklar, P., et al. 2007. PLINK: A Tool Set for Whole-Genome Association and Population-Based Linkage Analyses. *The American Journal of Human Genetics*. 81(3):559–575.

Puyal, J., Ginet, V., Grishchuk, Y., Truttmann, A.C. & Clarke, P.G.H. 2012. Neuronal autophagy as a mediator of life and death: Contrasting roles in chronic neurodegenerative and acute neural disorders. *Neuroscientist*. 18(3):224–236.

R Core Team. 2020. [Online], Available: https://www.r-project.org/.

Radwanska, K., Medvedev, N.I., Pereira, G.S., Engmann, O., Thiede, N., Moraes, M.F.D., Villers, A., Irvine, E.E., et al. 2011. Mechanism for long-term memory formation when synaptic strengthening is impaired. *Proceedings of the National Academy of Sciences of the United States of America*. 108(45):18471–18475.

Rapoport, J., Chavez, A., Greenstein, D., Addington, A. & Gogtay, N. 2009. Autism spectrum disorders and childhood-onset schizophrenia: Clinical and biological contributions to a relation revisited. *Journal of the American Academy of Child and Adolescent Psychiatry*. 48(1):10–18.

Rapoport, J.L., Giedd, J.N. & Gogtay, N. 2012. Neurodevelopmental model of schizophrenia: Update 2012. *Molecular Psychiatry*. 17(12):1228–1238.

Ravikumar, B., Duden, R. & Rubinsztein, D.C. 2002. Aggregate-prone proteins with polyglutamine and polyalanine expansions are degraded by autophagy. *Human Molecular Genetics*. 11(9):1107–1117.

Ravikumar, B., Stewart, A., Kita, H., Kato, K., Duden, R. & Rubinsztein, D.C. 2003. Raised intracellular glucose concentrations reduce aggredation and cell death caused by mutant huntingtin exon 1 by decreasing mTOR phosphorylation and inducing autophagy. *Human Molecular Genetics*. 12(9):985–994.

Ravikumar, B., Vacher, C., Berger, Z., Davies, J.E., Luo, S., Oroz, L.G., Scaravilli, F., Easton, D.F., et al. 2004. Inhibition of mTOR induces autophagy and reduces toxicity of polyglutamine expansions in fly and mouse models of Huntington disease. *Nature Genetics*. 36(6):585–595.

Remington, G., Foussias, G., Fervaha, G., Agid, O., Takeuchi, H., Lee, J. & Hahn, M. 2016. Treating Negative Symptoms in Schizophrenia: an Update. *Current Treatment Options in Psychiatry*. 3(2):133–150.

Rietschel, M., Mattheisen, M., Degenhardt, F., Mühleisen, T.W., Kirsch, P., Esslinger, C., Herms, S., Demontis, D., et al. 2012. Association between genetic variation in a region on chromosome 11 and schizophrenia in large samples from Europe. *Molecular Psychiatry*. 17(9):906–917.

Riglin, L., Collishaw, S., Richards, A., Thapar, A.K., Maughan, B., O'Donovan, M.C. & Thapar, A. 2017. Schizophrenia risk alleles and neurodevelopmental outcomes in childhood: a population-based cohort study. *The Lancet Psychiatry*.

Ripke, S., O'Dushlaine, C., Chambert, K., Moran, J.L., Kähler, A.K., Akterin, S., Bergen, S.E., Collins, A.L., et al. 2013. Genome-wide association analysis identifies 13 new risk loci for schizophrenia. *Nature Genetics*. 45(10):1150–1159.

Rohé, C.F., Montagna, P., Breedveld, G., Cortelli, P., Oostra, B.A. & Bonifati, V. 2004. Homozygous PINK1 C-terminus mutation causing early-onset parkinsonism. *Annals of Neurology*. 56(3):427–431.

Rong, J., McGuire, J.R., Fang, Z.-H., Sheng, G., Shin, J.-Y., Li, S.-H. & Li, X.-J. 2006. Regulation of intracellular trafficking of huntingtin-associated protein-1 is critical for TrkA protein levels and neurite outgrowth. *The Journal of neuroscience : the official journal of the Society for Neuroscience*. 26(22):6019–30.

Rose, C., Menzies, F.M., Renna, M., Acevedo-Arozena, A., Corrochano, S., Sadiq, O., Brown, S.D. & Rubinsztein, D.C. 2010. Rilmenidine attenuates toxicity of polyglutamine expansions in a mouse model of Huntington's disease. *Human Molecular Genetics*. 19(11):2144–2153.

Ross, C.A. & Tabrizi, S.J. 2011.

Rstudio, T. 2020. [Online], Available: http://www.rstudio.com/.

Rubinsztein, D.C., DiFiglia, M., Heintz, N., Nixon, R.A., Qin, Z.H., Ravikumar, B., Stefanis, L. & Tolkovsky, A. 2005. Autophagy and its possible roles in nervous system diseases, damage and repair. *Autophagy*. 1(1):11–22.

Rubinsztein, D.C., Codogno, P. & Levine, B. 2012. Autophagy modulation as a potential therapeutic target for diverse diseases. *Nature Reviews Drug Discovery*. 11(9):709–730.

Ryskalin, L., Limanaqi, F., Frati, A., Busceti, C.L. & Fornai, F. 2018. mTOR-related brain dysfunctions in neuropsychiatric disorders. *International Journal of Molecular Sciences*. 19(8):11–13.

Saftig, P., Beertsen, W. & Eskelinen, E.L. 2008. LAMP-2: A control step fot phagosome and autophagosome maturation. *Autophagy*. 4(4):510–512.

Saha, S., Chant, D., Welham, J. & McGrath, J. 2005.

Samara, M.T., Dold, M., Gianatsi, M., Nikolakopoulou, A., Helfer, B., Salanti, G. & Leucht, S. 2016. Efficacy, acceptability, and tolerability of antipsychotics in treatment-resistant schizophrenia: A network meta-analysis. *JAMA Psychiatry*. 73(3):199–210.

Samuels, D.C., Burn, D.J. & Chinnery, P.F. 2009. Detecting new neurodegenerative disease genes: does phenotype accuracy limit the horizon? *Trends in Genetics*. 25(11):486–488.

De Santi, M., Baldelli, G., Diotallevi, A., Galluzzi, L., Schiavano, G.F. & Brandi, G. 2019. Metformin prevents cell tumorigenesis through autophagy-related cell death. *Scientific reports*. 9(1):66.

Sarkar, S. 2013. Regulation of autophagy by mTOR-dependent and mTOR-independent pathways: Autophagy dysfunction in neurodegenerative diseases and therapeutic application of autophagy enhancers. *Biochemical Society Transactions*. 41(5):1103–1130.

Sarkar, S., Krishna, G., Imarisio, S., Saiki, S., O'Kane, C.J. & Rubinsztein, D.C. 2008. A rational mechanism for

combination treatment of Huntington's disease using lithium and rapamycin. *Human Molecular Genetics*. 17(2):170–178.

Schneider, J.L., Miller, A.M. & Woesner, M.E. 2017. Autophagy and Schizophrenia: A Closer Look at How Dysregulation of Neuronal Cell Homeostasis Influences the Pathogenesis of Schizophrenia. *Einstein Journal of Biology and Medicine*. 31(1&2):34.

Schork, A.J., Won, H., Appadurai, V., Nudel, R., Gandal, M., Delaneau, O., Revsbech Christiansen, M., Hougaard, D.M., et al. 2019. A genome-wide association study of shared risk across psychiatric disorders implicates gene regulation during fetal neurodevelopment. *Nature Neuroscience*. 22(3):353–361.

Scott, R.C., Schuldiner, O. & Neufeld, T.P. 2004. Role and regulation of starvation-induced autophagy in the Drosophila fat body. *Developmental Cell*. 7(2):167–178.

Seshadri, S., Kamiya, A., Yokota, Y., Prikulis, I., Kano, S. -i., Hayashi-Takagi, A., Stanco, A., Eom, T.-Y., et al. 2010. Disrupted-in-Schizophrenia-1 expression is regulated by -site amyloid precursor protein cleaving enzyme-1-neuregulin cascade. *Proceedings of the National Academy of Sciences*. 107(12):5622–5627.

Sharif, Z. 2008. Medication adherence in schizophrenia: patient perspectives and the clinical utility of paliperidone ER. *Patient Preference and Adherence*. (December):233.

Shibata, M., Lu, T., Furuya, T., Degterev, A., Mizushima, N., Yoshimori, T., MacDonald, M., Yankner, B., et al. 2006. Regulation of intracellular accumulation of mutant huntingtin by beclin 1. *Journal of Biological Chemistry*. 281(20):14474–14485.

Shin, S.Y., Lee, K.S., Choi, Y.K., Lim, H.J., Lee, H.G., Lim, Y. & Lee, Y.H. 2013. The antipsychotic agent chlorpromazine induces autophagic cell death by inhibiting the Akt/mtor pathway in human U-87MG glioma cells. *Carcinogenesis*. 34(9):2080–2089.

Shrigley, S., Pircs, K., Barker, R.A., Parmar, M. & Drouin-Ouellet, J. 2018. Simple generation of a high yield culture of induced neurons from human adult skin fibroblasts. *Journal of Visualized Experiments*. 2018(132):56904.

Siegert, S., Seo, J., Kwon, E.J., Rudenko, A., Cho, S., Wang, W., Flood, Z., Martorell, A.J., et al. 2015. The schizophrenia risk gene product miR-137 alters presynaptic plasticity. *Nature Neuroscience*. 18(7):1008–1016.

Sim, N.-L., Kumar, P., Hu, J., Henikoff, S., Schneider, G. & Ng, P.C. 2012. SIFT web server: predicting effects of amino acid substitutions on proteins. *Nucleic acids research*. 40(Web Server issue):W452-7.

Sirugo, G., Williams, S.M. & Tishkoff, S.A. 2019. The Missing Diversity in Human Genetic Studies. *Cell*. 177(1):26–31.

Siskind, D., Siskind, V. & Kisely, S. 2017. Clozapine Response Rates among People with Treatment-Resistant Schizophrenia: Data from a Systematic Review and Meta-Analysis. *Canadian Journal of Psychiatry*. 62(11):772–777.

Smith, R.C., Leucht, S. & Davis, J.M. 2019. Maximizing response to first-line antipsychotics in schizophrenia: a review focused on finding from meta-analysis. *Psychopharmacology*. 236(2):545–559.

Solé, X., Guinó, E., Valls, J., Iniesta, R. & Moreno, V. 2006. SNPStats: A web tool for the analysis of association studies. *Bioinformatics*. 22(15):1928–1929.

Spencer, B., Potkar, R., Trejo, M., Rockenstein, E., Patrick, C., Gindi, R., Adame, A., Wyss-Coray, T., et al. 2009. Beclin 1 Gene Transfer Activates Autophagy and Ameliorates the Neurodegenerative Pathology in -Synuclein Models of Parkinson's and Lewy Body Diseases. *Journal of Neuroscience*. 29(43):13578–13588.

Stahlberg, O., Soderstrom, H., Rastam, M. & Gillberg, C. 2004. Bipolar disorder, schizophrenia, and other psychotic disorders in adults with childhood onset AD/HD and/or autism spectrum disorders. *Journal of Neural Transmission*. 111(7):891–902.

Stamatakou, E., Wróbel, L., Hill, S.M., Puri, C., Son, S.M., Fujimaki, M., Zhu, Y., Siddiqi, F., et al. 2020.

Mendelian neurodegenerative disease genes involved in autophagy. *Cell Discovery*. 6(1):24.

Sullivan, P.F., Magnusson, C., Reichenberg, A., Boman, M., Dalman, C., Davidson, M., Fruchter, E., Hultman, C.M., et al. 2012. Family history of schizophrenia and bipolar disorder as risk factors for autism. *Archives of general psychiatry*. 69(11):1099–1103.

Tabrizi, S.J., Scahill, R.I., Owen, G., Durr, A., Leavitt, B.R., Roos, R.A., Borowsky, B., Landwehrmeyer, B., et al. 2013. Predictors of phenotypic progression and disease onset in premanifest and early-stage Huntington's disease in the TRACK-HD study: Analysis of 36-month observational data. *The Lancet Neurology*. 12(7):637–649.

Tanaka, Y., Guhde, G., Suter, A., Eskelinen, E.L., Hartmann, D., Lüllmann-Rauch, R., Janssen, P.M.L., Blanz, J., et al. 2000. Accumulation of autophagic vacuoles and cardiomyopathy LAMP-2-deficient mice. *Nature*. 406(6798):902–906.

Tanji, K., Mori, F., Kakita, A., Takahashi, H. & Wakabayashi, K. 2011. Alteration of autophagosomal proteins (LC3, GABARAP and GATE-16) in Lewy body disease. *Neurobiology of Disease*. 43(3):690–697.

Taylor, S.F., Demeter, E., Phan, K.L., Tso, I.F. & Welsh, R.C. 2014. Abnormal GABAergic function and negative affect in schizophrenia. *Neuropsychopharmacology*. 39(4):1000–1008.

du Toit, A., Hofmeyr, J.H.S., Gniadek, T.J. & Loos, B. 2018. Measuring autophagosome flux. *Autophagy*. 14(6):1060–1071.

Travassos, L.H., Carneiro, L.A.M., Ramjeet, M., Hussey, S., Kim, Y.G., Magalhes, J.G., Yuan, L., Soares, F., et al. 2010. Nod1 and Nod2 direct autophagy by recruiting ATG16L1 to the plasma membrane at the site of bacterial entry. *Nature Immunology*. 11(1):55–62.

Valente, E.M., Bentivoglio, A.R., Dixon, P.H., Ferraris, A., Lalongo, T., Frontali, M., Albanese, A. & Wood, N.W. 2001. Localization of a novel locus for autosomal recessive early-onset parkinsonism, PARK6, on human chromosome 1p35-p36. *American Journal of Human Genetics*. 68(4):895–900.

Valente, E.M., Abou-Sleiman, P.M., Caputo, V., Muqit, M.M.K., Harvey, K., Gispert, S., Ali, Z., Del Turco, D., et al. 2004. Hereditary early-onset Parkinson's disease caused by mutations in PINK1. *Science*. 304(5674):1158–1160.

Valenti, O. & Grace, A.A. 2010. Antipsychotic drug-induced increases in ventral tegmental area dopamine neuron population activity via activation of the nucleus accumbens-ventral pallidum pathway. *The international journal of neuropsychopharmacology*. 13(7):845–60.

Valionyte, E., Yang, Y., Roberts, S.L., Kelly, J., Lu, B. & Luo, S. 2020. Lowering Mutant Huntingtin Levels and Toxicity: Autophagy-Endolysosome Pathways in Huntington's Disease. *Journal of Molecular Biology*. 432(8):2673–2691.

Vassos, E., Di Forti, M., Coleman, J., Iyegbe, C., Prata, D., Euesden, J., O'Reilly, P., Curtis, C., et al. 2017. An Examination of Polygenic Score Risk Prediction in Individuals With First-Episode Psychosis. *Biological Psychiatry*.

Vázquez, P., Arroba, A.I., Cecconi, F., de la Rosa, E.J., Boya, P. & de Pablo, F. 2012. Atg5 and Ambra1 differentially modulate neurogenesis in neural stem cells. *Autophagy*. 8(2):187–99.

Velligan, D.I., Weiden, P.J., Sajatovic, M., Scott, J., Carpenter, D., Ross, R., Docherty, J.P. & Expert Consensus Panel on Adherence Problems in Serious and Persistent Mental Illness. 2009. The Expert Consensus Guideline Series. *The Journal of Clinical Psychiatry*. 70(suppl 4):01–48.

Vicente, M.M., Talloczy, Z., Wong, E., Tang, G., Koga, H., Kaushik, S., Arias, E., Harris, S., et al. 2010. Inefficient Autophagy in Huntington's Disease. *Nature Neuroscience*. 13(5):567–576.

Victor, M.B., Richner, M., Olsen, H.E., Lee, S.W., Monteys, A.M., Ma, C., Huh, C.J., Zhang, B., et al. 2018. Striatal neurons directly converted from Huntington's disease patient fibroblasts recapitulate age-associated disease phenotypes. *Nature Neuroscience*. 21(3):341–352.

Vierbuchen, T., Ostermeier, A., Pang, Z.P., Kokubu, Y., Südhof, T.C. & Wernig, M. 2010. Direct conversion of

fibroblasts to functional neurons by defined factors. *Nature*. 463(7284):1035–1041.

Vithlani, M., Terunuma, M. & Moss, S.J. 2011. The dynamic modulation of GABAa receptor trafficking and its role in regulating the plasticity of inhibitory synapses. *Physiological Reviews*. 91(3):1009–1022.

Vucicevic, L., Misirkic-Marjanovic, M., Paunovic, V., Kravic-Stevovic, T., Martinovic, T., Ciric, D., Maric, N., Petricevic, S., et al. 2014. Autophagy inhibition uncovers the neurotoxic action of the antipsychotic drug olanzapine. *Autophagy*. 10(12):2362–2378.

Vucicevic, L., Misirkic-Marjanovic, M., Harhaji-Trajkovic, L., Maric, N. & Trajkovic, V. 2018. Mechanisms and therapeutic significance of autophagy modulation by antipsychotic drugs. *Cell Stress*. 2(11):282–291.

Vulih-Shultzman, I., Pinhasov, A., Mandel, S., Grigoriadis, N., Touloumi, O., Pittel, Z. & Gozes, I. 2007. Activity-dependent neuroprotective protein snippet NAP reduces tau hyperphosphorylation and enhances learning in a novel transgenic mouse model. *Journal of Pharmacology and Experimental Therapeutics*. 323(2):438–449.

Wade, M., Tai, S., Awenat, Y. & Haddock, G. 2017. A systematic review of service-user reasons for adherence and nonadherence to neuroleptic medication in psychosis. *Clinical Psychology Review*. 51:75–95.

Wang, H., Bedford, F.K., Brandon, N.J., Moss, S.J. & Olsen, R.W. 1999. GABA(A)-receptor-associated protein links GABA(A) receptors and the cytoskeleton. *Nature*. 397(6714):69–72.

Wei, S., Wang, L.E., Mchugh, M.K., Han, Y., Xiong, M., Amos, C.I., Spitz, M.R. & Wei, Q.W. 2012. Genome-wide gene-environment interaction analysis for asbestos exposure in lung cancer susceptibility. *Carcinogenesis*. 33(8):1531–1537.

Weinberger, D.R. 1987. Implications of Normal Brain Development for the Pathogenesis of Schizophrenia. *Archives of General Psychiatry*. 44(7):660–669.

Weinberger, D.R. 2017. Future of Days Past: Neurodevelopment and Schizophrenia. *Schizophrenia bulletin*. 43(6):1164–1168.

Wenzel, A. 2017. *Diagnostic and Statistical Manual of Mental Disorders, Fifth Edition (DSM-5)*.

Whirl-Carrillo, M., McDonagh, E.M., Hebert, J.M., Gong, L., Sangkuhl, K., Thorn, C.F., Altman, R.B. & Klein, T.E. 2012. Pharmacogenomics knowledge for personalized medicine. *Clinical Pharmacology and Therapeutics*. 92(4):414–417.

Whiteford, H.A., Degenhardt, L., Rehm, J., Baxter, A.J., Ferrari, A.J., Erskine, H.E., Charlson, F.J., Norman, R.E., et al. 2013. Global burden of disease attributable to mental and substance use disorders: Findings from the Global Burden of Disease Study 2010. *The Lancet*. 382(9904):1575–1586.

Wigginton, J.E., Cutler, D.J. & Abecasis, G.R. 2005. A note on exact tests of Hardy-Weinberg equilibrium. *American Journal of Human Genetics*. 76(5):887–893.

Wold, M.S., Lim, J., Lachance, V., Deng, Z. & Yue, Z. 2016. ULK1-mediated phosphorylation of ATG14 promotes autophagy and is impaired in Huntington's disease models. *Molecular Neurodegeneration*. 11(1):76.

Wong, E. & Cuervo, A.M. 2010. Autophagy gone awry in neurodegenerative diseases. *Nature Neuroscience*. 13(7):805–811.

Wong, E.H.F., Yocca, F., Smith, M.A. & Lee, C.M. 2010. Challenges and opportunities for drug discovery in psychiatric disorders: The drug hunters' perspective. *International Journal of Neuropsychopharmacology*. 13(9):1269–1284.

Wulff, S., Nielsen, M.O., Rostrup, E., Svarer, C., Jensen, L.T., Pinborg, L. & Glenthoj, B.Y. 2019. The relation between dopamine D2 receptor blockade and the brain reward system: A longitudinal study of first-episode schizophrenia patients. *Psychological Medicine*. 50(2):220–228.

Xia, J., Benner, M.J. & Hancock, R.E.W. 2014. NetworkAnalyst - integrative approaches for protein–protein interaction network analysis and visual exploration. *Nucleic Acids Research*. 42(W1):W167–W174.

Xia, J., Gill, E.E. & Hancock, R.E.W. 2015. NetworkAnalyst for statistical, visual and network-based meta-

analysis of gene expression data. *Nature Protocols*. 10(6):823–844.

Xu, J., Yang, Y., Pang, S., Huang, W., Qin, X., Hawley, R.G. & Yan, B. 2013. Identification of a novel 21bp-insertion variant within the LC3B gene promoter in sporadic Parkinson's disease. *Translational Research*. 161(5):441–443.

Yang, Z. & Klionsky, D.J. 2010. Mammalian autophagy: Core molecular machinery and signaling regulation. *Current Opinion in Cell Biology*. 22(2):124–131.

Yates, A.D., Achuthan, P., Akanni, W., Allen, J., Allen, J., Alvarez-Jarreta, J., Amode, M.R., Armean, I.M., et al. 2020. Ensembl 2020. *Nucleic Acids Research*. 48(D1):D682–D688.

Yim, W.W.-Y. & Mizushima, N. 2020. Lysosome biology in autophagy. *Cell Discovery*. 6(1):6.

Yolken, R.H., Torrey, E.F., Lieberman, J.A., Yang, S. & Dickerson, F.B. 2011. Serological evidence of exposure to Herpes Simplex Virus type 1 is associated with cognitive deficits in the CATIE schizophrenia sample. *Schizophrenia Research*. 128(1–3):61–65.

Youle, R.J. & Narendra, D.P. 2011. Mechanisms of mitophagy. *Nature Reviews Molecular Cell Biology*. 12(1):9–14.

Young, S.L., Taylor, M. & Lawrie, S.M. 2015. "first do no harm." A systematic review of the prevalence and management of antipsychotic adverse effects. *Journal of Psychopharmacology*. 29(4):353–362.

Yu, L., Chen, Y. & Tooze, S.A. 2018. Autophagy pathway: Cellular and molecular mechanisms. *Autophagy*. 14(2):207–215.

Yuan, Y., Wang, H., Wei, Z. & Li, W. 2015. Impaired autophagy in hilar mossy cells of the dentate gyrus and its implication in schizophrenia. *Journal of Genetics and Genomics*. 42(1):1–8.

Zhang, J.P. & Malhotra, A.K. 2013. Pharmacogenetics of antipsychotics: Recent progress and methodological issues. *Expert Opinion on Drug Metabolism and Toxicology*. 9(2):183–191.

Zhang, J.P., Gallego, J.A., Robinson, D.G., Malhotra, A.K., Kane, J.M. & Correll, C.U. 2013. Efficacy and safety of individual second-generation vs. first-generation antipsychotics in first-episode psychosis: A systematic review and meta-analysis. *International Journal of Neuropsychopharmacology*. 16(6):1205–1218.

Zhang, L., Yu, J., Pan, H., Hu, P., Hao, Y., Cai, W., Zhu, H., Yu, A.D., et al. 2007. Small molecule regulators of autophagy identified by an image-based high-throughput screen. *Proceedings of the National Academy of Sciences of the United States of America*. 104(48):19023–19028.

Zhong, Y., Kinio, A. & Saleh, M. 2013. Functions of NOD-Like Receptors in Human Diseases. *Frontiers in Immunology*. 4:333.

Zhou, G., Soufan, O., Ewald, J., Hancock, R.E.W., Basu, N. & Xia, J. 2019. NetworkAnalyst 3.0: a visual analytics platform for comprehensive gene expression profiling and meta-analysis. *Nucleic Acids Research*. 47(W1):W234–W241.

Zhou, J., Tan, S.H., Nicolas, V., Bauvy, C., Yang, N. Di, Zhang, J., Xue, Y., Codogno, P., et al. 2013. Activation of lysosomal function in the course of autophagy via mTORC1 suppression and autophagosome-lysosome fusion. *Cell Research*. 23(4):508–523.

Zhu, X., Casadesus, G., Webber, K.M., Atwood, C.S., Bowen, R.L., Perry, G. & Smith, M.A. 2008. Parallels Between Neurodevelopment and Neurodegeneration: A Case Study of Alzheimer's Disease. *Handbook of Neurochemistry and Molecular Neurobiology*. 147–155.

Zufferey, R., Nagy, D., Mandel, R.J., Naldini, L. & Trono, D. 1997. Multiply attenuated lentiviral vector achieves efficient gene delivery in vivo. *Nature biotechnology*. 15(9):871–5.

I. APPENDIX A

1. Supplementary data

Supplementary table 1. RegulomeDB Scoring Categories

Score	Description
Likely to affect binding and linked to expression of a gene target	
1a	eQTL + TF binding + matched TF motif + matched DNase footprint + DNase peak
1b	eQTL + TF binding + any motif + DNase footprint + DNase peak
1c	eQTL + TF binding + matched TF motif + DNase peak
1d	eQTL + TF binding + any motif + DNase peak
1e	eQTL + TF binding + matched TF motif
1f	eQTL + TF binding/ DNase peak
Likely to affect binding	
2a	TF binding + matched TF motif + matched DNase footprint + DNase peak
2b	TF binding + any motif + DNase footprint + DNase peak
2c	TF binding + matched TF motif + DNase peak
Less likely to affect binding	
3a	TF binding + any motif + DNase peak
3b	TF binding + matched TF motif
Minimal binding evidence	
4	TF binding + DNase peak
5	TF binding or DNase peak
6	Motif hit

According to Boyle *et al*., 2012.

Supplementary table 2. Candidate genes association with autophagy, antipsychotic treatment response, neuropsychiatric disorders, and neurodegenerative diseases

Gene	Gene association as per the literature search*	Study reference	Population/Type of model/Review
AMBRA1	Autophagy, Central Nervous System Development	Maria Fimia *et al.*, 2007	Animal model, *in vitro*
ATG3	Autophagy, indirectly associated with Parkinson's disease (*ATG3* is part of the LC3 conjugation system)	Nath *et al.*, 2014; Xu, Yang, Pang, *et al.*, 2013	East Asian, *in vitro*
ATG7	Autophagy, Parkinson's disease	Chen, Pang, Feng, *et al.*, 2013	East Asian
ATG12	Autophagy, Parkinson's disease	Li, Huang, Pang, *et al.*, 2017	East Asian
ATG13	Autophagy, Schizophrenia, Autism spectrum disorder	Ryskalin, Limanaqi, Frati, *et al.*, 2018	Review
ATG14	Autophagy, Parkinson's disease, Alzheimer's disease, Drug response (indirectly *via* ULK complex)	Heras-Sandoval, Pérez-Rojas, Hernández-Damián, *et al.*, 2014; Kim *et al.*, 2018, 2017	Animal model, Review
ATG16L1	Autophagy, Schizophrenia	Glatt, Chandler, Bousman, *et al.*, 2009	North American
BECN1	Autophagy, Schizophrenia, Alzheimer's disease, Parkinson's disease	Bieri, Lucin, O'Brien, *et al.*, 2018; Merenlender-Wagner *et al.*, 2015; Spencer, Potkar, Trejo, *et al.*, 2009	Australian, *In vitro,* Animal model
GABARAP	Autophagy, Schizophrenia, Parkinson's disease	Tanji *et al.*, 2011; Xu *et al.*, 2013; El Haddad, Serrano, Moal, *et al.*, 2020	East Asian, *In vitro,* European
PINK1	Autophagy, Parkinson's disease, Amyotrophic lateral sclerosis	Hedrich, Hagenah, Djarmati, *et al.*, 2006; Ibáñez, Lesage, Lohmann, *et al.*, 2006; Li, Tomiyama, Sato, *et al.*, 2005; Rohé, Montagna, Breedveld, *et al.*, 2004; Valente, Bentivoglio, Dixon, *et al.*, 2001	European, African, East Asian

*Literature search association includes data obtained *via* NGHRI-EBI GWAS Catalog.

Supplementary table 3. Electronic sources utilised within study

Tool	Website	Accession date
Enrichr	https://amp.pharm.mssm.edu/Enrichr/	June 2020, July 2020
Ensembl Genome Browser release 102	https://www.ensembl.org/index.html	June, July 2020
NetworkAnalyst 3.0	https://www.networkanalyst.ca/	October 2020
NHGRI-EBI GWAS Catalogue	https://www.ebi.ac.uk/gwas/	March - May 2019, May - June 2020
PharmGKB	https://www.pharmgkb.org/	June 2020
PolymiRTS	http://compbio.uthsc.edu/miRSNP/home.php	August 2020
PolyPhen-2	http://genetics.bwh.harvard.edu/pph2/	July 2020
PubMed	https://www.ncbi.nlm.nih.gov/pubmed/	March - May 2019, May - June 2020
RegulomeDB 2.0	https://regulomedb.org/regulome-search	August 2020
rSNPBase	http://rsnp.psych.ac.cn/	August 2020
SIFT	https://sift.bii.a-star.edu.sg/	August 2020
SNP2TFBS	https://ccg.epfl.ch//snp2tfbs/	August 2020
SNPNexus	https://www.snp-nexus.org/v4/	July 2020
SNPStats	https://www.snpstats.net/start.htm	July 2020

Supplementary table 4. Functional impact of prioritised variants

Gene	Chr	SNP rsID	MAF	Alleles		Ensembl		SNPNexus		SIFT	Polyphen-2
				Minor	Major	Position GRCh37	Functional Consequence	SIFT	Polyphen	SIFT prediction	
AMBRA1	11	rs11819869	0.466	*T*	*C*	46539130	Intronic	*NA*	*NA*	*NA*	*NA*
	11	rs17197116	0.078	*C*	*T*	46498752	Intronic/Upstream	*NA*	*NA*	*NA*	*NA*
ATG3	3	rs2131008	0.422	*T*	*C*	112531572	Downstream/Upstream	*NA*	*NA*	*NA*	*NA*
	3	rs2969896	0.211	*G*	*A*	112537783	Synonymous/3' UTR/NMD target/Non-coding transcript exon/Downstream/Upstream	*NA*	*NA*	Tolerated	*NA*
ATG7	3	rs11128552	0.194	*G*	*T*	11498481	Intronic	*NA*	*NA*	*NA*	*NA*
	3	rs12636305	0.238	*G*	*T*	11377450	Intronic	*NA*	*NA*	*NA*	*NA*
	3	rs2442772	0.388	*A*	*G*	11452452	Intronic	*NA*	*NA*	*NA*	*NA*
	3	rs2442795	0.123	*T*	*G*	11509726	Intronic	*NA*	*NA*	*NA*	*NA*
	3	rs2454512	0.170	*A*	*G*	11446032	Intronic	*NA*	*NA*	*NA*	*NA*
	3	rs2594967	0.189	*T*	*G*	11308274	Intronic/NMD target/Downstream/Upstream	*NA*	*NA*	*NA*	*NA*
	3	rs2594992	0.157	*C*	*A*	11319523	Intronic/Downstream/ NMD target/Non-coding	*NA*	*NA*	*NA*	*NA*
	3	rs2606736	0.485	*A*	*G*	11358775	Downstream/Upstream/ Intronic	*NA*	*NA*	*NA*	*NA*
	3	rs6442259	0.427	*T*	*C*	11536677	Intronic	*NA*	*NA*	*NA*	*NA*
ATG12	5	rs26534	0.471	*A*	*G*	115840004	Intronic/NMD target/Upstream/Downstream	*NA*	*NA*	*NA*	*NA*
	5	rs26536	0.432	*A*	*G*	115840892	Non-coding transcript exonic/Upstream/3' UTR/NMD target/ Intronic	*NA*	*NA*	*NA*	*NA*
	5	rs6594908	0.209	*G*	*A*	115839806	Intronic/NMD target/Upstream/Downstream	*NA*	*NA*	*NA*	*NA*
ATG13	11	rs10769204	0.354	*T*	*C*	46654807	Intronic/Non-coding/Upstream	*NA*	*NA*	*NA*	*NA*
	11	rs10838610	0.354	*A*	*G*	46664710	Upstream/TFBS/Intronic/Non-coding/Downstream	*NA*	*NA*	*NA*	*NA*
	11	rs11038965	0.076	*T*	*G*	46670046	Intronic/Upstream/Downstream	*NA*	*NA*	*NA*	*NA*
	11	rs13448	0.354	*C*	*T*	46673864	Intronic/Non-coding/3' UTR/Downstream	*NA*	*NA*	*NA*	*NA*
	11	rs4606447	0.388	*G*	*A*	46670187	Downstream/Upstream/Intronic	*NA*	*NA*	*NA*	*NA*
ATG14	14	rs1538257	0.325	*T*	*G*	55412559	Upstream/Downstream	*NA*	*NA*	*NA*	*NA*
	14	rs57295720	0.068	*T*	*C*	55411648	Missense/Downstream (Valine to Isoleucine)	Tolerated	Benign	Tolerated	Benign
	14	rs7150763	0.314	*G*	*A*	55373083	Intronic/Non-coding	*NA*	*NA*	*NA*	*NA*
	14	rs8003279	0.186	*G*	*A*	55397412	Synonymous/Upstream	*NA*	*NA*	Tolerated	*NA*

	2	rs1045095	0.277	*T*	*C*	233294901	3' UTR/NMD target/Downstream/Non-coding transcript exon	*NA*	*NA*	*NA*	*NA*
	2	rs10803619	0.121	*T*	*C*	233295230	3' UTR/ NMD target/Downstream/Non-coding transcript exon	*NA*	*NA*	*NA*	*NA*
	2	rs2241879	0.340	*A*	*G*	233274822	Intronic/NMD target/Downstream/Upstream/Intronic/Non-coding	*NA*	*NA*	*NA*	*NA*
ATG16L1	2	rs2241880	0.340	*G*	*A*	233274722	Missense/3' UTR/NMD target/Non-coding transcript exon/Upstream/Downstream (Threonine to Alanine)	*NA*	*NA*	Tolerated	Benign
	2	rs3792106	0.471	*T*	*C*	233282094	Intronic/NMD target/Downstream/Intronic/Non-coding	*NA*	*NA*	*NA*	*NA*
	2	rs3792109	0.335	*A*	*G*	233275771	Intronic/NMD target/Intronic/Non-coding/Non-coding transcript exon/Upstream/Downstream	*NA*	*NA*	*NA*	*NA*
	2	rs3828309	0.335	*G*	*A*	233271764	Intronic/NMD target/Upstream/ Intronic/Non-coding	*NA*	*NA*	*NA*	*NA*
	2	rs6758317	0.286	*T*	*C*	233260305	Intronic/NMD target/Non-coding	*NA*	*NA*	*NA*	*NA*
GABARAP	17	rs222843	0.170	*G*	*A*	7242662	Upstream/Downstream/Intronic/NMD target/Non-coding transcript exon	*NA*	*NA*	*NA*	*NA*
	1	rs1043424	0.330	*C*	*A*	20650507	Missense/Non-coding transcript exon/Downstream (Asparagine to Threonine)	*NA*	*NA*	Tolerated	Benign
	1	rs16824318	0.053	*C*	*A*	20651181	3' UTR/Non-coding transcript exon/Downstream	*NA*	*NA*	*NA*	*NA*
PINK1	1	rs3102071	0.175	*A*	*G*	20641518	Intronic/Non-coding/Upstream/Downstream	*NA*	*NA*	*NA*	*NA*
	1	rs3738136	0.073	*A*	*G*	20645618	Missense/Non-coding transcript exon (Alanine to Threonine)	Tolerated	Benign	Tolerated	Benign
	1	rs650616	0.452	*A*	*G*	20651565	Downstream/Non-coding transcript exon	*NA*	*NA*	*NA*	*NA*

3': 3-prime end; NMD: Nonsense-mediated mRNA decay; UTR: untranslated region.

Supplementary table 5. Regulatory impact of prioritised variants

Gene	SNP rsID	RegulomeDB	PolymiRTs	SNP2TFBS	rSNPBase				eQTL	mirTarBase/ miRNA	*CpG island*
					rSNP	Proximal	Distal	RNA binding protein mediated regulation			
AMBRA1	rs11819869	5	*NA*	*NA*	Yes	No	Yes	Yes	Yes	*NA*	*NA*
	rs17197116	4	*NA*	*NA*	*NA*	*NA*	*NA*	*NA*	*NA*	*NA*	*NA*
ATG3	rs2131008	1f	*NA*	*NA*	No	No	No	No	Yes	*NA*	*NA*
	rs2969896	7	*NA*	*NA*	Yes	Yes	No	Yes	Yes	Yes	*NA*
ATG7	rs11128552	3a	*NA*	*NA*	Yes	No	Yes	Yes	No	*NA*	*NA*
	rs12636305	3a	*NA*	*NA*	Yes	No	No	Yes	Yes	*NA*	*NA*
	rs2442772	3a	*NA*	*NA*	Yes	No	No	Yes	No	*NA*	*NA*
	rs2442795	2b	*NA*	*NA*	Yes	No	No	Yes	No	*NA*	*NA*
	rs2454512	2b	*NA*	Yes	Yes	No	No	Yes	Yes	*NA*	*NA*
	rs2594967	3a	*NA*	*NA*	Yes	Yes	No	Yes	No	*NA*	*NA*
	rs2594992	5	*NA*	*NA*	Yes	No	Yes	Yes	Yes	*NA*	*NA*
	rs2606736	5	*NA*	*NA*	Yes	Yes	Yes	Yes	No	*NA*	*NA*
	rs6442259	2b	*NA*	*NA*	Yes	No	Yes	Yes	No	NA	*NA*
ATG12	rs26534	1d	*NA*	*NA*	*NA*	*NA*	*NA*	*NA*	*NA*	*NA*	*NA*
	rs26536	2b	*NA*	*NA*	*NA*	*NA*	*NA*	*NA*	*NA*	*NA*	*NA*
	rs6594908	3a	*NA*	*NA*	Yes	Yes	Yes	Yes	Yes	*NA*	*NA*
ATG13	rs10769204	5	*NA*	*NA*	Yes	Yes	No	Yes	No	*NA*	*NA*
	rs10838610	2a	*NA*	*NA*	Yes	Yes	No	Yes	Yes	*NA*	*NA*
	rs11038965	3a	*NA*	*NA*	*NA*	*NA*	*NA*	*NA*	*NA*	*NA*	*NA*
	rs13448	3a	*NA*	Yes	Yes	Yes	Yes	Yes	Yes	*NA*	*NA*
	rs4606447	2b	*NA*	*NA*	Yes	Yes	No	Yes	Yes	*NA*	*NA*
ATG14	rs1538257	1f	*NA*	*NA*	Yes	Yes	Yes	No	Yes	*NA*	*NA*
	rs57295720	4	*NA*	*NA*	*NA*	*NA*	*NA*	*NA*	*NA*	*NA*	*NA*
	rs7150763	3a	*NA*	*NA*	Yes	No	No	Yes	Yes	*NA*	*NA*
	rs8003279	5	*NA*	*NA*	Yes	Yes	Yes	Yes	Yes	*NA*	*NA*
ATG16L1	rs1045095	5	Yes	*NA*	Yes	Yes	Yes	Yes	Yes	*NA*	*NA*
	rs10803619	5	Yes	*NA*	Yes	Yes	Yes	Yes	No	*NA*	*NA*
	rs2241879	7	*NA*	*NA*	Yes	Yes	No	Yes	Yes	*NA*	*NA*
	rs2241880	7	*NA*	*NA*	Yes	Yes	No	Yes	Yes	*NA*	*NA*

ATG16L1	rs3792106	5	*NA*	*NA*	Yes	No	Yes	Yes	Yes	*NA*	*NA*
	rs3792109	5	*NA*	*NA*	Yes	Yes	No	Yes	Yes	Yes	*NA*
	rs3828309	4	*NA*	*NA*	Yes	Yes	Yes	Yes	Yes	*NA*	*NA*
	rs6758317	3a	*NA*	*NA*	Yes	Yes	Yes	Yes	Yes	*NA*	*NA*
GABARAP	rs222843	1d	*NA*	*NA*	Yes	Yes	Yes	No	Yes	*NA*	*NA*
PINK1	rs1043424	4	*NA*	Yes	Yes	No	Yes	Yes	Yes	*NA*	*NA*
	rs16824318	3a	*NA*	*NA*	*NA*	*NA*	*NA*	*NA*	*NA*	*NA*	*NA*
	rs3102071	1f	*NA*	*NA*	Yes	Yes	Yes	Yes	Yes	*NA*	*NA*
	rs3738136	3a	*NA*	*NA*	*NA*	*NA*	*NA*	*NA*	*NA*	*NA*	*NA*
	rs650616	2b	*NA*	*NA*	Yes	Yes	Yes	Yes	Yes	*NA*	*NA*

NA: not available.

Supplementary table 6. Literature search concerning prioritised variants

Gene	Variants	NGHRI-EBI GWAS Catalog Association	Literature Search*	Study Accession	Ethnicity
AMBRA1	rs11819869	*NA*	Schizophrenia-related risk variant	PMID: 21747397	European
	rs17197116	Cigarettes smoked per day	*NA*	PMID: 30643251	European
ATG3	rs2131008	*NA*	*NA*	*NA*	*NA*
	rs2969896	*NA*	*NA*	*NA*	*NA*
ATG7	rs2594967	*NA*	*NA*	*NA*	*NA*
	rs2594992	Systolic blood pressure	*NA*	PMID27618452	European
	rs2606736	Systolic blood pressure and HDL cholesterol	Associated with reduced risk of clear cell renal cell carcinoma	PMID24097068; PMID27618447; PMID: 30827239	South Asian, East Asian, European, Latin American, African American
	rs12636305	*NA*	*NA*	*NA*	*NA*
	rs2454512	*NA*	*NA*	*NA*	*NA*
	rs2442772	*NA*	*NA*	*NA*	*NA*
	rs11128552	*NA*	*NA*	*NA*	*NA*
	rs2442795	*NA*	*NA*	*NA*	*NA*
	rs6442259	*NA*	*NA*	*NA*	*NA*
ATG12	rs6594908	*NA*	*NA*	*NA*	*NA*
	rs26534	*NA*	*NA*	*NA*	*NA*
	rs26536	*NA*	*NA*	*NA*	*NA*
ATG13	rs10769204	Age at first intercourse	*NA*	PMID:27089180	European
	rs10838610	*NA*	*NA*	*NA*	*NA*
	rs4606447	Reaction time	*NA*	PMID:29844566	European
	rs13448	*NA*	Associated with lower rate of hypertension	PMID: 28347919	European
	rs11038965	*NA*	*NA*	*NA*	*NA*
ATG14	rs7150763	*NA*	*NA*	*NA*	*NA*
	rs8003279	*NA*	Associated with treatment response in non-small lung cancer	PMID:28420621	East Asian
	rs1538257	*NA*	*NA*	*NA*	*NA*
	rs57295720	*NA*	*NA*	*NA*	*NA*

	rs6758317	Bilirubin levels	Associated to ankylosing spondylitis disease	PMID:32084209; PMID: 28952203	East Asian
	rs3828309	Crohn's disease	*NA*	PMID:18587394	European
	rs2241880	Crohn's disease	Ass. w/ hepatocellular carcinoma susceptibility and crohn's disease susceptbility	PMID:25048429; PMID: 17200669; PMID:17435756; PMID:20570966; PMID22412388; PMID:31484215	European, East Asian
ATG16L1	rs2241879	*NA*	Associated with susceptibility to Crohn's disease, and risk for IBD	PMID: 18162085; PMID: 32099608	West Asian, European
	rs3792109	Crohn's disease	Part of a haplotype associated with IBD	PMID:22936669; PMID:21102463; PMID: 28542425	European, South Asian
	rs3792106	*NA*	Associated with susceptibility to Crohn's disease; Part of a haplotype associated with IBD	PMID: 22833393; PMID: 28542425	South Asian
	rs1045095	*NA*	*NA*	*NA*	*NA*
	rs10803619	*NA*	*NA*	*NA*	*NA*
GABARAP	rs222843	*NA*	Associated with vulnerability to nicotine dependence	PMID: 17164261	European-Americans
	rs3102071	*NA*	*NA*	*NA*	*NA*
	rs1043424	*NA*	Predicts outcome in colorectal cancer	DOI: 10.1200/JCO.2019.37.15_suppl.3595	European
PINK1	rs650616	*NA*	*NA*	*NA*	*NA*
	rs3738136	*NA*	Potential marker for co-segregation of PINK1 with Parkinson's disease locus in familial cases	PMID: 19889566	South Asian
	rs16824318	*NA*	*NA*	*NA*	*NA*

IBD: inflammatory bowel disease; NA: not available; w/: with.

Supplementary table 7. Associations between genetic variants of the autophagy pathway and antipsychotic treatment response as defined by the change in log-transformed PANSS scores over 12 months under the genotypic model of inheritance

$\alpha = 2.08 \times 10^{-4}$

Genotypic model of inheritance

Gene	dbSNPID	PANSS Domain	Contrast	ATR	Effect estimate	95% CI	P-value
AMBRA1	**rs11819869**	**Negative**	***TT vs CC***	**Worsened**	**4.56E-03**	**2.04e-03 to 7.07e-03**	**0.000411****
	rs2454512	General	*AA vs GG*	Worsened	9.72E-03	2.28E-03 to 1.72E-02	1.06E-02
	rs2442795	General	*TT vs GG*	Worsened	1.05E-02	2.39E-03 to 1.87E-02	1.14E-02
	rs11128552	General	*GT vs TT*	Worsened	2.13E-03	1.84E-04 to 4.07E-03	3.18E-02
	rs2594967	General	*TT vs GG*	Worsened	4.80E-03	5.91E-04 to 9.00E-03	2.55E-02
	rs2442795	Negative	*TT vs GG*	Worsened	1.13E-02	2.957E-03 to 1.96E-02	8.05E-03
	rs2454512	Negative	*AA vs GG*	Worsened	1.00E-02	2.38E-03 to 1.77E-02	1.03E-02
	rs2442795	Negative	*TG vs GG*	Improved	-2.51E-03	-4.62E-03 to -3.98E-04	1.99E-02
	rs2442772	Negative	*AG vs GG*	Improved	-2.25E-03	-4.26E-03 to -2.44E-04	2.80E-02
	rs2442772	Negative	*AA vs GG*	Improved	-2.59E-03	-5.09E-03 to -9.54E-05	4.20E-02
	rs6442259	Negative	*TC vs CC*	Worsened	2.72E-03	6.32E-04 to 4.81E-03	1.08E-02
ATG7	rs2594992	Negative	*CA vs AA*	Worsened	2.65E-03	5.80E-04 to 4.73E-03	1.23E-02
	rs6442259	Positive	*TT vs CC*	Worsened	4.54E-03	1.31E-03 to 7.77E-03	5.89E-03
	rs2442772	Positive	*AG vs GG*	Improved	-3.23E-03	-5.82E-03 to -6.23E-04	1.50E-02
	rs2442772	Positive	*AA vs GG*	Improved	-4.19E-03	-7.43E-03 to -9.52E-04	1.13E-02
	rs2606736	Positive	*AA vs GG*	Worsened	4.33E-03	1.02E-03 to 7.64E-03	1.04E-02
	rs2454512	Total	*AA vs GG*	Worsened	9.65E-03	2.50E-03 to 1.68E-02	8.27E-03
	rs2442795	Total	*TG vs GG*	Improved	-2.43E-03	-4.41E-03 to -4.51E-04	1.62E-02
	rs2442772	Total	*AA vs GG*	Improved	-2.50E-03	-4.84E-03 to -1.52E-04	3.70E-02
	rs6442259	Total	*TC vs CC*	Worsened	2.00E-03	4.54E-05 to 3.95E-03	4.50E-02
	rs6442259	Total	*TT vs CC*	Worsened	2.47E-03	1.32E-04 to 4.81E-03	3.85E-02
	rs2442795	Total	*TT vs GG*	Worsened	1.04E-02	2.61E-03 to 1.82E-02	9.07E-03
ATG13	rs10769204	Negative	*TT vs CC*	Improved	-4.11E-03	-7.15E-03 to -1.06E-03	8.27E-03
	rs13448	Negative	*CT vs TT*	Worsened	2.21E-03	2.14E-04 to 4.21E-03	3.00E-02

ATG14	rs1538257	General	*AC vs CC*	Worsened	2.61E-03	6.92E-04 to 4.52E-03	7.72E-03
	rs8003279	General	*GG vs AA*	Improved	-6.29E-03	-1.20E-02 to -6.12E-04	3.00E-02
	rs1538257	**Negative**	***TG vs GG***	**Worsened**	**3.34E-03**	**1.39E-03 to 5.30E-03**	**0.000841****
	rs7150763	Negative	*GG vs AA*	Improved	-4.19E-03	-7.35E-03 to -1.03E-03	9.50E-03
	rs8003279	Total	*GG vs AA*	Improved	-5.44E-03	-1.09E-02 to -6.91E-06	4.98E-02
	rs1538257	Total	*AC vs CC*	Worsened	2.23E-03	3.92E-04 to 4.07E-03	1.76E-02
ATG16L1	rs6758317	Positive	*TT vs CC*	Worsened	6.01E-03	1.30E-03 to 1.07E-02	1.24E-02
	rs10803619	Positive	*TC vs CC*	Worsened	3.64E-03	4.44E-04 to 6.84E-03	2.57E-02
	rs10803619	Total	*TT vs CC*	Worsened	4.94E-03	3.43E-04 to 9.53E-03	3.53E-02
GABARAP	**rs222843**	**Negative**	***GG vs AA***	**Worsened**	**8.52E-03**	**3.62E-03 to 1.34E-02**	**0.000678****
	rs222843	Total	*GG vs AA*	Worsened	4.65E-03	2.45E-05 to 9.27E-03	4.89E-02

ATR: antipsychotic treatment response, indicates relative response to treatment over time between genotypes; CI: confidence interval; effect estimate: difference in log-transformed PANSS scores between the different genotypes, multiplied by time; ** illustrates P-value below the uncorrected threshold of 0.001. P-values with no asterisk have met an uncorrected threshold of P-value ≤ 0.05.

Supplementary table 8. Associations between genetic variants of the autophagy pathway and antipsychotic treatment response as defined by the change in log-transformed PANSS scores over 12 months under the additive allelic model of inheritance

			$\alpha = 2.08 \times 10^{-4}$				
			Additive allelic model of inheritance				
Gene	**dbSNPID**	**PANSS Domain**	**Contrast**	**ATR**	**Effect estimate**	**95% CI**	**P-value**
AMBRA1	**rs11819869**	**Negative**	**Each *T* allele**	**Worsened**	**2.20E-03**	**9.46E-04 to 3.46E-03**	**0.000613****
ATG7	rs2594992	Negative	Each *C* allele	Worsened	2.63E-03	8.59E-04 to 4.40E-03	3.68E-03
	rs2442772	Negative	Each *A* allele	Improved	-1.46E-03	-2.67E-03 to -2.49E-04	1.83E-02
	rs2442772	Positive	Each *A* allele	Improved	-2.29E-03	-3.86E-03 to -7.24E-04	4.25E-03
	rs6442259	Positive	Each *T* allele	Worsened	2.19E-03	5.96E-04 to 3.79E-03	7.22E-03
	rs2606736	Positive	Each *A* allele	Worsened	2.15E-03	4.96E-04 to 3.81E-03	1.10E-02
	rs2442772	Total	Each *A* allele	Improved	-1.30E-03	-2.43E-03 to -1.62E-04	2.52E-02
	rs6442259	Total	Each *T* allele	Worsened	1.29E-03	1.35E-04 to 2.45E-03	2.88E-02
ATG13	rs10769204	Negative	Each *T* allele	Improved	-1.92E-03	-3.28E-03 to -5.58E-04	5.80E-03
ATG16L1	rs10803619	General	Each *T* allele	Worsened	2.16E-03	3.89E-04 to 3.93E-03	1.69E-02
	rs10803619	Positive	Each *T* allele	Worsened	3.27E-03	9.26E-04 to 5.62E-03	6.35E-03
	rs6758317	Positive	Each *T* allele	Worsened	1.95E-03	6.37E-05 to 3.83E-03	4.28E-02
	rs10803619	Total	Each *T* allele	Worsened	2.30E-03	6.07E-04 to 4.00E-03	7.89E-03
GABARAP	rs222843	General	Each *G* allele	Worsened	1.88E-03	2.83E-04 to 3.48E-03	2.11E-02
	rs222843	Negative	Each *G* allele	Worsened	2.49E-03	8.62E-04 to 4.12E-03	2.79E-03
	rs222843	Total	Each *G* allele	Worsened	1.88E-03	3.45E-04 to 3.41E-03	1.65E-02

ATR: antipsychotic treatment response, indicates relative response to treatment over time with each additional minor allele; CI: confidence interval; effect estimate: difference in log-transformed PANSS scores with each additional minor allele, multiplied by time; ** illustrates P-value ≤ 0.001. No asterisks represent P-value ≤ 0.05.

Supplementary table 9. Associations between genetic variants of the mitophagy pathway and antipsychotic treatment response as defined by the change in log-transformed PANSS scores over 12 months under the genotypic model of inheritance

			$\alpha = 7.81 \times 10^{-4}$				
			Genotypic model of inheritance				
Gene	**dbSNPID**	**PANSS Domain**	**Contrast**	**ATR**	**Effect estimate**	**95% CI**	**P-value**
AMBRA1	**rs11819869**	**Negative**	***TT vs CC***	**Worsened**	**4.56E-03**	**2.04E-03 to 7.07E-03**	**0.000411*** **
GABARAP	**rs222843**	**Negative**	***GG vs AA***	**Worsened**	**8.52E-03**	**3.62E-03 to 1.34E-02**	**0.000678*** **
	rs222843	Total	*GG vs AA*	Worsened	4.65E-03	2.45E-05 to 9.27E-03	4.89E-02
PINK1	rs1043424	General	*CC vs AA*	Worsened	2.91E-03	9.63E-06 to 5.81E-03	4.93E-02
	rs650616	General	*AA vs GG*	Improved	-2.80E-03	-5.39E-03 to -1.95E-04	3.52E-02
	rs1043424	**Negative**	***CC vs AA***	**Worsened**	**5.96E-03**	**3.02E-03 to 8.90E-03**	**0.0000756*** **
	rs650616	Negative	*AA vs GG*	Improved	-3.09E-03	-5.75E-03 to -4.25E-04	2.32E-02
	rs1043424	Positive	*CA vs AA*	Improved	-3.41E-03	-5.91E-03 to -9.19E-04	7.40E-03

ATR: antipsychotic treatment response, indicates relative response to treatment over time between genotypes; CI: confidence interval; effect estimate: difference in log-transformed PANSS scores between the different genotypes, multiplied by time; *** illustrates P-value below the Bonferroni-corrected threshold α-value. No asterisks represent P-value ≤ 0.05.

Supplementary table 10. Associations between genetic variants of the mitophagy pathway and antipsychotic treatment response as defined by the change in log-transformed PANSS scores over 12 months under the additive allelic model of inheritance

			$\alpha = 7.81 \times 10^{-4}$ Additive allelic model of inheritance				
Gene	**dbSNPID**	**PANSS Domain**	**Contrast**	**ATR**	**Effect estimate**	**95% CI**	**P-value**
AMBRA1	**rs11819869**	**Negative**	**Each *T* allele**	**Worsened**	**2.20E-03**	**9.46E-04 to 3.46E-03**	**0.000613*** **
GABARAP	rs222843	General	Each *G* allele	Worsened	1.88E-03	2.83E-04 to 3.48E-03	2.11E-02
	rs222843	Negative	Each *G* allele	Worsened	2.49E-03	8.62E-04 to 4.12E-03	2.79E-03
	rs222843	Total	Each *G* allele	Worsened	1.88E-03	3.45E-04 to 3.41E-03	1.65E-02
PINK1	rs650616	General	Each *A* allele	Improved	-1.34E-03	-2.62E-03 to -5.22E-05	4.14E-02
	rs1043424	Negative	Each *C* allele	Worsened	2.00E-03	6.64E-04 to 3.33E-03	3.38E-03
	rs650616	Negative	Each *A* allele	Improved	-1.59E-03	-2.91E-03 to -2.79E-04	1.76E-02

ATR: antipsychotic treatment response, indicates relative response to treatment over time with each additional minor allele; CI: confidence interval; effect estimate: difference in log-transformed PANSS scores with each additional minor allele, multiplied by time; *** illustrates P-value below the Bonferroni-corrected threshold α-value. No asterisks represent P-value ≤ 0.05.

Supplementary table 11. Associations between genetic variants of the NOD-like receptor signalling pathway and antipsychotic treatment response as defined by the change in log-transformed PANSS scores over 12 months under the genotypic model of inheritance

			$\alpha = 6.94 \times 10^{-4}$ Genotypic model of inheritance				
Gene	**dbSNPID**	**PANSS Domain**	**Contrast**	**ATR**	**Effect estimate**	**95% CI**	**P-value**
ATG16L1	rs6758317	Positive	*TT vs CC*	Worsened	6.01E-03	1.30E-03 to 1.07E-02	1.24E-02
	rs10803619	Positive	*TC vs CC*	Worsened	3.64E-03	4.44E-04 to 6.84E-03	2.57E-02
	rs10803619	Total	*TT vs CC*	Worsened	4.94E-03	3.43E-04 to 9.53E-03	3.53E-02
GABARAP	**rs222843**	**Negative**	***GG vs AA***	**Worsened**	**8.52E-03**	**3.62E-03 to 1.34E-02**	**0.000678*** **
	rs222843	Total	*GG vs AA*	Worsened	4.65E-03	2.45E-05 to 9.27E-03	4.89E-02

ATR: antipsychotic treatment response, indicates relative response to treatment over time between genotypes; CI: confidence interval; effect estimate: difference in log-transformed PANSS scores between the different genotypes, multiplied by time; *** illustrates P-value below the Bonferroni-corrected threshold α-value. No asterisks represent P-value ≤ 0.05.

Supplementary table 12. Associations between genetic variants of the NOD-like receptor signalling pathway and antipsychotic treatment response as defined by the change in log-transformed PANSS scores over 12 months under the additive allelic model of inheritance

			$\alpha = 6.94 \times 10^{-4}$				
			Additive allelic model of inheritance				
Gene	**dbSNPID**	**PANSS Domain**	**Contrast**	**ATR**	**Effect estimate**	**95% CI**	**P-value**
ATG16L1	rs10803619	General	Each *T* allele	Worsened	2.16E-03	3.89E-04 to 3.93E-03	1.69E-02
	rs10803619	Positive	Each *T* allele	Worsened	3.27E-03	9.26E-04 to 5.62E-03	6.35E-03
	rs6758317	Positive	Each *T* allele	Worsened	1.95E-03	6.37E-05 to 3.83E-03	4.28E-02
	rs10803619	Total	Each *T* allele	Worsened	2.30E-03	6.07E-04 to 4.00E-03	7.89E-03
GABARAP	rs222843	General	Each *G* allele	Worsened	1.88E-03	2.83E-04 to 3.48E-03	2.11E-02
	rs222843	Negative	Each *G* allele	Worsened	2.49E-03	8.62E-04 to 4.12E-03	2.79E-03
	rs222843	Total	Each *G* allele	Worsened	1.88E-03	3.45E-04 to 3.41E-03	1.65E-02

ATR: antipsychotic treatment response, indicates relative response to treatment over time with each additional minor allele; CI: confidence interval; effect estimate: difference in log-transformed PANSS scores with each additional minor allele, multiplied by time; P-values have met an uncorrected threshold of P-value ≤ 0.05.

Supplementary table 13. Associations between genetic variants of the KSHV infection pathway and antipsychotic treatment response as defined by the change in log-transformed PANSS scores over 12 months under the genotypic model of inheritance

$\alpha = 8.93 \times 10^{-4}$

Genotypic model of inheritance

Gene	dbSNPID	PANSS Domain	Contrast	ATR	Effect estimate	95% CI	P-value
ATG14	rs1538257	General	*TG vs GG*	Worsened	2.61E-03	6.92E-04 to 4.52E-03	7.72E-03
	rs8003279	General	*GG vs AA*	Improved	-6.29E-03	-1.20E-02 to -6.12E-04	3.00E-02
	rs1538257	**Negative**	*TG vs GG*	**Worsened**	**3.34E-03**	**1.39E-03 to 5.30E-03**	**0.000841*** **
	rs7150763	Negative	*GG vs AA*	Improved	-4.19E-03	-7.35E-03 to -1.03e-03	9.50E-03
	rs8003279	Total	*GG vs AA*	Improved	-5.44E-03	-1.09E-02 to -6.91E-06	4.98E-02
	rs1538257	Total	*TG vs GG*	Worsened	2.23E-03	3.92E-04 to 4.07E-03	1.76E-02
GABARAP	**rs222843**	**Negative**	***GG vs AA***	**Worsened**	**8.52E-03**	**3.62E-03 to 1.34E-02**	**0.000678*** **
	rs222843	Total	*GG vs AA*	Worsened	4.65E-03	2.45E-05 to 9.27E-03	4.89E-02

ATR: antipsychotic treatment response, indicates relative response to treatment over time between genotypes; CI: confidence interval; effect estimate: difference in log-transformed PANSS scores between the different genotypes, multiplied by time; *** illustrates P-value below the Bonferroni-corrected threshold α-value. No asterisks represent P-value ≤ 0.05.

Supplementary table 14. Associations between genetic variants of the KSHV infection pathway and antipsychotic treatment response as defined by the change in log-transformed PANSS scores over 12 months under the additive allelic model of inheritance

$\alpha = 8.93 \times 10^{-4}$

Additive allelic model of inheritance

Gene	dbSNPID	PANSS Domain	Contrast	ATR	Effect estimate	95% CI	P-value
GABARAP	rs222843	General	Each *G* allele	Worsened	1.88E-03	2.83E-04 to 3.48E-03	2.11E-02
	rs222843	Negative	Each *G* allele	Worsened	2.49E-03	8.62E-04 to 4.12E-03	2.79E-03
	rs222843	Total	Each *G* allele	Worsened	1.88E-03	3.45E-04 to 3.41E-03	1.65E-02

ATR: antipsychotic treatment response, indicates relative response to treatment over time with each additional minor allele; CI: confidence interval; effect estimate: difference in log-transformed PANSS scores with each additional minor allele, multiplied by time; P-values have met an uncorrected threshold of P-value ≤ 0.05.

Supplementary table 15. Associations between genetic variants of the schizophrenia pathway and antipsychotic treatment response as defined by the change in log-transformed PANSS scores over 12 months under the genotypic model of inheritance

			$\alpha = 5.21 \times 10^{-4}$ Genotypic model of inheritance				
Gene	**dbSNPID**	**PANSS Domain**	**Contrast**	**ATR**	**Effect estimate**	**95% CI**	**P-value**
AMBRA1	**rs11819869**	**Negative**	***TT vs CC***	**Worsened**	**4.56E-03**	**2.04E-03 to 7.07E-03**	**0.000411*** **
ATG13	rs10769204	Negative	*TT vs CC*	Improved	-4.11E-03	-7.15E-03 to -1.06E-03	8.27E-03
	rs13448	Negative	*CT vs TT*	Worsened	2.21E-03	2.14E-04 to 4.21E-03	3.00E-02
ATG16L1	rs6758317	Positive	*TT vs CC*	Worsened	6.01E-03	1.30E-03 to 1.07E-02	1.24E-02
	rs10803619	Positive	*TC vs CC*	Worsened	3.64E-03	4.44E-04 to 6.84E-03	2.57E-02
	rs10803619	Total	*TT vs CC*	Worsened	4.94E-03	3.43E-04 to 9.53E-03	3.53E-02
GABARAP	**rs222843**	**Negative**	***GG vs AA***	**Worsened**	**8.52E-03**	**3.62E-03 to 1.34E-02**	**0.000678****
	rs222843	Total	*GG vs AA*	Worsened	4.65E-03	2.45E-05 to 9.27E-03	4.89E-02

ATR: antipsychotic treatment response, indicates relative response to treatment over time between genotypes; CI: confidence interval; effect estimate: difference in log-transformed PANSS scores between the different genotypes, multiplied by time; ** illustrates P-value ≤ 0.001; *** illustrates P-value below the Bonferroni-corrected threshold α-value. No asterisks represent P-value ≤ 0.05.

Supplementary table 16. Associations between genetic variants of the schizophrenia pathway and antipsychotic treatment response as defined by the change in log-transformed PANSS scores over 12 months under the additive allelic model of inheritance

			$\alpha = 5.21 \times 10^{-4}$				
			Additive allelic model of inheritance				
Gene	**dbSNPID**	**PANSS Domain**	**Contrast**	**ATR**	**Effect estimate**	**95% CI**	**P-value**
AMBRA1	**rs11819869**	**Negative**	**Each *T* allele**	**Worsened**	**2.20E-03**	**9.46E-04 to 3.46E-03**	**0.000613****
ATG13	rs10769204	Negative	Each *T* allele	Improved	-1.92E-03	-3.28E-03 to -5.58E-04	5.80E-03
ATG16L1	rs10803619	General	Each *T* allele	Worsened	2.16E-03	3.89E-04 to 3.93E-03	1.69E-02
	rs10803619	Positive	Each *T* allele	Worsened	3.27E-03	9.26E-04 to 5.62E-03	6.35E-03
	rs6758317	Positive	Each *T* allele	Worsened	1.95E-03	6.37E-05 to 3.83E-03	4.28E-02
	rs10803619	Total	Each *T* allele	Worsened	2.30E-03	6.07E-04 to 4.00E-03	7.89E-03
	rs2241880	Total	Each *G* allele	Improved	-1.30E-03	-2.52E-03 to -7.17E-05	3.80E-02
GABARAP	rs222843	General	Each *G* allele	Worsened	1.88E-03	2.83E-04 to 3.48E-03	2.11E-02
	rs222843	Negative	Each *G* allele	Worsened	2.49E-03	8.62E-04 to 4.12E-03	2.79E-03
	rs222843	Total	Each *G* allele	Worsened	1.88E-03	3.45E-04 to 3.41E-03	1.65E-02

ATR: antipsychotic treatment response, indicates relative response to treatment over time with each additional minor allele; CI: confidence interval; effect estimate: difference in log-transformed PANSS scores with each additional minor allele, multiplied by time; ** illustrates P-value ≤ 0.001. No asterisks represent P-value ≤ 0.05.

Supplementary table 17. Associations between genetic variants of the neurodegenerative disease pathway and antipsychotic treatment response as defined by the change in log-transformed PANSS scores over 12 months under the genotypic model of inheritance

			Genotypic model of inheritance				
Gene	**dbSNPID**	**PANSS Domain**	**Contrast**	**ATR**	**Effect estimate**	**95% CI**	**P-value**
ATG7	rs2594967	General	*TT vs GG*	Worsened	4.80E-03	5.91E-04 to 9.00E-03	2.55E-02
	rs2442795	General	*TT vs GG*	Worsened	1.05E-02	2.39E-03 to 1.87E-02	1.14E-02
	rs11128552	General	*GT vs TT*	Worsened	2.13E-03	1.84E-04 to 4.07E-03	3.18E-02
	rs2454512	General	*AA vs GG*	Worsened	9.72E-03	2.28E-03 to 1.72E-02	1.06E-02
	rs2442795	Negative	*TT vs GG*	Worsened	1.13E-02	2.95E-03 to 1.96E-02	8.05E-03
	rs2442795	Negative	*TG vs GG*	Improved	-2.51E-03	-4.62E-03 to -3.98E-04	1.99E-02
	rs2442772	Negative	*AG vs GG*	Improved	-2.25E-03	-4.26E-03 to -2.44E-04	2.80E-02
	rs2442772	Negative	*AA vs GG*	Improved	-2.59E-03	-5.09E-03 to -9.54E-05	4.20E-02
	rs2454512	Negative	*AA vs GG*	Worsened	1.00E-02	2.38E-03 to 1.77E-02	1.03E-02
	rs6442259	Negative	*TC vs CC*	Worsened	2.72E-03	6.32E-04 to 4.81E-03	1.08E-02
	rs2594992	Negative	*CA vs AA*	Worsened	2.65E-03	5.80E-04 to 4.73E-03	1.23E-02
	rs6442259	Positive	*TT vs CC*	Worsened	4.54E-03	1.32E-03 to 7.77E-03	5.89E-03
	rs2442772	Positive	*AG vs GG*	Improved	-3.23E-03	-5.82E-03 to -6.29E-04	1.50E-02
	rs2442772	Positive	*AA vs GG*	Improved	-4.19E-03	-7.43E-03 to -9.52E-04	1.13E-02
	rs2606736	Positive	*AA vs GG*	Worsened	4.33E-03	1.02E-03 to 7.64E-03	1.04E-02
	rs2442795	Total	*TT vs GG*	Worsened	1.04E-02	2.61E-03 to 1.82E-02	9.07E-03
	rs2454512	Total	*AA vs GG*	Worsened	9.65E-03	2.50E-03 to 1.68E-02	8.27E-03
	rs2442795	Total	*TG vs GG*	Improved	-2.43E-03	-4.41E-03 to -4.51E-04	1.62E-02
	rs2442772	Total	*AA vs GG*	Improved	-2.50E-03	-4.84E-03 to -1.52E-04	3.70E-02
	rs2454512	Total	*AA vs GG*	Worsened	9.65E-03	2.50E-03 to 1.68E-02	8.27E-03
	rs6442259	Total	*TC vs CC*	Worsened	2.00E-03	4.54E-05 to 3.95E-03	4.50E-02
	rs6442259	Total	*TT vs CC*	Worsened	2.47E-03	1.32E-04 to 4.81E-03	3.85E-02
ATG14	rs1538257	General	*AC vs CC*	Worsened	2.61E-03	6.92E-04 to 4.52E-03	7.72E-03
	rs8003279	General	*GG vs AA*	Improved	-6.29E-03	-1.20E-02 to -6.12E-04	3.00E-02
	rs1538257	**Negative**	***TG vs GG***	**Worsened**	**3.34E-03**	**1.39E-03 to 5.30E-03**	**0.000841****
	rs7150763	Negative	*GG vs AA*	Improved	-4.19E-03	-7.35E-03 to -1.03E-03	9.50E-03
	rs8003279	Total	*GG vs AA*	Improved	-5.44E-03	-1.09E-02 to -6.91E-06	4.98E-02
	rs1538257	Total	*AC vs CC*	Worsened	2.23E-03	3.92E-04 to 4.07E-03	1.76E-02

GABARAP	**rs222843**	**Negative**	***GG vs AA***	**Worsened**	**8.52E-03**	**3.62E-03 to 1.34E-02**	**0.000678****
	rs222843	Total	*GG vs AA*	Worsened	4.65E-03	2.45E-05 to 9.27E-03	4.89E-02
PINK1	rs1043424	General	*CC vs AA*	Worsened	2.91E-03	9.63E-06 to 5.81E-03	4.93E-02
	rs650616	General	*AA vs GG*	Improved	-2.80E-03	-5.39E-03 to -1.95E-04	3.52E-02
	rs1043424	**Negative**	***CC vs AA***	**Worsened**	**5.96E-03**	**3.02E-03 to 8.90E-03**	**0.0000756*****
	rs650616	Negative	*AA vs GG*	Improved	-3.09E-03	-5.75E-03 to -4.25E-04	2.32E-02
	rs1043424	Positive	*CA vs AA*	Improved	-3.41E-03	-5.91E-03 to -9.19E-04	7.40E-03

ATR: antipsychotic treatment response, indicates relative response to treatment over time between genotypes; CI: confidence interval; effect estimate: difference in log-transformed PANSS scores between the different genotypes multiplied by time; ** illustrates P-value ≤ 0.001; *** illustrates P-value below the Bonferroni-corrected threshold α-value. No asterisks represent P-value ≤ 0.05.

Supplementary table 18. Associations between genetic variants of the neurodegenerative disease pathway and antipsychotic treatment response as defined by the change in log-transformed PANSS scores over 12 months under the additive allelic model of inheritance

$\alpha = 2.60 \times 10^{-4}$

Additive allelic model of inheritance

Gene	dbSNPID	PANSS Domain	Contrast	ATR	Effect estimate	95% CI	P-value
ATG7	rs2594992	Negative	Each *C* allele	Worsened	2.63E-03	-7.53E-04 to 2.40E-03	3.68E-03
	rs2442772	Negative	Each *A* allele	Improved	-1.46E-03	-2.67E-03 to -2.49E-04	1.83E-02
	rs2442772	Positive	Each *A* allele	Improved	-2.29E-03	-3.86E-03 to -7.24E-04	4.25E-03
	rs6442259	Positive	Each *T* allele	Worsened	2.19E-03	5.96E-04 to 3.79E-03	7.22E-03
	rs2606736	Positive	Each *A* allele	Worsened	2.15E-03	4.96E-04 to 3.81E-03	1.10E-02
	rs2442772	Total	Each *A* allele	Improved	-1.30E-03	-2.43E-03 to -1.62E-04	2.52E-02
	rs6442259	Total	Each *T* allele	Worsened	1.29E-03	1.35E-04 to 2.45E-03	2.88E-02
GABARAP	rs222843	General	Each *G* allele	Worsened	1.88E-03	2.83E-04 to 3.48E-03	2.11E-02
	rs222843	Negative	Each *G* allele	Worsened	2.49E-03	8.62E-04 to 4.12E-03	2.79E-03
	rs222843	Total	Each *G* allele	Worsened	1.88E-03	3.45E-04 to 3.41E-03	1.65E-02
PINK1	rs650616	General	Each *A* allele	Improved	-1.34E-03	-2.62E-03 to -5.22E-05	4.14E-02
	rs1043424	Negative	Each *C* allele	Worsened	2.00E-03	6.64E-04 to 3.33E-03	3.38E-03
	rs650616	Negative	Each *A* allele	Improved	-1.59E-03	-2.91E-03 to -2.79E-04	1.76E-02

ATR: antipsychotic treatment response, indicates relative response to treatment over time with each additional minor allele; CI: confidence interval; effect estimate: difference in log-transformed PANSS scores with each additional minor allele, multiplied by time; P-values have met an uncorrected threshold of P-value ≤ 0.05.

Supplementary table 19. Associations between all prioritised variants and antipsychotic treatment response as defined by the change in log-transformed PANSS scores over 12 months under the genotypic model of inheritance

			$\alpha = 1.79 \times 10^{-4}$				
			Genotypic model of inheritance				
Gene	**dbSNPID**	**PANSS Domain**	**Contrast**	**ATR**	**Effect estimate**	**95% CI**	**P-value**
AMBRA1	**rs11819869**	**Negative**	***TT vs CC***	**Worsened**	**4.56E-03**	**2.04E-03 to 7.07E-03**	**0.000411****
ATG7	rs2454512	General	*AA vs GG*	Worsened	9.72E-03	2.28E-03 to 1.72E-02	1.06E-02
	rs2594967	General	*TT vs GG*	Worsened	4.80E-03	5.91E-04 to 9.00E-03	2.55E-02
	rs2442795	General	*TT vs GG*	Worsened	1.05E-02	2.39E-03 to 1.87E-02	1.14E-02
	rs11128552	General	*GT vs TT*	Worsened	2.13E-03	1.84E-04 to 4.07E-03	3.18E-02
	rs2442795	Negative	*TT vs GG*	Worsened	1.13E-02	2.95E-03 to 1.96E-02	8.05E-03
	rs2454512	Negative	*AA vs GG*	Worsened	1.00E-02	2.38E-03 to 1.77E-02	1.03E-02
	rs2442795	Negative	*TG vs GG*	Improved	-2.51E-03	-4.62E-03 to -3.98E-04	1.99E-02
	rs2442772	Negative	*AG vs GG*	Improved	-2.25E-03	-4.26E-03 to -2.44E-04	2.80E-02
	rs2442772	Negative	*AA vs GG*	Improved	-2.59E-03	-5.09E-03 to -9.54E-05	4.20E-02
	rs6442259	Negative	*TC vs CC*	Worsened	2.72E-03	6.32E-04 to 4.81E-03	1.08E-02
	rs2606736	Positive	*AA vs GG*	Worsened	4.33E-03	1.02E-03 to 7.64E-03	1.04E-02
	rs2454512	Total	*AA vs GG*	Worsened	9.65E-03	2.50E-03 to 1.68E-02	8.27E-03
	rs2442795	Total	*TT vs GG*	Worsened	1.04E-02	2.61E-03 to 1.82E-02	9.07E-03
	rs2442795	Total	*TG vs GG*	Improved	-2.43E-03	-4.41E-03 to -4.51E-04	1.62E-02
	rs2442795	Total	*TT vs GG*	Worsened	1.04E-02	2.61E-03 to 1.82E-02	9.07E-03
	rs2442772	Total	*AA vs GG*	Improved	-2.50E-03	-4.84E-03 to -1.52E-04	3.70E-02
	rs6442259	Total	*TC vs CC*	Worsened	2.00E-03	4.54E-05 to 3.95E-03	4.50E-02
	rs6442259	Total	*TT vs CC*	Worsened	2.47E-03	1.32E-04 to 4.81E-03	3.85E-02
ATG13	rs13448	Negative	*CT vs TT*	Worsened	2.21E-03	2.14E-04 to 4.21E-03	3.00E-02
	rs10838610	Negative	*AA vs GG*	Improved	-4.11E-03	-7.15E-03 to -1.06E-03	8.27E-03
ATG16L1	rs6758317	Positive	*TT vs CC*	Worsened	6.01E-03	1.30E-03 to 1.07E-02	1.24E-02
	rs10803619	Positive	*TC vs CC*	Worsened	3.64E-03	4.44E-04 to 6.84E-03	2.57E-02
	rs10803619	Total	*TT vs CC*	Worsened	4.94E-03	3.43E-04 to 9.53E-03	3.53E-02

	rs1538257	General	*TG vs GG*	Worsened	2.61E-03	6.92E-04 to 4.52E-03	7.72E-03
	rs8003279	General	*GG vs AA*	Improved	-6.29E-03	-1.20E-02 to -6.12E-04	3.00E-02
	rs1538257	General	*TG vs GG*	Worsened	2.61E-03	6.92E-04 to 4.52E-03	7.72E-03
ATG14	**rs1538257**	**Negative**	***TG vs GG***	**Worsened**	**3.34E-03**	**1.39E-03 to 5.30E-03**	**0.000841****
	rs7150763	Negative	*GG vs AA*	Improved	-4.19E-03	-7.35E-03 to -1.03E-03	9.50E-03
	rs8003279	Total	*GG vs AA*	Improved	-5.44E-03	-1.09E-02 to -6.91E-06	4.98E-02
	rs1538257	Total	*AC vs CC*	Worsened	2.23E-03	3.92E-04 to 4.07E-03	1.76E-02
GABARAP	**rs222843**	**Negative**	***GG vs AA***	**Worsened**	**8.52E-03**	**3.62E-03 to 1.34E-02**	**0.000678****
	rs222843	Total	*GG vs AA*	Worsened	4.65E-03	2.45E-05 to 9.27E-03	4.89E-02
	rs1043424	General	*CC vs AA*	Worsened	2.91E-03	9.63E-06 to 5.81E-03	4.93E-02
	rs650616	General	*AA vs GG*	Improved	-2.80E-03	-5.39E-03 to -1.95E-04	3.52E-02

ATR: antipsychotic treatment response, indicates relative response to treatment over time between genotypes; CI: confidence interval; effect estimate: difference in log-transformed PANSS scores between the different genotypes multiplied by time; ** illustrates P-value ≤ 0.001; *** illustrates P-value below the Bonferroni-corrected threshold α-value. No asterisks represent P-value ≤ 0.05.

Supplementary table 20. Associations between all prioritised variants and antipsychotic treatment response as defined by the change in log-transformed PANSS scores over 12 months under the additive allelic model of inheritance

			$\alpha = 1.79 \times 10^{-4}$				
			Additive allelic model of inheritance				
Gene	**dbSNPID**	**PANSS Domain**	**Contrast**	**ATR**	**Effect estimate**	**95% CI**	**P-value**
AMBRA1	**rs11819869**	**Negative**	**Each *T* allele**	**Worsened**	**2.20E-03**	**9.46E-04 to 3.46E-03**	**0.000613****
ATG7	rs2594992	Negative	Each *C* allele	Worsened	2.63E-03	8.59E-04 to 4.40E-03	3.68E-03
	rs2442772	Negative	Each *A* allele	Improved	-1.46E-03	-2.67E-03 to -2.49E-04	1.83E-02
	rs2442772	Positive	Each *A* allele	Improved	-2.29E-03	-3.86E-03 to -7.24E-04	4.25E-03
	rs2606736	Positive	Each *A* allele	Worsened	2.15E-03	4.96E-04 to 3.81E-03	1.10E-02
	rs6442259	Positive	Each *T* allele	Worsened	2.19E-03	5.96E-04 to to 3.79E-03	7.22E-03
	rs2442772	Total	Each *A* allele	Improved	-1.30E-03	-2.43E-03 to -1.62E-04	2.52E-02
	rs6442259	Total	Each *T* allele	Worsened	1.29E-03	1.35E-04 to 2.45E-03	2.88E-02
ATG13	rs10838610	Negative	Each *A* allele	Improved	-1.92E-03	-3.28E-03 to -5.58E-04	5.80E-03
ATG16L1	rs10803619	General	Each *T* allele	Worsened	2.16E-03	3.89E-04 to 3.93E-03	1.69E-02
	rs6758317	Positive	Each *T* allele	Worsened	1.95E-03	6.37E-05 to 3.83E-03	4.28E-02
	rs10803619	Positive	Each *T* allele	Worsened	3.27E-03	9.26E-04 to 5.62E-03	6.35E-03
	rs10803619	Total	Each *T* allele	Worsened	2.30E-03	6.07E-04 to 4.00E-03	7.89E-03
GABARAP	rs222843	General	Each *G* allele	Worsened	1.88E-03	2.83E-04 to 3.48E-03	2.11E-02
	rs222843	Negative	Each *G* allele	Worsened	2.49E-03	8.62E-04 to 4.12E-03	2.79E-03
	rs222843	Total	Each *G* allele	Worsened	1.88E-03	3.45E-04 to 3.41E-03	1.65E-02
PINK1	rs650616	General	Each *A* allele	Improved	-1.34E-03	-2.62E-03 to -5.22E-05	4.14E-02
	rs650616	Negative	Each *A* allele	Improved	-1.59E-03	-2.91E-03 to -2.79E-04	1.76E-02
	rs1043424	Negative	Each *C* allele	Worsened	2.00E-03	6.64E-04 to 3.33E-03	3.38E-03

ATR: antipsychotic treatment response, indicates relative response to treatment over time with each additional minor allele; CI: confidence interval; effect estimate: difference in log-transformed PANSS scores with each additional minor allele, multiplied by time; ** illustrates P-value ≤ 0.001. No asterisks represent P-value ≤ 0.05.

Supplementary table 21. Enriched pathways for candidate genes (extended)

Pathway	P-value	Adjusted P-value	Odds Ratio	Combined Score	Genes
Autophagy*	2.02E-17	6.21E-15	138.89	5339.20	*ATG3; ATG16L1; AMBRA1; ATG14; ATG13; ATG7; GABARAP; ATG12*
Mitophagy*	2.71E-06	4.18E-04	102.56	1314.58	*PINK1; AMBRA1; GABARAP*
NOD-like receptor signaling*	5.60E-05	5.75E-03	37.45	366.69	*ATG16L1; GABARAP; ATG12*
Kaposi sarcoma-associated herpesvirus infection pathway*	6.38E-05	4.91E-03	35.84	346.23	*ATG3; ATG14; GABARAP*
FoxO signaling*	1.51E-03	9.30E-02	33.67	218.71	*GABARAP; ATG12*
Ferroptosis*	1.79E-02	9.17E-01	55.56	223.62	*ATG7*
RIG-I-like receptor signaling*	3.11E-02	1.00E+00	31.75	110.21	*ATG12*
GABAergic synapse*	3.94E-02	1.00E+00	24.97	80.78	*GABARAP*
Longevity regulating*	4.50E-02	1.00E+00	21.79	67.57	*ATG13*
Apelin signaling*	6.00E-02	1.00E+00	16.22	45.64	*GABARAP*
Parkinson's disease*	6.21E-02	1.00E+00	15.65	43.48	*PINK1*
Schizophrenia	*Previously reported association in literature*				*ATG13; ATG16L1; GABARAP; AMBRA1*
Neurodegenerative disease	*Previously reported association in literature*				*ATG12; ATG14; ATG3; ATG7; GABARAP; PINK1*

*Predicted *via* Enrichr, available at https://amp.pharm.mssm.edu/Enrichr/, accessed June 2020.

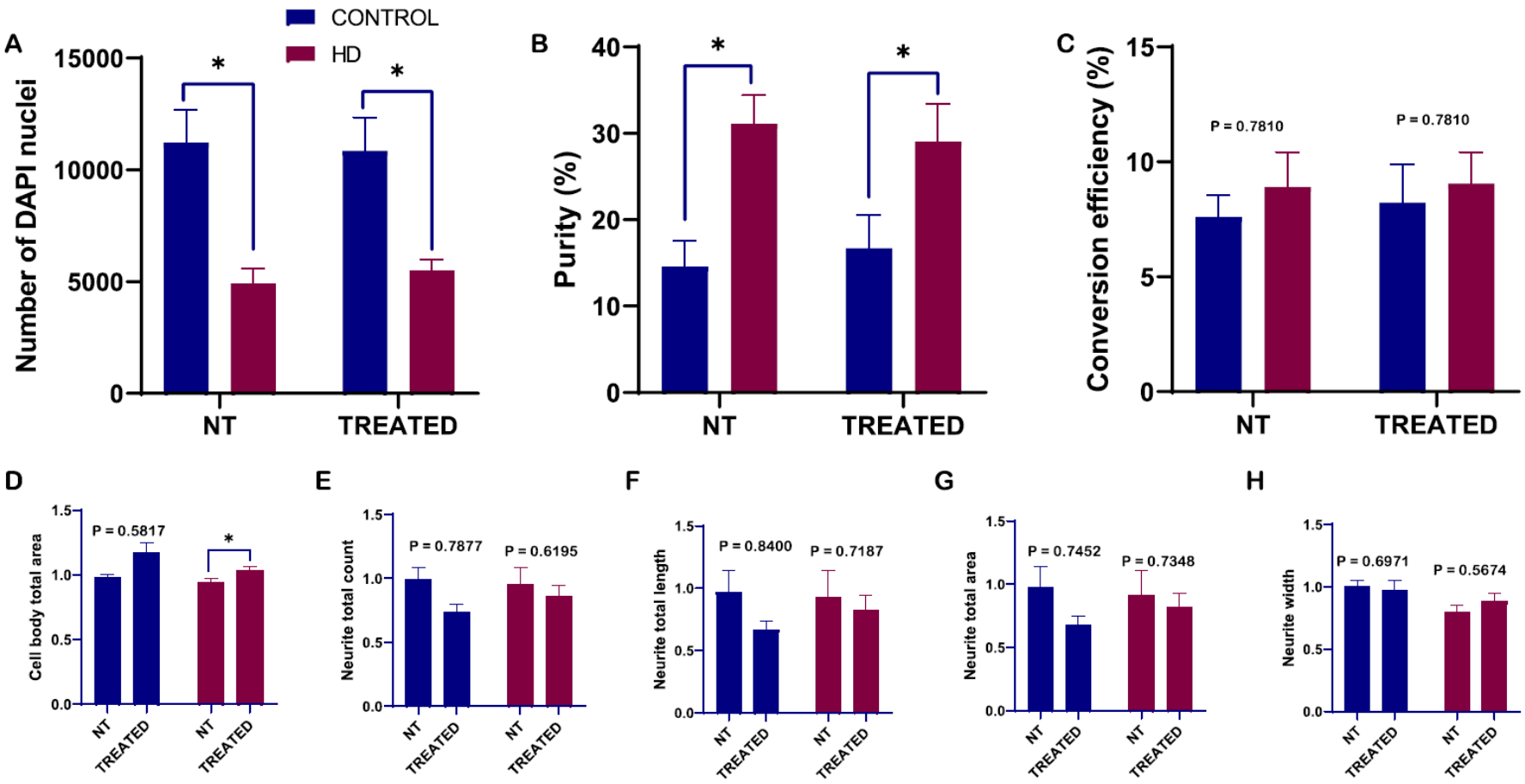

Supplementary figure 1. Treatment of Huntington's disease and control induced neurons with autophagy inducing drug Torin1 (extended).
A) Quantification of average neuronal yields per DAPI following 28 days of conversion. (n = 3 for control, 14 wells analysed in total and n = 3 for HD, 14 wells analysed in total). B - C) Quantification of average neuronal purity and efficiency of reprogrammed adult human dermal fibroblasts. (n = 3 for control, 14 wells analysed in total and n = 3 for HD, 14 wells analysed in total). D - H) Quantification of relative cell body area, neurite area, length, count, and width per cell calculated by HCS analysis defined by MAP2+ neurons. (n = 3 for control, 14 wells analysed in total and n = 3 for HD, 14 wells analysed in total). HD: Huntington's disease; HCS: High-content screening; NT: Non-treated. Data are expressed as mean ±SEM and are from biological replicates (n = 3) of 3 control lines and 3 HD lines. An unpaired unequal student's t-test was used in D - H to test differences between two groups. P-value < 0.05 set for significance (indicated by *). Cell lines have been normalised to 1.

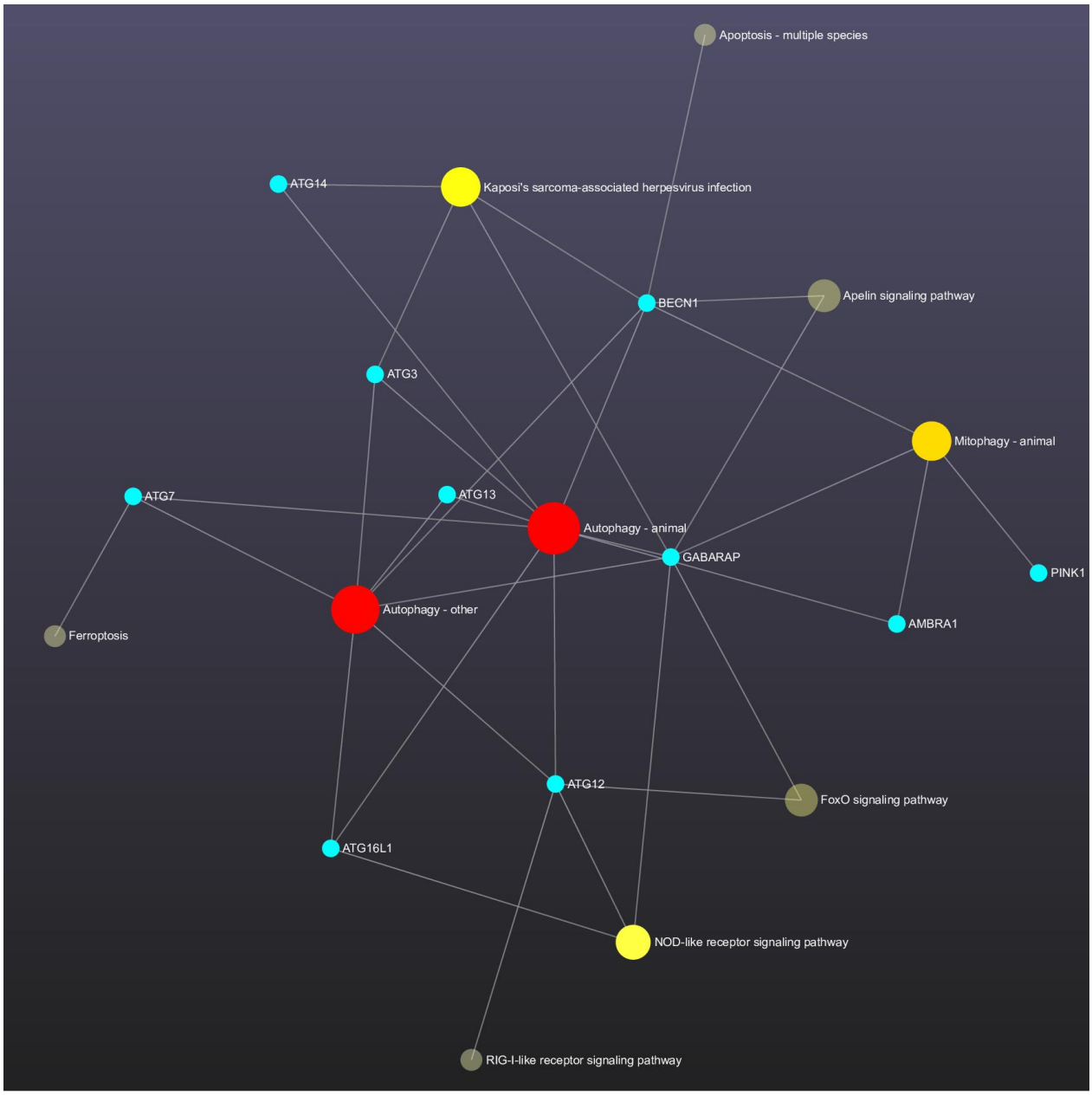

Supplementary figure 2. Network depicting the expected interaction of signal transduction pathways enriched for the candidate genes as determined by KEGG.

Nodes representing gene sets (signal transduction pathways) are colour-coded according to their enrichment score (P-value) with red representing the lowest P-value (most significant) and dull yellow representing the largest P-value (less significant). Additionally, nodes are sized according to the number of genes from the gene set that are on the analysed gene list (*ATG3, ATG7, ATG12, ATG13, ATG14, ATG16L1, AMBRA1, BECN1, GABARAP, PINK1*). Created using NetworkAnalyst (www.networkanalyst.ca) in October 2020. FoxO: Forkhead box protein O; NOD: nucleotide-binding oligomerization domain; RIG-I: retinoic acid-inducible gene I.

Supplementary table 22. Expected gene-signal transduction pathway interaction as determined by KEGG database

Signalling pathway	Gene hits	P-value	Adjusted P-value
Autophagy - animal	*AMBRA1, ATG3, ATG7, ATG12 ATG13, ATG14, ATG16L1, BECN1, GABARAP*	6.9×10^{-16}	1.94×10^{-13}
Autophagy - other	*ATG3, ATG7, ATG12, ATG13, ATG16L1, BECN1, GABARAP*	1.22×10^{-15}	1.94×10^{-13}
Mitophagy - animal	*AMBRA1, BECN1, GABARAP, PINK1*	9.17×10^{-7}	9.73×10^{-5}
Kaposi's sarcoma-associated	*ATG3, ATG14, BECN1*	6.06×10^{-5}	4.82×10^{-3}
NOD-like receptor	*ATG12, ATG16L1, GABARAP*	1.28 x 10-3	8.11×10^{-2}
FoxO	*ATG12, GABARAP*	1.19×10^{-2}	5.8×10^{-1}
Apelin	*BECN1, GABARAP*	1.28×10^{-2}	5.8×10^{-1}
Apoptosis - multiple species	*BECN1*	4.19×10^{-2}	1
Ferroptosis	*ATG7*	5.05×10^{-2}	1
RIG-I-like receptor	*ATG12*	8.69×10^{-2}	1

Network data generated using NetworkAnalyst (www.networkanalyst.ca).

II. APPENDIX B

1. Conference attendance

a. 2nd Nordic Huntington Disease Research Meeting 2019 (delegate)
b. 28th World Congress of Psychiatric Genetics 2020 (delegate)
c. The Network for European CNS Transplantation and Restoration (NECTAR) Conference 2020 (delegate)

2. Journal article output

Preprint available on bioRxiv: doi: https://doi.org/10.1101/2021.03.01.433433

Distinct sub-cellular autophagy impairments occur independently of protein aggregation in aged induced neurons from patients with Huntington's disease

Karolina Pircs[1], Janelle Drouin-Ouellet[4, 8], Jeovanis G. Valdés[2], Melinda Rezeli[3], Daniela A. Grassi[1], Raquel Garza[1], Yogita Sharma[1], Isabelle St-Amour[6], Marie E. Jönsson[1], Pia A. Johansson[1], Kate Harris[5], Romina Vuono[5], Tom Stoker[5], Bob A. Hersbach[1], Kritika Sharma[1], Jessica Lagerwall[1], Stina Lagerström[1], Petter Storm[8], Vivien Horváth[1], Elena Cattaneo[7], Sébastien S. Hébert[6], György Marko-Varga[3], Malin Parmar[8], Roger A. Barker[5], [7] & Johan Jakobsson[1*]

[1]Laboratory of Molecular Neurogenetics, Department of Experimental Medical Science, Wallenberg Neuroscience Center and Lund Stem Cell Center, BMC A11, Lund University, 221 84 Lund, Sweden.

[2]Oncology and Pathology, Kamprad Lab, Lund University, Lund, Sweden.

[3]Clinical Protein Science and Imaging, Department of Biomedical Engineering, Lund University, Lund, Sweden.

[4]Faculty of Pharmacy, University of Montreal, Montreal, Quebec, Canada.

[5]John van Geest Centre for Brain Repair & Department of Neurology, Department of Clinical Neurosciences, University of Cambridge, Forvie Site, Cambridge CB2 0PY, UK.

[6]Axe Neurosciences, Centre de recherche du CHU de Québec – Université Laval, CHUL, Québec, QC G1V 4G2, Canada.

[7]Laboratory of Stem Cell Biology and Pharmacology of Neurodegenerative Diseases, Department of Biosciences, University of Milan, 20122 Milan, Italy.

[8]Developmental and Regenerative Neurobiology, Department of Experimental Medical Science, Wallenberg Neuroscience Center and Lund Stem Cell Center, BMC A11, Lund University, 221 84 Lund, Sweden.

*Lead Contact:

Johan Jakobsson

Dept of Experimental Medical Science

Wallenberg Neuroscience Center

BMC A11

221 84

Lund

SWEDEN

Email: johan.jakobsson@med.lu.se

Phone: +46 46 2224225

Fax: +46 46 2220559